Gene Targeting: A Focus on Acute Myeloid Leukemia Gene Silencing and Detection of Methylated DNA by Exploring the Use of Synthetic Nanocarriers and Nucleic Acid Analogs

by

Anyeld Maria Ubeda

A thesis submitted in partial fulfillment of the requirements for the degree of

Master of Science
in
Biomedical Sciences

Department of Biomedical Engineering
University of Alberta

Abstract

Research in the field of nucleic acids and molecular genetics has enormously enhanced our knowledge about the genetic origins of a myriad of disease. Currently from this knowledge, various gene-targeted therapies and biomarker detection and diagnostic assays are being developed, which are discussed in Chapter 1, as targeting sequences of interest is deemed a simpler task compared to protein targeting. The treatment and understanding of Acute Myeloid Leukemia (AML) development has greatly benefited from the advances in molecular characterization and the World Health Organization (WHO) recognizes certain recurrent genetic abnormalities as diagnosis for the disease. In this thesis, we first demonstrate how we can develop gene silencing therapeutic options targeting messenger RNA (mRNA) in AML cells by delivering small interfering RNAs (siRNA) using polyethylenimine (PEI) carriers. Next, we show how we can target the aberrant formation of DNA adducts in the sequence of the *KRAS* oncogene using synthetic nucleobase analogs.

More specifically, in Chapter 2, we explored the use of RNA silencing as a promising candidate to be used in conjunction with traditional treatments as it has the potential to act in synergy to lower doses, length of treatments and side effects.

We identified molecular targets using lipid modified PEI delivery systems that could be used as the basis of therapy during AML progression using the stem-cell like KG1a cell line and primary cells. We identified linoleic acid and lauric acid modified PEI as effective and versatile carriers and showed how they can effectively downregulate the mRNA levels of genes including *BCR5* (survivin), and *BCL2L12* leading to a reduction in proliferation of the cells. Moreover, we highlight the versatility of the synthetic delivery systems and how gene silencing allows for personalized and targeted patient treatment.

In Chapter 3, we showed the versatility of incorporating DNA base analogs to oligonucleotide sequences for the detection of *O*^{6}-methylguanine (O^6-meG), a DNA adduct that is highly mutagenic. The base analogs were synthesized by the Sturla group in ETH Zurich to have higher affinity to the methylated guanine in comparison to the non-methylated form. Our main objective was to develop a templated-ligation based detection assay and identify parameters that enhance the selectivity of the synthetic base for downstream sequence amplification. The templated ligation reaction would simplify previously reported detection methods for the same adduct and also give sequence specificity of the location of interest which a lot of previous methods lacked. We examined different parameters of the ligation reaction, modified the reacting probes, and reaction conditions to increase the detection limit of our assay in the presence of non-methylated background DNA. By enhancing the selectivity of the ligation reaction, we aimed to increase the selectivity of the O^6-meG detection retaining sequence specificity so that in the future we can design a fast screening test for adduct formation that can be used as a biomarker test for hotspot mutation sites.

Preface

The work presented in this thesis was guided by the supervision of Dr. Julianne Gibbs and Dr. Hasan Uludağ.

Chapter 1 is a literature review to provide background about the current therapeutic and detection developments that have resulted from the advances in molecular biology and genetic sequencing with a focus in cancer. We discuss genetic therapies exploring their aim to enhance gene function by introducing a sequence of interest to target cells or downregulate an aberrant gene by ultimately inducing mRNA degradation. In Chapter 1 we also discuss some examples of personalized medicine and how biomarker detection and sequencing enhance the treatment strategies for individual patients. More specifically, we discuss how detecting DNA lesions such as methylation of bases can provide real-time information about the progress of treatment using alkylating chemotherapeutic agents. Hence, we highlight the versatility of the work being done with nucleic acids and gene targeting and how it provides alternatives for new treatments and diagnostics. Figure1.3 and Figure 1.5 were utilized in Chapter 1 with permission from the respective publishers. More specifically Figure 1.3 was published in an open access article by Su Yin Lim and co-workers in the journal of Molecular Cancer, 2018 under the Creative Commons Attribution 4.0 International License ((http://creativecommons.org/licenses/by/4.0/). Figure 1.5 was utilized with permission granted by the American Chemical Society (ACS) in the journal of Chemical Research in Toxicology. The figure is the work of Alessia Stornetta and co-workers (https://pubs.acs.org/doi/10.1021/acs.chemrestox.6b00380). Further permissions related to the material excerpted should be directed to ACS.

Chapter 2 continues the work started by Dr. Breanne Landry and Dr. Hilal Gul-Uludağ focusing on gene therapies to treat acute myeloid leukemia via RNA interference using lipid substituted polyethylenimines. The primary patient samples were obtained thanks to Dr. Joseph Brandwein and Zoulika Zak. The RT-qPCR experiments presented in Chapter 2 were

performed with the generous help from Cezary Kucharski. All lipopolymers used for Chapter 2 were synthesized by Dr. Remant K.C. My role in the project was the design of experiments, cell culture, analysis and processing of data. All contributors to Chapter 2 were members of the University of Alberta at the time the studies were conducted.

Chapter 3 continues the work started by Dr. Shana Sturla and Dr. Ioannis Trantakis from the laboratory of toxicology from the Swiss Federal Institute of Technology in Zurich (ETH Zurich) in collaboration with Dr. Julianne Gibbs and Dr. Eiman Osman from the University of Alberta. Dr. Trankakis provided the ExBIM modified oligonucleotides utilized in all experiments presented and Dr. Eiman Osman was involved in the synthesis of the oligonucleotides prepared at the University of Alberta.

Acknowledgements

None of the opportunities that have allowed me to complete this thesis would have been possible without the support and encouragement of the amazing individuals in my life. First, I would like to thank my supervisors Dr. Hasan Uludağ and Dr. Julianne Gibbs for providing me with mentorship and guidance while working with them. I am truly fortunate to have had two supervisors that genuinely care about the growth and scholarship of their students. I would also like to thank Dr. David Eisenstat for being part of my supervisory committee and his questions and suggestions for my work. Moreover, I would like to thank the Alberta/Technical University of Munich International Graduate School for Hybrid Functional Materials (ATUMS), Leah Veinot and Dr. John Veinot for providing me the opportunity and funding to participate in an incredible program for graduate students at the University of Alberta and allowing me to complete a research exchange term in Munich. Thank you Dr. Job Boehkhoven for hosting me in your laboratory at the Technical University of Munich (TUM) and giving me an invaluable experience to do research overseas and learn more about advanced materials.

I would also like to thank everyone that I had the pleasure of working with during my graduate studies. In the Uludağ lab, I would like to give special thanks to Cezary Kucharski for his mentorship and guidance when performing experiments, you keep us in check Cezy. I would also like to give special thanks to my officemates, Eleni Tsekoura, Dr. Manoj Parmar and Dr. Juliana Valencia-Serna for being role models, challenging me and taking their time to discuss about science and non-scientific topics in and out of the lab. In addition, I got to work with an excellent team that quickly became some of my closest friends in Edmonton, thank you Dr. Deniz Meneksedag-Erol, Dr. Remant K.C., Daniel Nisakar, Aysha Ansari, Mahsa Mohseni, Bindu Thapa, Teo Dick, Yousef Nademi, Beste Avci, and Adam Manfrin. In the Gibbs lab, I also had the pleasure of working with great individuals and researchers including Dr. Eiman Osman, Sarah Hales, Benjamin Rehl, Hansol Park, Yuning Liu, Safeenaz Alladin-

Mustan, Dr. Akemi Darlington, Mokhtar Rashwan, and Shyam Parshotam. Thank you for answering all of my basic chemistry questions and being great company to work with. I would also like to thank Kenwick Ng for being my friend in the BME department and going through the same journey as me.

Finally, the opportunity to study abroad in Canada would really not have been possible without my family. Thank you mom (Sandra Gutierrez), dad (Larry Ubeda) and sister (Sandra Ubeda), Minnie, CindyLu, Coco and extended family for being my motivation to do better every day. Thank you for being so supportive, loving and caring. You truly are the best role models I could ever have. Thanks to my uncle's and aunt's families (Tio Pablo, Tia Ana, Tia Margarita, Tio Alfredo, David, Nora, Javier, Hugo, Ana, and Fausto) in Canada for receiving me with open arms when I first came and making me feel at home. Thanks for all your motivation and care, I am very lucky to have you. In addition, I would also like to thank Henry Li and my Cantonese friends and family in Edmonton for also making me feel at home and sharing your culture and encouragement with me. Thank you, Anna Wong, David Li, Carmen Li, Jason Lee, Ahreum Lee, Patrick Li, Mahmah and Minnie Li for sharing your delicious meals and laughter throughout my studies.

Table of Contents

List of Tables

List of Figures

Chapter 1. Background and Scope

1.1 Introduction

Since the discovery of nucleic acids in 1868 by Friedrich Miescher, scientists have developed a greater understanding of the complexity of our genetic code and unveiled a myriad of opportunities in medicine, material science, biotechnology, pharmaceuticals, and more [1-6]. In this thesis project, I demonstrate how we can use the current knowledge about the molecular makeup of different types of cancer to develop gene therapies and biomarker detection methods. Moreover, I show how we can pair synthetic materials with nucleic acids to extend their applications given that working with nucleic acids alone has limitations that prevent them from being used to their full potential.

Advances in molecular biology in the 1980s and 1990s allowed scientists to categorize cancer as a genetic disorder or disease, a classification that is still accepted by the National Institutes of Health (NIH) [7-8]. At this time, it was elucidated that the onset of carcinogenesis involved different environmental and endogenous factors that affected the DNA structure or composition due to chemical alterations or by the addition, duplication, or deletion of bases, or chromosomal insertions, rearrangements, and translocations which ultimately caused changes in amplification, transcription, and gene expression altering cellular homeostasis [9-10]. As more information was collected about the genetic alterations involved in carcinogenesis, different gene categories were established that had higher potential to be correlated with the onset or progression of cancer. Two main broad categories for such genes are: (i) proto-oncogenes, which are genes involved in promoting cellular growth and (ii) tumor-suppressor genes, which are involved in regulating apoptosis or cell death and slowing down growth [11]. More specifically, these categories include genes involved in intracellular signaling pathways, cell proliferation, migration, cell cycle and differentiation, DNA repair, transcription regulation, apoptosis, motility, adhesion, angiogenesis stress responses, and immune regulation [11-12]. In summary, the vast knowledge obtained through the advances in cancer genetics highlighted the fine balance and precise regulation of the growth-promoting

and growth-suppressing genes and proteins involved in cellular homeostasis and the complexity of their interactions. Even though the genetic basis of cancer is extremely complex, sequencing advances, especially after the launch of The Cancer Genome Atlas (TCGA) in 2005 by the US National Institutes of Health (NIH), have identified countless targets that have allowed for the development of more precise and targeted therapies, diagnostics and preventative measures [13-21]. In April 2018, the TCGA program ended with the publication of the Pan-Cancer Atlas, and its data portal now includes 3,142,246 mutations in 22,872 genes involved in different types of cancer [22]. Such tremendous work provides a panoramic collection of interconnected interactions, events and networks which elucidate on further understanding of oncogenic processes and how they originate.

1.1.2 Genetic Therapies in Oncology

1.1.2.1 Gene expression-based therapies

With the knowledge gained about the genetic basis of cancer, gene therapies have become attractive as advanced alternatives for novel treatments, providing precise targeting of the disease at the genome level. Advances in gene therapies for cancer started with attempts to suppress oncogenes, replace or/and enhance tumor suppressor gene activity, modulate anti-cancer immune responses, and genetically sensitize cells to chemotherapeutic agents among other approaches [23]. China was the first country to approve the first gene therapy medication, Gendicine for the treatment of head and neck cancer, which introduces an adenovirus as vector to insert the P*53* gene into cancer cells to reduce their growth. *P53,* the most commonly mutated gene in human cancers and also referred to as "the guardian of the genome", is a tumor suppressor gene mutated in 60-80% of cancers and thus is one of the most studied targets to date. It is known to be involved in the cell cycle, DNA repair, and apoptosis and its loss of function usually leads to over proliferation of cells promoting development of different cancers [24-26]. A recent gene therapy to be approved by the U.S. Food and Drug Administration (FDA) was an immunotherapeutic approach, with the

development of chimeric antigen receptor (CAR) T cell therapies to treat acute lymphoblastic leukemias (ALL) in children and advanced lymphomas in adults [27]. CAR T cell therapy works by the introduction of CAR genes into T cells reprogramming them to express a receptor that targets specific cancer cell antigens with the ability to be expanded in vivo. CARs include an antigen recognition domain and a signaling domain that allows for the T cells to have enhanced activation, expansion and overall more effective targeting [28-29]. Currently, Kymriah® (tisagenlecleucel) by Novartis and Yescarta® (axicabtagene ciloleucel) by Kite pharma both work by reprograming T cells to target the CD19 receptor that is commonly present in B-cell malignancies [30]. Besides the treatment of hematologic malignancies, a second type of gene therapy, Luxtruna® (voretigene neparvovec-rzyl) also obtained FDA approval in December 2017 targeting patients with a *RPE65*-mediated inherited retinal dystrophy [31]. *RPE65* is responsible for the expression of the RPE65 protein that is essential for normal vision producing the retinal pigment epithelium. Patients with biallelic *RPE65* mutations usually experience vision loss and have the risk of suffering from complete blindness [32]. Luxtruna™ then works by reintroducing the *RPE65* gene directly into retinal cells by an adeno-associated viral vector [33]. The mentioned therapies are summarized in Table 1.1. Currently there are hundreds of ongoing clinical trials that focus on gene therapies as an intervention and with the recent FDA approvals we can only expect to have an exponential increase in the upcoming years.

Table 1.1 Recently approved gene-based therapies.

Name of therapy	Disease	Target	Mechanism
Gendicine	Head and neck cancer	P53	Adenovirus vector introduces p53 to target cells
Kymriah	B-cell acute lymphoblastic leukemia	CD19	Chimeric antigen receptor T cell treatment
Yescarta	Non-Hodgkin lymphoma	CD19	Chimeric antigen receptor T cell treatment
Luxtruna	Inherited retinal dystrophy	RPE65	Adeno-associated vector introduces *RPE65* gene into retinal epithelium

1.1.2.2 Gene downregulation-based therapies

In contrast to introducing new genes, gene silencing aims at down-regulating or repressing genes that are over-expressed or mutated in cancer cells. Some of the most commonly activated oncogenes belong to the ras family, encoding a group of protein receptors critical for signal transduction pathways involving DNA synthesis, metabolism, proliferation, and cytoskeleton organization [34-35]. Therefore, the *ras* oncogenes have become common targets for silencing and down-regulation for cancer treatments and have been extensively studied in the past [36-39]. Other common targets for downregulation are ones that prevent or de-regulate apoptosis, as the evasion of apoptosis is amongst the hallmarks of cancer playing a central role in its development and in chemoresistance [40].

There are three main pathways that can lead to apoptosis;

(i) the extrinsic pathway mediated by death receptors,

(ii) the intrinsic pathway driven by mitochondrial stimuli, and

(iii) the perforin/granzyme pathway driven by cytotoxic T cells [41].

All pathways converge in the activation of caspase 3 which induces the activation of endonucleases and proteases with the exception of the granzyme A-arm of the

perforin/granzyme pathway which can promote cell death by DNA cleavage [41]. In the case of the intrinsic pathway, a balance between apoptotic and anti-apoptotic proteins, of the BCL-2 family of proteins, dictate the oligomerization of two proteins, BAX and BAK at the outer mitochondrial membrane which commits the cell to apoptosis through permeabilization of the membrane [42]. The anti-apoptotic proteins, BCL-2, BCL-W, BCL-XL, MCL-1, and BFL-1 amongst others can act by inhibiting BAX/BAK oligomerization directly or by sequestering pro-apoptotic proteins [43-46]. Therefore, it is unsurprising that the BCL-2 family of anti-apoptotic proteins get constantly upregulated in many cancer types and targeting them is a popular approach for therapeutic development. Within the past couple of years Venclexta® (venetoclax, ABT-199), a first-in-class BCL-2 inhibitor, received FDA approval for patients with chronic lymphocytic leukemia (CLL), small lymphocytic lymphoma (SLL) and acute myeloid leukemia (AML) [47]. In addition to the development of small molecule inhibitors, several gene therapy attempts have been made for the inhibition of the anti-apoptotic BLC family proteins. For example, as it is known that MCL-1 and BCL-XL have cooperative functions and resistance to ABT-199 can arise by their upregulation [48], silencing RNA (siRNA) has been used as an alternative for targeting both MCL-1 and BCL-XL in combination inducing apoptosis in pancreatic cancer cells [49] mesothelioma cells [50-51]. Another creative combinatorial gene therapeutic approach was done by Ma et al., who developed a bifunctional vector containing small-hairpin RNA (shRNA) to silence BCL-2 and single stranded RNA (ssRNA) as a Toll-like receptor 7 (TLR7) stimulator for the downstream activation of an antitumor immune response [52-53]. Their dual approach promoted apoptosis in gastric cancer cells and also stimulated TLR7-mediated immune responses in mice by the activation of natural killer (NK) cells [53].

Methods for gene silencing can be divided into two: (i) those that act post-transcription including the use of antisense oligonucleotides, RNA interference (RNAi), ribozyme transcript degradation, and (ii) those that edit the DNA directly before transcription including zinc finger nucleases, transcription activator-like effector nucleases, and CRISPR/CAS9 [54-59]. In

Chapter 2 I will focus on gene silencing post-transcriptionally by the use of silencing RNA (siRNA). Here I present other alternatives to siRNA as a background. The first post-transcriptional gene silencing approach was by the use of antisense oligonucleotides (ASOs) in 1978 to inhibit viral replication *in vitro* [60]. The first ASOs that were developed were single stranded deoxynucleotides that could base pair to target mRNA leading to its degradation by endonucleases and thus inhibiting protein production [60]. However, the original ASOs were highly unstable and new strategies to enhance their efficacy have been developed; modifications were attempted on their backbone, sugar moiety or nucleobase offering a variety of options for improvement [61-62]. A common ASO modification is the incorporation of phosphorothioate backbones, shown in Fig. 1.1, to replace naturally occurring phosphodiester bonds, specifically by the introduction of a sulfur in the place of a non-binding oxygen atom in the natural phosphodiester bond. Phosphorothioate oligonucleotides (PS-ONs) are more biologically stable as they are more resistant to nuclease-degradation and activate RNase-H (the endonuclease that catalyzes the cleavage of DNA/RNA hybrids) more readily enhancing the gene silencing activity of ASOs [63-65]. On the other hand, one drawback of PS-ONs is that they display low binding affinity to the target mRNA. To improve their binding, the sugar moieties of ASOs have been enhanced by modifying their 2' position, which differentiates the DNA from RNA. In this way, the DNA/RNA hybrids can better mimic RNA/RNA duplexes and have increased affinity [62]; common substitutions include 2'-*O*-Methyl (2'-OMe), 2'-*O*-methoxy ethyl (2'-OMOE) and locked nucleic acids, which have a modification that connects the 2' oxygen with the 4' carbon of the ribose [62, 66-67]. Another category of ASOs are splice switching oligonucleotides (SSOs) which target pre-mRNA and modify their normal splicing pattern [68]. RNA splicing requires precise sequence recognition of the splicesosome machinery for the proper translation of the desired protein after the mRNA has been processed. When SSOs are used, they cause a steric block in the normal protein:RNA or RNA:RNA recognition that would normally occur as part of the splicing process and thus inhibit translation [69]. In addition, SSOs have been commonly used to promote exon skipping

in diseases where mutations arising from specific exons are the cause of an aberrant protein expression that leads to disease, such as Duchenne muscular dystrophy (DMD) where the majority of mutations can be targeted by this approach [70-71].

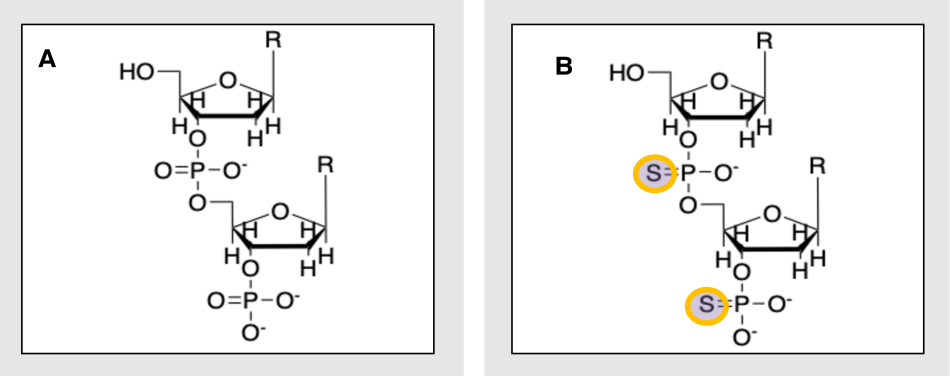

Figure 1.1. Representation of DNA phosphodiester bond (A) compared to DNA phosphorothioate bond, highlighting the sulfur substitution (B).

In contrast to ASOs which may work independently from cellular enzymes, mRNA downregulation via RNAi requires the activity of the RNA-induced silencing complex (RISC) which takes short double stranded RNA (20-30 nucleotides in length), processes it and as a result promotes the cleavage of its cognate target [72]. The mRNA cleavage by RISC starts by dsRNA entering the cell by synthetic methods or by being transcribed from the nucleus. Once in the cytoplasm the dsRNA is processed by the Dicer ribonuclease III, or Dicer for short, which cleaves the dsRNA into shorter duplexes usually of 21-23 nucleotides in length with two 3' overhangs. The short dsRNAs or siRNA then get recognized by RISC which becomes activated. Then the endonuclease argonaute 2 (AGO2) endonuclease which is part of RISC cleaves the siRNA sense strand and allows for the antisense strand to bind to its target mRNA [72]. microRNAs (miRNA), short hairpin RNAs (shRNAs) and siRNA are used for silencing through RISC [72]. A few of the main differences are that miRNA can access multiple targets when compared to siRNA and shRNAs have a stem-loop conformation and need to be expressed in the nucleus usually by transduction with a viral vector [73-74]. After shRNAs are transported out of the nucleus to the cytoplasm, they are then processed into the same

format as siRNA for mRNA silencing, with the difference that shRNAs are expressed with greater stability than siRNAs, as the former are usually introduced directly into the cytoplasm [74]. The miRNAs and siRNAs are both recognized by RISC; however, the way they recognize their target mRNA is different. siRNA needs to be perfectly complementary to its mRNA target to initiate its endonucleolytic cleavage; on the other hand, mRNA has different recognition sites for individual miRNAs allowing partial binding. The partial binding of the miRNA to its target and the recognition of specific sites on the mRNA allow the miRNA to promote gene silencing by other pathways in addition to target degradation including repression of translation by sequestering targets from the translational machinery [75]. However, different studies have suggested that the miRNA mediated protein inhibition is only modest, reporting only about fourfold protein reduction [75]. In more rare cases, miRNA does fully bind its target and then promotes cleavage similarly to siRNA [76]. As miRNAs are involved in the regulation of multiple targets, their disruption can contribute to the development of multiple diseases.

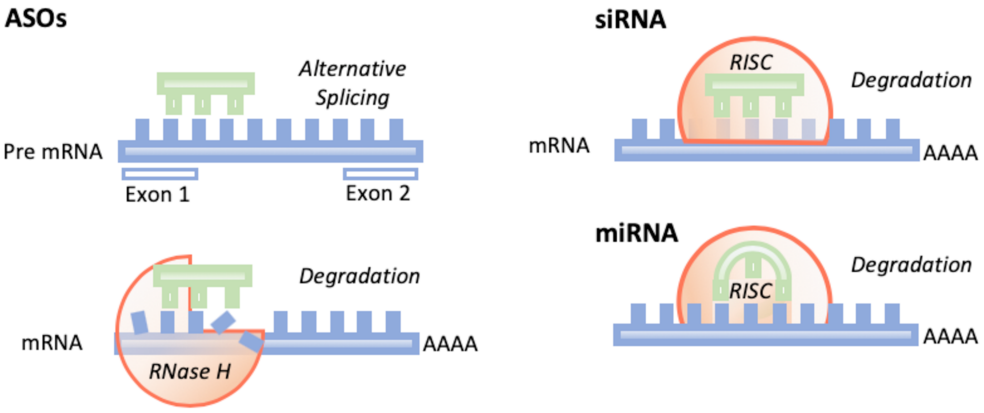

Figure 1.2. Mechanisms of post transcriptional gene silencing including antisense oligonucleotides (ASOs), silencing RNA (siRNA) and microRNA (miRNA).

The miRNAs can also be used as biomarkers of relevant diseases and act as a surrogate for diagnostic purposes [77]. Specifically, miRNAs have been observed to be upregulated or downregulated at various tumour sites acting as oncogenes (oncomiRs) or tumor suppressor genes (tumor suppressor miRNAs) which can be targeted or employed in replacement

therapies [78]. Both siRNA and miRNA are emerging therapeutic agents in the development of targeted cancer treatments and almost one-third of the current ongoing clinical trials using them are directed towards cancer as the clinical application [79]. Figure 1.2. illustrates the different examples discussed that result in post-transcriptional gene silencing.

In this thesis, I will also highlight how molecular therapies or detection methods that focus on nucleic acids offer tremendous versatility and ease in the design process as changing a nucleic acid probe or effector molecule is by nature simpler than changing a small molecule inhibitor, including the production of a monoclonal antibody or a chemical moiety. As we now have vast sequence information of the basis of many diseases, in the future we expect more precise and personalized nucleic acid-based therapies and detection methods to be employed in clinics or in point of care devices.

1.1.3 Nucleic Acid Biomarker Detection Methods

Another area that has benefited from the extensive effort into disease-associated nucleic acid identification/sequencing research has been early biomarker detection in different types of cancer. A biomarker is defined as "any substance, biological structure or process that can be measured in a bio-specimen and may be associated with health-related outcomes" [80]. As genetic variations by themselves can dictate the course or susceptibility of a person to a disease, sequencing and early diagnostics of these changes is of great importance for improving patient prognosis and extensive genome comparison studies have been performed in the past to analyze differences between patients [81]. A milestone even more impressive than devising a therapy to achieve complete remission in patients would be the ability to detect and address early disease onset markers preventing the development of oncogenesis all together. At the same time, biomarker detection methods have as an overall goal to improve patient prognosis by dictating and personalizing therapeutic regimes, predicting

outcomes to therapies and monitoring the progress of the patient once a therapy has been administered (Fig 1.3) [82].

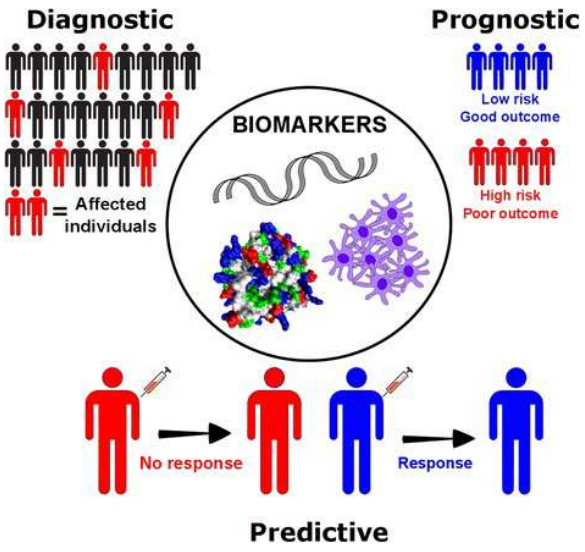

Figure 1.3. Clinical applications of biomarkers including their use for diagnostics, prognostic assessment and predictions of therapeutic outcomes. This image is public domain material, distributed under the terms of the Creative Commons Attribution 4.0 which permits unrestricted use, distribution, and reproduction of the material published. [82. Lim, S.Y. et al., Mol Cancer. 2018; 17: 8. DOI: 10.1186/s12943-018-0757-5].

In the genome, biomarkers are commonly found in the forms of single nucleotide polymorphisms (SNPs), short tandem repeats (STRs), deletions or insertions. More recently circulating tumor-associated DNAs have also been elucidated as a more convenient pool of biomarkers [81-83]. Another change that has also been considered as a biomarker is DNA hypermethylation more commonly in gene promoter regions [83-84]. In the example of acute myeloid leukemia (AML), patients that are screened for molecular abnormalities at diagnosis have a clearer understanding of the prognosis, remission rates, disease-free survival, and risk of relapse [85-87]. Currently, the World Health Organization (WHO) encourages the search for genetic defects during AML diagnosis as differences in mutations could identify different subsets or pathologies of the disease that can be treated specifically with particular drugs and highly improve the outcome of treatment [88-89]. The mutation that is most involved in AML

prognosis is the internal tandem duplication in the *FLT3* gene (FLT3-ITD) [90]. *FLT3* encodes a membrane-bound receptor with a tyrosine kinase domain that when activated relays a cascade of phosphorylation reactions involving the MAP kinase, STAT and AKT/PI3 kinase signal transduction pathways responsible for the regulation of cell differentiation, proliferation, apoptosis and cellular survival [91]. The FLT3-ITD mutation then renders the resultant protein constitutively active dysregulating the former pathways [92]. Approximately 30-40% of AML patients have the FLT3-IDT mutation and this subset of patients is strongly associated with poor patient prognosis and reduced disease-free survival and overall survival [93-95]. Thus, given the specificity of the FLT3-IDT mutation, multiple AML targeted therapeutics have been developed including Midostaurin (Rydapt) which in 2017 became the first targeted therapy for FLT3-positive AML patients after almost 40 years of having no new drugs approved for the treatment of AML [96-99].

1.1.3.1 Interrogation of nucleic acid methylation

Besides specific genetic mutations, other changes in the genome that have been used as important biomarkers in cancer include DNA methylation patterns. DNA methylation is a common and important process for cellular processes including transcriptional regulation; methylation patterns are considered epigenetic marks in the genome which can be heritable [100]. DNA methylation by itself can also induce gene silencing and it is known that in early stages of tumorigenesis DNA methylation can be involved in the downregulation of tumor suppressor genes [101]. Moreover, changes in methylation patterns or dysfunctions are involved in the onset and progression of different types of cancer [100]. In this case, the addition of the extra methyl group happens in the C-5 position of the cytosine (5-mC) ring of the DNA by a DNA methyltransferase which can appear in any position of the genome yet 98% of it happens in CpG islands, genomic regions rich in cytosine and guanine usually found near transcription sites, in somatic cells [102-106]. In Chapter 3, we discuss another type of DNA methylation which is caused by environmental exposure or endogenously, for example

by the S-adenosylmethionine methyl group donor, leading to the formation of methylated DNA bases other than cytosine. In particular, we focus on the detection of the O^6-methylguanine (O^6-meG) adduct which has the greatest mutagenic and carcinogenic potential [107]. The presence of O^6-meG along with other DNA adducts, which are DNA bases that have been covalently modified compared to canonical bases, are also considered biomarkers of the effective dose of exposure to a particular carcinogen [108-109]. Common carcinogens have included polycyclic aromatic hydrocarbons (PAHs), aromatic amines, heterocyclic amines, aflatoxins, nitrosamines, cancer chemotherapeutic agents, styrene, and malondialdehyde and even dietary sources. However, the use of DNA adducts as biomarkers has been limited by their short half-lives in the body as they are usually repaired by different enzymes [110-112]. Nevertheless, their early detection could be very beneficial to understand disease onset and enhance patient care. The most common ways to detect adducts have been radiolabeling, antibodies that are specific to a certain adduct, modified DNA, or structural characterization methods using analytical instrumentations and detection limits are usually of 1 adduct/10^9 nucleotides [113].

1.1.3.2 Detection of DNA methylation

To detect DNA methylation, the gold standard is the bisulfite sequencing technique as current sequencing methods by themselves cannot distinguish between methylated or non-methylated cytosine [114]. Instead, bisulfite treatment converts the cytosine sugar into uracil, but not the methylated cytosine, by deamination and these converted residues are then detected as thymines after PCR-amplification and subsequent sequencing [115]. Now, this method is applied to entire genomes and methylation patterns are commonly assessed. However, this method is still challenging in its own regard as complete conversion is essential and post-sequencing analysis can be difficult as bisulfite treatment might lead to DNA fragmentation or have other effects on its structure [115]. To avoid some of the limitations, it is also common to enrich a sequence of interest before the analysis and specifically isolate

CpG islands [115]. One of the main hallmarks of the bisulfite conversion method paired with sequencing is that it is quantitative, but it also offers sequence specificity of the methylation. Before introducing sequencing analysis, methylation detection methods focused on quantification of the modification and mass spectroscopy was a common analysis which was highly sensitive, yet it required sample hydrolysis. Mass spectroscopy was also paired with liquid chromatography and the sensitivity of the analysis was furthered improved being able to detect down to 0.05% methylated bases in a sample of interest [116]. An advantage that the mass spectrometry analysis offered compared to bisulfite treatment is that poor-quality DNA samples can be analyzed [116-118]. However, just like sequencing techniques these methods require expensive equipment and highly trained personnel to analyze a sample. Novel detection techniques have focused on reducing the number of modification steps or hydrolyzation steps prior to the detection with the development of nanosensors that are able to detect current changes when a methylated base is read through a detector compared to a non-methylated base [119-121]. Microarray chip systems have also been developed that are able to examine the entire genome and analyzed for specific DNA damage using immunoprecipitation [122].

As mentioned above, methylation can also occur in other bases besides cytosine, mainly by chemical exposure or by cellular metabolic pathways and the most common sites for alkylation are the Nitrogen (N) and Oxygen (O) atoms in DNA, as they are nucleophilic targets of alkylating agents which are electrophilic: *N*-methylpurines (N^3 and N^7 of guanine, N^1 and N^3 of adenine), and O^6 of guanine [123]. However, in contrast to 5-mC, these methylated bases are often found in low abundance in the genome [111-112] making their detection and analysis more challenging. Some chemotherapeutic agents act by inducing methylation, including temozolomide and dacarbazine for the treatment of high-grade glioma and melanoma [124]. By inducing DNA methylation, these therapeutic agents can lead to double strand breaks after different repair pathways remove the adduct causing cytotoxicity and reduction of the malignant cells [125]. In this manner, monitoring the methylation

achieved in the target cells can also be useful for tracking the progress of the treatment and its effectiveness. The presence of O^6-meG, for example has been monitored in tissues before by antibody staining and ultra-performance liquid chromatography-tandem mass spectrometry (UPLC-MS/MS), a highly sensitive approach that offers the most accurate quantification analysis of the adduct and allows for dose-response monitoring of treatment in liver and colon tissues with O^6-meG; however, single base resolution in a sequence is not possible through this method [126]. For sequence specific resolution, Sturla and co-workers have created several DNA base surrogates that are able to preferentially bind adducts compared to non-modified bases. In a previous report they were able to engineer a KlenTaq DNA polymerase, which is able to bypass various DNA lesions, to specifically incorporate one of their surrogates across from any O^6-meG or O^6-carboxymethylguanine (O^6-CMG) [127-128]. Their modified polymerase was able to incorporate their synthetic bases across from O^6-meG and/or O^6-CMG with a catalytic advantage of up to 150-fold when compared to guanine. However, the polymerase also incorporated canonical dNTPs across from O^6-meG bypassing the lesion but not across from O^6-CMG and stalling instead without the addition of the surrogate base. Thus, even though their surrogate had specificity towards O^6-meG compared to guanine they needed to develop a more sensitive system to perform the amplification [127].

In Chapter 3, we discuss another method for the sequence-specific detection of O^6-meG by introducing a "second-generation" surrogate from the Sturla group. When it was first introduced, Trantakis et al. designed an approach in which they achieved colorimetric detection of O^6-meG with sequence specificity. To do this, they designed "detection probes" and "discrimination probes" with the surrogate bases and functionalized them to gold nanoparticles (AuNPs) so that when a target was present in solution, the AuNPs would lead to a colorimetric change based on their intrinsic properties as they formed aggregates [129]. More specifically, in their assay they designed 13-nucleotides long targets (13-mer) that had either O^6-meG or guanine in the middle position and their respective complementary probes

containing their surrogates or cytosine. The probes were modified with thiol groups at the 5' position that allowed them to conjugate them to AuNPs. The two probes that allowed for the detection: the detection or discrimination probe were composed of a spacer that separated the complementary sequence from the NPs and the complementary sequence itself. Each probe was functionalized on separate NPs so that in the presence of the target half of it would be bound with the detection probe and the other half with the discriminating probe which contained the surrogate. In this way, the two probes would align in a tail-to-tail order and bring together the AuNPs to which they were attached [129]. AuNPs exhibit surface plasmon resonance allowing them display different colours when they are in suspension (red) compared to when they are aggregated (purple) (Scheme 1). Thus, AuNPs are extensively used for colorimetric detection assays [130-131].

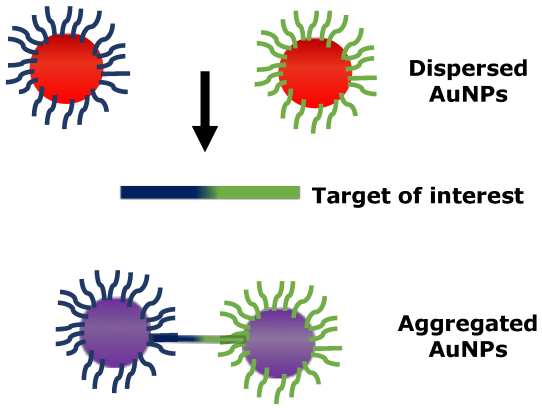

Figure 1.4. Simplified representation of changes in gold nanoparticles when a target of interest is present.

One of their main advantages is that when used for nucleic acid detection like in the example, AuNPs are very sensitive to discriminate between mismatches. The Mirkin group explained their sensitivity on the basis that they require short probes for detection: a mismatch in a short oligonucleotide is more destabilizing than a mismatch in a longer sequence. In addition, AuNPs exhibit a sharp and clear transition in absorbance upon aggregation attributed to the cooperative binding of the duplexes [132-133]. Thus, by using

these properties, Trantakis et al. were able to develop an assay that was able to detect a 1.6% O^6-meG containing target compared to non-specific background DNA or 96 fmol of O^6-meG target in the presence of 6 pmol background DNA [129].

One of the points for improvement in their assay was the analysis of longer sequences, as the sensitivity of the hybridization of the probes is highly dependent on the destabilization due to the mismatch, a longer probe then would be more tolerable to said destabilization. In their article, they also analyzed a 17-mer probe which require some modifications to their AuNP probes; however, they managed to still achieve discrimination [129]. In Chapter 3, we extend the use of the modified surrogate probes into a ligation-mediated detection method which would allow for downstream exponential amplification and thus be able to further enhance the limit of detection of the system and potentially reduce the time needed to complete the detection as AuNP aggregation in their case was performed in 6 hours. The development of synthetic base surrogates that preferentially bind adducts is an exciting field as in the future sequencing methods could be developed that are able to detect these unnatural base pairs and give very precise information about their position, quantity and be able to track changes as treatments are administered.

1.1.4 Personalized Cancer Therapy at the Intersection of Molecular Therapy and Diagnostics

Both efforts to develop nucleic acid-based genetic therapies and detection methods for early genetic biomarkers of oncogenesis have as a main goal to support the advances in personalized medicine and attempt to understand and address the molecular basis of disease on a more personalized patient basis (Fig. 1.5). It is well known that patients with the 'apparent' same type of cancer may not respond in the same way to treatment as the genetic alterations present in their disease could be completely different [134]. Acute Myeloid Leukemia is a case in-point for the need for personalized medicine. As mentioned before, the sequencing work performed in the past has led to the development of specific therapeutics like the ones targeting the *FLT3* mutation. Currently AML includes around 11 categories in

which patients can be grouped into depending on sequencing analysis and cytogenetics and more than 20 subsets when considering cellular differentiation states [135-136]. Recently the Druker group also reported an extensive genomic analysis on 562 AML patients where they examined correlations between gene mutation signatures and drug responses [137]. In their studies, they reported how mutations in certain genes including *TP53* and *KRAS* could lead to broad patterns of drug resistance and analyzed which drugs would be best tolerated when these mutations were present [137]. Moreover, utilizing genetic interrogation to predict drug sensitivity patterns can be highly beneficial in the understanding and treatment of patients like in the example with AML given that hundreds of patients with seemingly the "same" disease can have unique gene mutation patterns that can effectively differentiate them to design treatments that improve their prognosis [137].

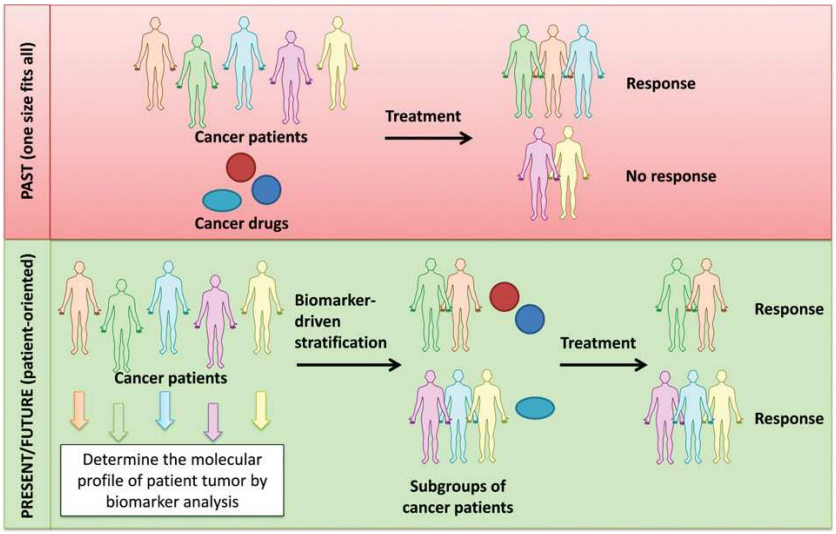

Figure 1.5. Schematic representation of the shift towards personalized cancer treatments driven by the molecular profile of each patient [138].

Published in: Alessia Stornetta; Maike Zimmermann; George D. Cimino; Paul T. Henderson; Shana J. Sturla; Chem. Res. *Toxicol.* 2017, 30, 388-409. DOI: 10.1021/acs.chemrestox.6b00380. Copyright © 2016 American Chemical Society, permissions related to the material excerpted should be directed to the ACS.

Theranostics, as the name implies, is an area of research that combines detection and diagnostic information with therapy with the focus of developing more effective, safer and treatments that can be tracked once administered. In theranostics, the biomarker that is the detected is the same target of therapy and thus the therapeutic agent is only active in its presence [139-140]. Other examples of theranostic developments are nano-delivery systems that are loaded with anti-cancer agents which are able of being tracked once in the tumor and only then receive a signal to delivery their cargo [139-140]. For example, Wu et a., developed a polyethylenimine (PEI) passivated carbon dot nanoparticle with folate on the surface of particles to effectively target their cells of interest which have upregulated folate receptors [141]. Because of the carbon dot component, the particles were able to emit visible light and the PEI allowed them to encapsulate siRNA at the same time as PEI and siRNA can form complexes due to electrostatic interactions. One of the main advantages in the development of these systems is that for *in vivo* studies the nanoparticles can be tracked and their biodistribution assessed at the same time that they deliver their therapeutic outcome [141]. The particles were administered via the intrapulmonary route to access lung cancer cells in mice and showed retention and accumulation at the lung region providing a multifunctional example of the potential of nanomaterials for the administration of precise therapeutic agents [141].

Overall, in the future the most effective and personalized cancer treatment will combine efforts in multidisciplinary fields, using the knowledge obtained from sequencing information, molecular biology synthetic chemistry and biology, nanotechnology, and materials science. In the following 2 chapters, I will combine a few examples from the advances gained in the molecular therapy and diagnostics areas to analyze two projects individually focusing on detection of biomarkers and nucleic acid (siRNA) based therapy.

Chapter 2. RNA Interference for the treatment of Acute Myeloid Leukemia

2.1 Introduction

Acute myeloid leukemia (AML) is the most prevalent myeloid disorder in adults [142], with a mortality rate exceeding 90% for those diagnosed over the age of 65 [143]. AML originates in the hematopoietic stem and progenitor cells and it is characterized by the increase of immature myeloblasts or "blasts" in circulation overcrowding healthy cells and the space in the bone marrow. The abnormal growth and differentiation of the myeloblast cell population is driven by mutations and chromosomal alterations that lead to differentiation blocks which arrest the cells in immature stages of development [144]. Over the years, the molecular features of AML have been extensively characterized and now AML is classified as a highly heterogeneous disease from a molecular and pathological point of view [145-146]. A plethora of mutations may lead to the development of the disease and as a result, multiple molecular targets have been exploited to date. Due to the advances in molecular characterization, the World Health Organization recognizes certain recurrent genetic abnormalities in patients as basis for diagnostics for AML [88]. Being the most prevalent acute leukemia in adults and second most common in children, ongoing research has led to a better understanding about the disease and treatment options [145-149]. However, until the introduction of new targeted therapies last year, treatments had not significantly changed for almost 30 years, and cytotoxic chemotherapy was still the standard [148]. Still, hematopoietic stem cell transplantation (HSCT) best allows for the prevention of AML recurrence and for increased disease-free survival but has the highest treatment-related morbidity and mortality, especially in older patients [148]. Another challenge with current treatment options is that most AML patients become chemo-resistant [150], making new treatment options of urgent need, especially for patients that endure high risks with chemotherapy and who are not eligible for HSCT. In this thesis, we explore the use of RNA interference using polymeric delivery systems to identify molecular targets that can be silenced and inhibit leukemic cell

survival and proliferation. We hypothesize that we can use RNA interference using polymeric carriers to explore potent AML treatments that are less cytotoxic and can become an alternative for patients. With this strategy, we aim to develop versatile therapies that in the future can be tailored in a per-patient basis and can be better translated to clinical applications.

2.1.2 Leukemic cell model

In AML it is thought that a subset of leukemic stem cells (LSCs) are the primary cause of malignancy and disease relapse [150]. LSCs have self-renewal potential and resistance to apoptosis amongst other characteristics that aid in their survival in the face of drug treatment. This resiliency also makes them capable of re-initiating the disease once thought to be eradicated [151]. For this reason, treatment options that can target LSCs are highly sought-after. Thus, in the presented studies we focus on the effects of the silencing therapy on primary cells and KG1/KG1a cell lines, which are relevant cell line models for LSCs [152]. KG1a have been found to keep their self-renewal potential and be inherently resistant to chemotherapy and drug treatments, including daunorubicin (DNR) and mitoxantrone [154] induced apoptosis [154], TNFα [155] and natural killer cell killing [152].

2.1.3 RNA interference

In 1998, RNA interference by double stranded RNA was first discovered in the nematode *Caenorhabditis elegans* by Fire, Mello and colleagues as a method to control gene expression [156]. The process of RNA interference or gene silencing starts with the formation of short interfering RNA (siRNA) by the Dicer enzyme triggering the beginning of the RNAi process. The siRNA is incorporated into the effector nuclease, the RNA-induced silencing complex (RISC) where the sense strand is cleaved by the Argonaute proteins and the antisense strand guides it to cleave mRNA sequences that are complementary [157]. In 2001 the Tuschl group found that RNAi was also present in mammalian cells and multiple biomedical applications for RNAi have been developed ever since [158]. With advances in molecular

genetics and sequencing, RNAi offers a novel and alternative form of targeted therapy for countless malignancies and diseases, including AML [159]. In this project, we make use of post-transcriptional gene silencing by introducing exogenous therapeutic siRNAs, which are introduced directly to the RISC complex, targeting specific genes responsible for the survival, proliferation and self-renewal of leukemic cells and analyze the capacity of mRNA silencing to induce cell death and reduce proliferation. Using siRNA as the therapeutic agent may provide advantages compared to small molecule inhibitors which can lead to some known drawbacks as they have been shown to be costly, toxic, and pose risk of immunogenicity [160]. The main limitation that gene therapy with siRNA would address is that proteins and small molecule drugs cannot access every disease-causing protein or aberrant gene, whereas siRNA can be easily designed to target any disease-causing genetic sequence [161]. Moreover, unlike targeting protein activity alone, typical of conventional drugs, RNAi agents can eradicate the protein all together in the cell.

2.1.4 Synthetic delivery systems

Even though siRNA has great potential for therapeutic applications, some obstacles prevent siRNA to be readily used: it is easily degraded by nucleases and cleared by glomerular filtration, it is also highly hydrophilic and negatively charged making it almost impossible to cross lipophilic cell membranes on its own [162-163]. Thus, the development of delivery systems to bring RNAi into clinics is a high priority and countless materials have been developed to circumvent these obstacles, the most advanced being nanoparticle formulations [164]. Carriers are generally categorized into two main groups: synthetic or viral; however, due to toxicities and undesired immune responses associated with viral vectors as well as their scalability limitations [165], we focused this project on non-viral carriers. Given their ease of synthesis and chemical flexibility with the incorporation of countless functional groups, we used modified polymers to address siRNA delivery [166]. More specifically, we used low molecular weight polyethylenimine (PEI) modified with aliphatic groups, which have shown to

make PEI into an effective delivery system for AML cells [167]. PEI is a cationic polymer that complexes and encapsulates the siRNA by electrostatic interactions forming a polyplex, i.e., polymer-siRNA complex [166]. PEI is also known to have a high proton buffering capacity in the endosome once it has been taken up by the cell, allowing it to be bound to endosome entrapped H^+, increasing the endosomal osmotic pressure that ultimately ruptures the endosomal membrane [168-169]. However, the complete process of endosomal escape with PEI complexes is yet to be fully elucidated.

2.1.5 AML therapy

The therapeutic regimen for AML patients is dictated by the patients' age, cytogenetic or molecular markers and abnormalities, comorbidities, performance status, and antecedent hematologic disorders [170-171]. For most patients, intensive therapy is administered which is divided into two stages: remission induction and consolidation therapy which might include a stem cell transplantation. Depending on the risk of administration and age of the patient, the intensity of the induction therapy is customized. The chemotherapeutic options that are most commonly administered include cytarabine and an anthracycline (daunorubicin or its analog idarubicin), which have both drastically increased disease-free survival in the AML population [172-174]. Advances in therapeutic agents have made AML curable in 35-40% of patients who are 60 years or younger compared to a disease that was incurable about 50 years ago [172]. Even though cytarabine, amongst other nucleoside analogs developed after, and the anthracyclines are essential for the treatment of AML, they have broad mechanisms of action which induce cytotoxicity and comorbidities that targeted treatments wish to overcome. For example, anthracyclines are known to have cardiotoxic effects exposing patients to cardiovascular morbidities and mortalities [175]. Additionally, 15–30% of patients show no response to cytarabine treatment and 30–80% of patients experience relapse [176]. Changes and optimization in the intensity and dosage of cytarabine depending on the patient are common, however, even though high dose cytarabine increases the probability of relapse-

free survival the high dosing induces greater side effects which can be fatal and not recommended for older patients [174, 176]. In more than 30 years until 2017, no new drugs had been approved by the US Food and Drug Administration (FDA) for the treatment of AML [177]. 2017 marked an exciting year for the introduction of four new targeted therapies for the treatment of AML. In April, August and September, novel targeted therapies were introduced: Midostaurin for treating fms-like tyrosine kinase 3 (*FLT3)*-mutated AML, enasidenib for relapsed or refractory AML patients with an isocitrate dehydrogenase-2 (IDH2) mutation, CPX-351 for newly diagnosed therapy-related patients or with myelodysplasia-related changes, and gemtuzumab ozogamicin (GO) for the treatment of adults with newly diagnosed CD33+ AML [177-181]. More recently, in July 2018, ivosidenib also received FDA approval for relapsed or refractory patients with an IDH1 mutation [182]. Midostaurin first emerged as a kinase inhibitor aimed to increase the selectivity of the staurosporine inhibitor of protein kinase C and was investigated to treat solid tumors and in ophthalmologic applications [177, 179-180]. Now, midostaurin is used as a multi-kinase inhibitor for two patient groups with AML: newly diagnosed patients with *FLT3*-mutations, which are found in about one third of patients with AML, and for patients with advanced systemic mastocytosis [180]. Enasidenib, is a small-molecule inhibitor of the IDH2 mutant enzyme that affects 12% of AML patients leading to DNA and histone hypermethylation which prevents cellular differentiation [183]. Similarly, ivosidenib targets the IDH1 mutated gene which is present in 6-10% of patients with AML and also leads to aberrant differentiation [183-184]. In contrast, CPX-351 is not directed to a new target but is a new liposomal formulation of cytarabine and daunorubicin in a 5:1 ratio which showed lower toxicity and increased survival rates compared than the conventional treatment regime [185-186]. GO consists of the anthracycline, calicheamicin, conjugated to an anti-CD33 monoclonal antibody, as CD33 is readily seen in leukemic blasts [178, 181]. GO was first given accelerated approval by the FDA in 2000; however, soon after its introduction different studies could not demonstrate the efficacy of the drug and showed increased toxicities causing its withdrawal in 2010. After treatment

optimization and more advanced studies, however, GO was re-approved in September of 2017 and has become the first antibody-drug conjugate for humans [181].

Table 2.1. Recently approved targeted therapies for acute myeloid leukemia

Name of therapy	Target	Functional Goal
Midostaurin	FLT3	Multi-kinase inhibitor of the FLT3 mutation inducing cytotoxicity
Enasidenib	IDH-2	Inhibit IDH-2 and promote cellular differentiation
CPX-351	-	Dual-drug liposomal formulation of cytarabine and daunorubicin in 5:1 ratio
Gemtuzumab ozogamicin	CD-33	Anti-CD33 monoclonal antibody
Ivosidenib	IDH-1	Inhibit IDH-1 and promote cellular differentiation

Besides the introduction of the new targeted molecules, not too many therapeutic advances have been achieved for the older patient population (older than 65); despite the attainment of ~50% complete remission at some point, these patients still achieve only a 2-year survival rate of 15-20% [187-188]. It is to be noted, however, that hypomethylating agents such as decitabine and azacitidine hold promise as they were shown to have a survival advantage for the older patient population [173,176]. Currently decitabine or low dose cytarabine are used for this population of patients. Another patient population that needs treatment alternatives are the adolescent and young adult patients. Recently, the adolescent and young adult patients, defined by the US National Cancer Institute to be of 15-39 years of age, have also been shown to have higher risk of treatment-related mortality (TRM) than younger patients and could have up to three times more TRM [189-191]. Hence, the development and use of more targeted therapies is highly desired in AML as dosage optimization does not convey the new innovative approaches currently being developed.

2.1.6 RNA interference as a treatment option for AML

In this thesis we focused on gene silencing as a targeted therapeutic approach, able to target specific genetic mutations or genes that get overexpressed in leukemic cells compared to healthy tissues. As the specificity of RNAi therapy is given by the siRNA sequence, using this type of approach can offer alternatives and potent combinations to treat AML other than relying on protein inhibitors or chemotherapeutic agents with broad mechanisms of action. In addition, the development of molecular databases, including disease gene databases, has strengthened the versatility of gene silencing, the ease for its rational design, and encouraged the identification of new targets and delivery systems for the treatment of AML along with many other diseases [192].

The Kiyosawa group in Japan and the Druker group in the United States were amongst the first to test RNAi in AML models. Kiyosawa et al., successfully targeted the Raf-1 kinase and the Bcl-2 oncoprotein as their overexpression had been demonstrated to be involved with chemo-resistance [193]. In their studies, they also compared siRNA to antisense oligodeoxynucleotides (AS-ODN or antisense DNA) and showed how siRNA was more effective at achieving gene silencing. Antisense DNA was the method for mRNA targeting and gene expression downregulation before the use of siRNA and had been previously employed in myeloid leukemia cells as well [193-196]. The second example of one of the first uses of RNAi in AML targeted *FLT3*, which plays an important role in the survival, proliferation and differentiation of blasts, and showed that siRNA treatment in combination with a small molecule inhibitor provided a more effective alternative for treatment than either method alone [196]. These two examples introduced RNAi as a potent and novel alternative for AML therapeutics, yet, also pointed to a few challenges to be overcome to introduce siRNAs to patients, highlighting the delivery challenge. In the case of Kiyosawa, 400 nM of siRNA had to be transfected with a synthetic reagent to achieve the desired level of silencing (Oligofectamine, from Invitrogen). Typically, concentrations in the order of 50-60 nM in

culture are considered viable to be translated to a clinical setting and concentrations of 0.3-0.01 mg/kg have been reported to be effective in mice and non-human primates with synthetic lipidic carriers [197-199]. In the case of the Druker group, the transfection was performed by electroporation, which is not suitable for in vivo delivery. The two examples portrayed chemical and physical transfection methods employed for siRNA delivery over the years, both facing unique challenges. Merkerova et al., compared some of the first chemical transfection methods used for leukemias, in a chronic myeloid leukemia model specifically, (Oligofectamine, Metafectene and siPORT Amine) to electroporation and revealed common concepts when comparing the two: synthetic carriers usually show very low delivery for patient cells and electroporation usually leads to high toxicity even though it has a higher capacity for transfection [197]. Currently, these delivery obstacles are addressed by the formulation of targeted synthetic carriers and materials that have improved chemical and physical transfections. Many approaches have been developed to address in vivo delivery as well as to improve the effectiveness of the siRNA to be delivered avoiding the high concentrations that were necessary before [197-199].

The transfection of hematopoietic cells poses yet another delivery challenge by the nature of these cells being able to grow in suspension (or freely unattached in the body). Compared to most other cells in our bodies, cells in suspension have reduced surface area available to encounter the transfection reagents and thus are more difficult to transfect. Also, compared to attachment-dependent cells, cells in suspension possess morphological differences at their surfaces that will have an effect on surface recognition and penetration [200-201]. Such molecules could act as non-specific receptors for highly cationic siRNA/nanoparticle formulations. To circumvent these challenges, our group has identified lipid-modified PEI as an effective delivery agent for leukemic cells in the past [167].

Here, we analyzed and compared different aliphatic groups that are able to improve the delivery potential of PEI with a focus on leukemic stem cell models and primary cells.

Combining the polymeric carrier with lipid modifications has shown to increase its hydrophobicity and therefore ease its interactions with the hydrophobic cellular membrane allowing for a more effective entry and cargo delivery to the cytoplasm [202-204]. We identified two main modifications that were able to consistently and effectively transfect our cells of interest at specific modification ratios: linoleic acid and lauric acid. We also utilized the modified polymers to downregulate the expression of genes that target the proliferation and apoptosis of the leukemic cells and focused on the BCL2 Like 12 (*BCL2L12*) and Baculoviral IAP Repeat Containing 5 (*BIRC5* or survivin) genes. BCL2L12 is an anti-apoptotic protein that has previously been shown to promote the proliferation of leukemic cells and when downregulated, the engraftment of the cells in mice models is impaired [205]. Thomadaki et al., evaluated the expression level of BCL2L12 of AML patients compared to healthy donors and observed that AML patients had increased expression, which gave them a predisposition for relapse [206]. BCL2L12 overexpression is also observed in chronic lymphocytic leukemia patients and it was predictive of a shorter overall survival [207]. Similarly, to BCL2L12, survivin is also part of an inhibitor of apoptosis family and has been shown to be overexpressed in the majority of cancer cells [208]. Specifically, in AML patients, survivin is an indicator of poor prognosis, associated with drug resistance and it is overexpressed in the leukemic stem cell population compared to the bulk leukemic cells making it a promising target for downregulation [209-210]. Its overexpression has also been shown to have a role in the initiation of AML making it a suitable target in the early stages of treatment [211].

As they have been proven to be potent targets in treatment of AML, we examined the silencing of both *BCL2L12* and *survivin* and showed how it leads to the decrease in proliferation of the KG1 and KG1A leukemic stem cell models at different time points. Also, by optimizing the transfection schedule we were able to enhance the effect of the siRNAs on proliferation over a period of 10 days. In addition, we showed how after selecting the proper modifications for PEI we are also able to target multiple genes including *MAP2K3, CDC 20,*

and *SOD-1* and observe decreased proliferation in the desired cells. The overall studies in this thesis demonstrated the versatility of siRNA delivery with modified PEI to elicit an effect in leukemic cells that are difficult to transfect as well as paramount therapeutic targets for AML, offering an alternative for more precise and targeted treatment options.

2.2 Materials and Methods

2.2.1 Materials

The low molecular weight 0.6, 1.2 and 2.0 kDa PEI, and 25 kDa PEI, linoleyl chloride, stearic acid, lauric acid, caprylic chloride, alpha-linoleyl acid, Hanks' Balanced Salt Solution (HBSS without phenol red), were obtained from Sigma–Aldrich (St. Louis, MO). Lipofectamine™ RNAiMAX was purchased from Invitrogen (Grand Island, NY). Penicillin (1000 U/mL) and streptomycin (10 mg/mL) were purchased from Invitrogen. Fetal bovine serum (FBS) was purchased from VWR (PAA, Ontario, Canada). RPMI Medium 1640 with L-glutamine was purchased from Qiagen (Huntsville, AL) and IMDM medium with GlutaMax from Thermo Fisher (Waltham, MA). Unlabeled, negative control siRNA as well as 6-carboxyfluorescein FAM-labeled siRNA were from IDT (Coralville, IA). The following siRNAs were also from IDT: survivin (Cat. No. HSC.RNAI. N001012271.12.1), BCL2L12 (Cat. No. HSS.RNAI. N001040668.12), CDC20 (Cat. No. HSC.RNAi. N001255.12.1), and SOD-1 (Cat. No. HSC.RNAI.N000454.12). MAP2K3 (Cat. No. AM16708) and RPS6KA5 siRNA (Cat. No. AM51334, unmodified) were obtained from Ambion.

2.2.2 Cell Culture

Suspension cells were cultured with Roswell Park Memorial Institute (RPMI) medium containing 10% FBS (heat inactivated at 56 ^{o}C for 30 min) and 1% penicillin/streptomycin under normal conditions (37 ^{o}C, 5% CO_2 under humidified atmosphere). KG1A and KG1 cell lines were obtained from the American Type Culture Collection (Rockville, MD, USA) and cultured under the same temperature and CO_2 conditions, with Iscove's Modified Dulbecco's Medium (IMDM) and 20% FBS. Primary cells were obtained frozen from the Canadian

Biosample Repository (University of Alberta) and belonged to AML patients with active disease at diagnosis from the University of Alberta Hospital. Experiments involving primary samples were performed within 24 hours of thawing after determining their viability with the Trypan blue staining method. For thawing, cells were transferred dropwise to a tube containing DNase I (100 µg/ml) and incubated for 2-4 minutes, then 5 mL of FBS were added to the DNase/cell mixture dropwise; the suspension was distributed into different 1.5 mL tubes and spun down at 600 rpm for 10 minutes. The supernatant was removed, and cell pellets were resuspended in IMDM supplemented with GlutaMAX (1x, Thermo Fisher Scientific). The medium was also supplemented with 100 ng/ml SCF (Shenandoah 100-04), 50 ng/ml FLT3L (Shenandoah 100-21), 20 ng/ml Il-3 (Shenandoah 100-80), 20 ng/ml G-CSF (Shenandoah 100-72), and 10^{-4} M of β-mercaptoethanol.

2.2.3 Synthesis of lipid modified polyethylenimine carriers

The low molecular weight (0.6, 1.2 or 2.0 kDa) PEI-modified polymers were synthesized in-house by published methods [167, 202, 204, 212-213] by grafting aliphatic lipids via N-acylation at different feed ratios. The modifications tested include linoleic acid (LA), alpha-linolenic acid, stearic acid (St), lauric acid (Lau), and caprylic acid (CA). The nomenclature of the polymers is exemplified as follows: PEI 0.6 CA 4 refers to a 0.6 kDa PEI modified with caprylic acid at a theoretical feed ratio of 4 caprylic acids per PEI.

Table 2.2 Chemical structure of lipid substitutions

Name (Chemical Formula)	**Structure**
Alpha-linolenic acid ($C_{18}H_{30}O_2$)	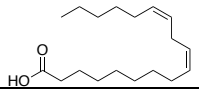
Linolenic acid ($C_{18}H_{32}O_2$)	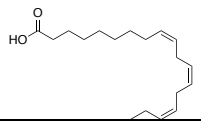
Stearic acid ($CH_3(CH_2)_{16}COOH$)	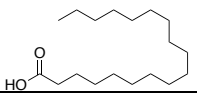

Lauric acid ($C_{12}H_{24}O_2$)	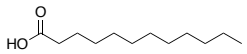
Caprylic acid ($C_8H_{16}O_2$)	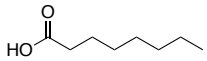

2.2.4 siRNA delivery to suspension cells

To assess the uptake of the complexes, FAM-labeled siRNA was delivered with a variety of modified carriers. Complexes were prepared by combining siRNA and polymers at different siRNA:polymer ratios (1:6, 1:8, 1:10) and incubating them for 30 minutes at room temperature in serum-free medium before introducing them to the cells. With RNAiMAX, a ratio of 1:2 was used as increasing this ratio has shown to be toxic in our previous experience. For delivery experiments, we used an siRNA concentration of 30 nM and approximately 45,000 cells in X-well plates. Cells were analyzed after 24 hours of transfections using flow cytometry. On the day of the analysis, the cells were prepared by collecting them in 1.5 mL Eppendorf tubes, centrifuging them at 14000 rpm for 5 minutes, washing twice with HBSS and fixing them to a final concentration of 1.2% formaldehyde. All transfections were performed in triplicate. To set the baseline for uptake and fluorescence a no treatment control was used, and a gate was set at approximately 1% uptake. For the uptake experiment in Figure 2.1 we utilized a cell line thought to be THP-1; however, after authentication they match the genetic profile of the Raji Burkitt's Lymphoma cell line. These cells were only used to generate Figure 2.1 as a model for suspension cells.

2.2.5 Analysis of cellular proliferation

The CyQUANT cell proliferation kit (Cat. No. C7026) was obtained from Thermo Fisher and the manufacturer's protocol was followed. Briefly, cells were transfected on "day 0" and analyzed after 3 days, 7 days or 10 days after treatment. For Figure 2.4 cells were analyzed on day 15. Cells were also transfected on day 7 for most studies, with the exception of Figure 2.4. On the day of the analysis, cells were lysed using lysis buffer prepared in house (0.5 mol/L 2-amino-2-methylpropan-1-ol and 0.1% Triton-X; pH 10.5). After 1 hour of incubation

in the lysis buffer, we prepared a DNA calibration curve including concentrations of 2.0, 1.0, 0.5, 0.25, 0.125 and 0.0 µg/mL of DNA by preparing serial dilutions of the DNA standards provided by the kit in the lysis buffer and adding 1x dye to the samples in a black 96-microwell plate (Thermo Fisher). The fluorescent intensity values were obtained with the Fluoroskan Ascent plate reader (Thermo Fisher) with λ_{ex}=485 and λ_{em}=530 nm and graphed against the DNA concentrations. The samples were prepared in a similar way by adding 50 µL of the lysed cells and 50 µL of 1x dye to the wells. The DNA concentration from the samples was then obtained using the fluorescent intensity and comparing it to the calibration curve from the standards. The results were plotted as a percentage of DNA by setting the no treatment control as the reference: [DNA from sample] / [DNA from no treatment control] x 100.

2.2.6 Apoptosis Analysis

To analyze the effect of siRNA delivery with the selected polymers, the cells were analyzed for apoptosis using the FITC-Annexin V and Propidium Iodide apoptosis assay kit from BD Biosciences (Cat. No. 556547) following the manufacturer's instructions. Briefly, the suspension cells were collected in 1.5 mL Eppendorf tubes, centrifuged and washed with the apoptosis binding buffer (1X) provided. The cells were then incubated with 2.5 µL of FITC-Annexin V and 2.5 µL of Propidium Iodide in the dark for 15 min at room temperature. Then, cells were analyzed with a flow cytometer within 30 min.

2.2.7 mRNA silencing of suspension cells

To determine the silencing effect of the transfections against specific genes, RT-qPCR was used to assess the level of intracellular mRNA. First, total RNA from the treated cells was extracted using the TRIZOL method according to the instructions from the manufacturer (Invitrogen), extracts were quantified with a NanoVue spectrophotometer (GE Healthcare Life Sciences). For primary cells, cDNA was synthesized using the SuperScript™ VILO™ cDNA Synthesis Kit from Thermo Fisher (Cat. No.11754050). Otherwise, we used the Invitrogen cDNA kit including Master Mix 1 (Oligo dT 0.5 µg/µL, random hexamers and dNTPS 10 mM)

and Master Mix 2 (5x Synthesis Buffer, DTT 0.1M, RNAout 1.8 U/µL and M-MLV RT enzyme). After adding Master Mix 1 to the samples (2000 ng of RNA) they were heated to 65 °C for 5 minutes. After adding Master Mix 2, the samples were heated at 25 °C for 10 min, 37 °C for 50 min and 70 °C for 15 min, then stored at 4 °C. For the quantitative PCR, human β-actin was used as the endogenous control (Forward: 5' GCG AGA AGA TGA CCC AGA T 3' and Reverse: 5' CCA GTG GTA CGG CCA GA3'). 5 µL of master mix containing 2X SYBR Green (FroggaBio Cat. No. BIO-92005, otherwise obtained from the Molecular Biology Facility MBSU at the University of Alberta) and 1.0 µL of each forward and reverse primer (10 µM) per sample were combined and added to 3 µL of cDNA (7.5 ng/µL). The samples were analyzed using a StepOne Real-Time PCR System (Applied Biosystems, Foster City, CA) based on the manufacturer's recommendations (initial denaturation for 10 min at 95 °C, followed by 40 cycles of denaturation at 95 °C for 15 sec and hybridization and elongation at 60 °C for 1 minute) results were then processed using the $2^{-\Delta\Delta CT}$ method and presented as relative quantities normalized to the β-actin housekeeping gene.

Table 2.3 List of Primers for RT-qPCR

BCL2L12 Forward	5' CCC GCC CCT ATG CCC TTT TT 3'
BCL2L12 Reverse	5' ACC GGC CCA GCG TAG AA 3'
CDC20 Forward	5' CGCTATATCCCCCATCGCAG 3'
CDC 20 Reverse	5' GATGTTCCTTCTTGGTGGGC 3'
MAP2K3 Forward	5' CGGCTGCAAGCCCTACAT 3'
MAP2K3 Reverse	5' CAGACGTCGGACTTGACATTGT 3'
RSP6KA5 Forward	5' GAC ACT GCA GCC CAG CAA 3'
RSP6KA5 Reverse	5' CCT AAG CTA CTG AGT CCG AGA ACT G3'
SOD-1 Forward	5' GCA CAC TGG TGG TCC ATG AAA 3'
SOD-1 Reverse	5' TGG GCG ATC CCA ATT ACA CC 3'
Survivin Forward	5' TGAGAACGA GCCAGACTTGG 3'
Survivin Reverse	5' ATGTTCCTCTATGGGGTCGT 3'

2.2.8 Statistical Analysis

All results were plotted as means of 3 replicate samples with standard deviations. Statistical significance was determined by the unpaired Student's *t*-test where an asterisk (*) represents ($p \leq 0.05$) and a plus sign (+) represents ($p \leq 0.1$). The analysis was performed by comparing the control siRNA (csiRNA) sample with the siRNA-treatment samples.

2.3 Results

2.3.1 Selection of carriers for siRNA delivery to AML cells

A library of low molecular weight PEI (0.6, 1.2, and 2.0 kDa) modified polymers including saturated and unsaturated lipid substitutions was analyzed using FAM-siRNA. We plotted the percentage uptake and mean fluorescence intensity in a suspension cell model, Raji Burkitt lymphoma cells (Fig. 2.1), KG1 (Fig. 2.2A) and KG1A cells (Fig. 2.2B) and AML patient cells (Fig. 2.3). RNAiMAX and PEI 25 were used as commercially available delivery reagents for reference. From the library screens, PEI 1.2 Lau 8 (C-12) was consistently the most effective carrier with uptake percentages of up to 95% and the highest fluorescent intensities for both, cell lines and patient samples (Fig. 2.1-2.3). In addition, PEI 1.2 LA 6 (C-18) was selected from our screens as the linoleic acid substitution had been previously shown to be highly effective at delivery of siRNA to AML cells [167, 214] and was effectively used to inhibit cell growth in up to 80% of MDA-MB-231 cells [213]. Also, the linoleic acid substitution was the only unsaturated carbon modification chosen in comparison to the rest of the modifications selected. In the past, we have hypothesized that the increased level of saturation gives the carrier more fluidity which allows it to have better interactions with the cell membrane [167]. Other polymers selected for further experiments in the case of KG1 and KG1A cells were PEI 0.6 Lau 4 (C-12), PEI 1.2 St 4 (C-18) and PEI 2 LA 9 (C-18). For the patient studies, PEI 0.6 St 4 (C-18) was also selected as it consistently delivered FAM-siRNA at higher percentages in 3/5 patients (Fig. 2.3)

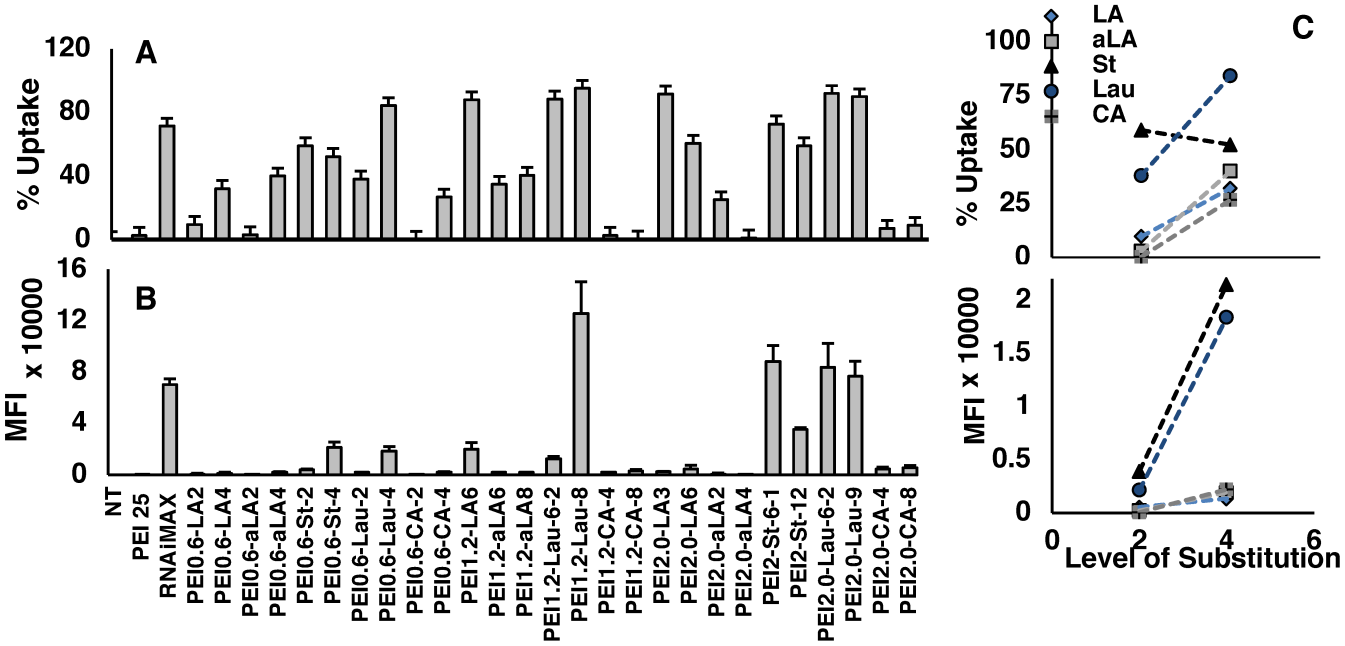

Figure 2.1. siRNA delivery to hematopoietic cell line.

Suspension cell lines were used to model uptake for the leukemia cells. PEI:siRNA ratio used was 10:1 and FAM-siRNA concentration was 30 nM, different molecular weights and substitutions were tested and analyzed for uptake percentage (percentage of cells that are positive for FAM) (A) and mean fluorescence intensity (MFI) (B) of the FAM-positive cells. The effect of increased doubling the substitution number for 0.6 PEI was also observed (C).

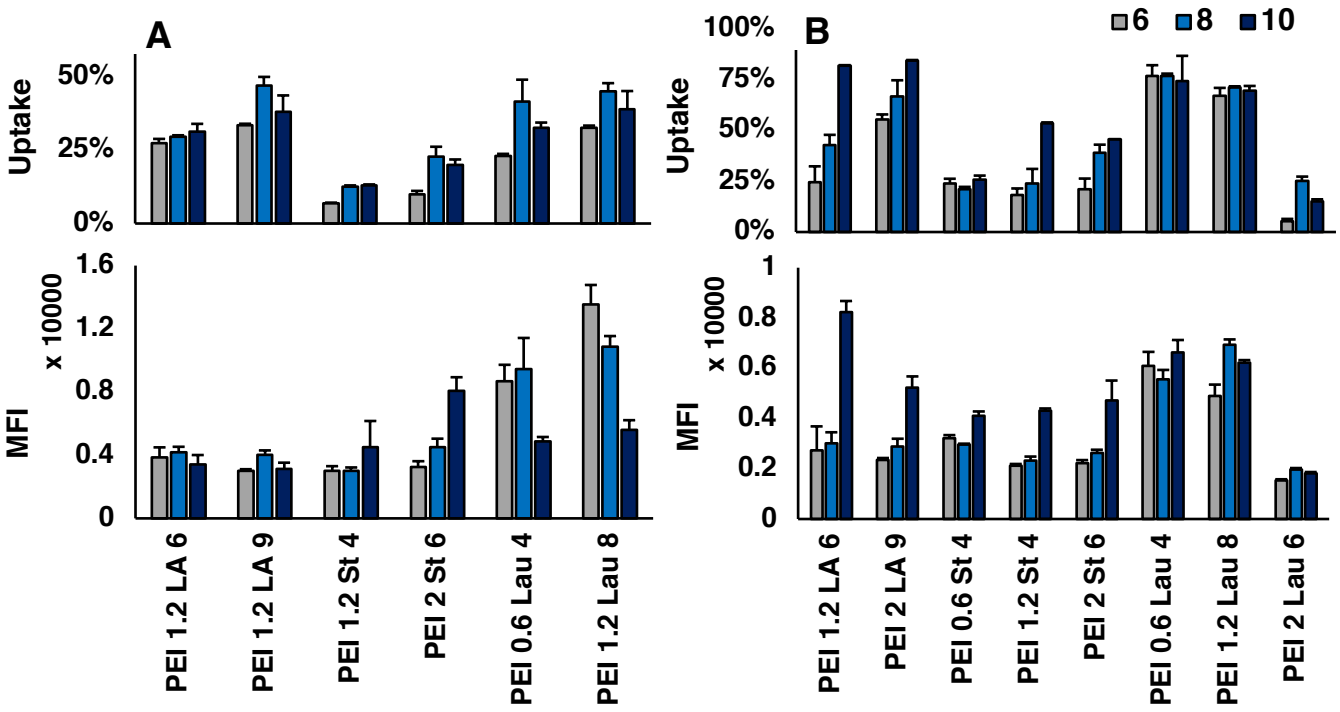

Figure 2.2. siRNA delivery to KG1 (A) and KG1A cells (B).

Delivery was examined with various PEI:siRNA ratios: 6:1, 8:1, and 10:1, FAM-siRNA concentration was 30 nM. Uptake percentage (percentage of cells that are positive for FAM) and mean fluorescence intensity (MFI) from the FAM-siRNA positive cells were assessed.

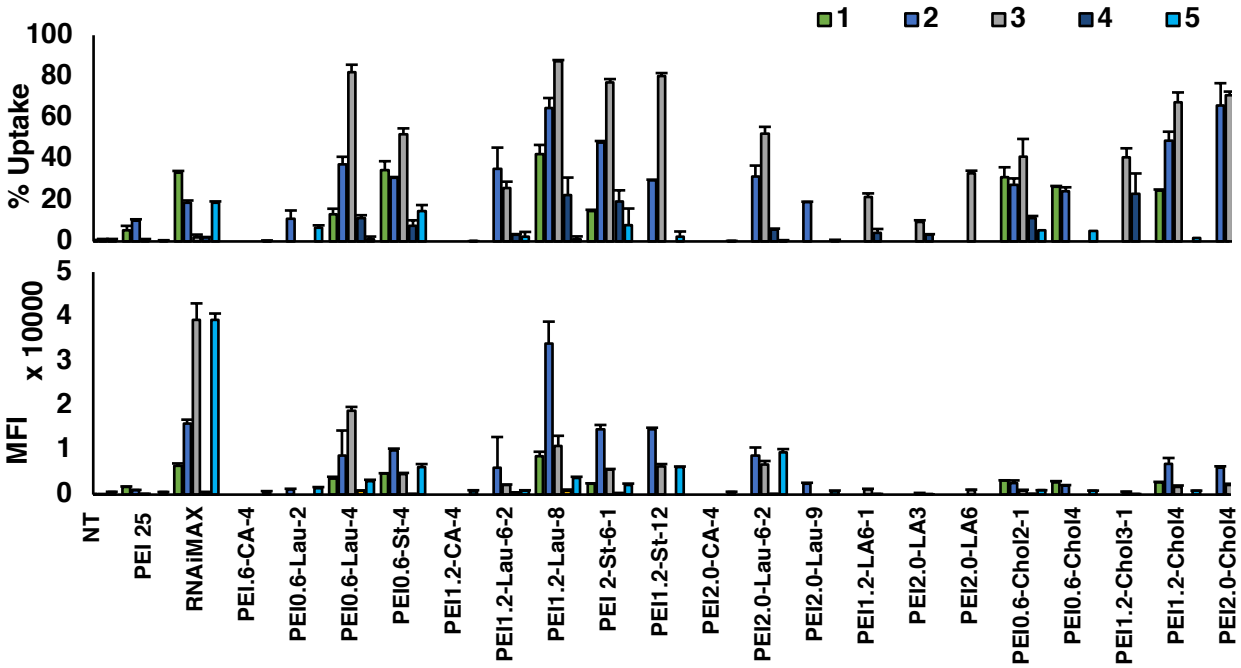

Figure 2.4. siRNA delivery to AML patient cells. 5 patient cell samples (JB 48, 50, 65, 80 and 117) were obtained and tested for the uptake of complexes using FAM-siRNA and a library of polymers. siRNA:PEI ratio was 1:10 and siRNA concentration 30 nM, uptake percentage (percentage of cells that are positive for FAM) and mean fluorescence intensity (MFI) from the FAM-siRNA positive cells were assessed.

2.3.2 Exploring growth inhibition in leukemic cells by siRNA delivery

To study the effect of siRNA delivery on AML cells over time, we first examined the growth inhibition in a hematopoietic cell model, Raji Burkitt lymphoma cells (Fig. 2.4). Different siRNAs were delivered on day 0 and cellular proliferation was assayed on days 7, 10 and 15 after the delivery, changing the media each time the cells were analyzed. The time points were selected to explore the outcomes of the delivery after longer periods of time than what we had previously reported [214-215]. From this analysis, we observed that the maximum cell growth inhibition was of 35% targeting CDC 20 with RNAiMAX on day 7. By day 15 the effect of siRNA on cell proliferation was lost in all the targets except in the case of survivin which retained about 12% of inhibition with both RNAiMAX and PEI 1.2 LA 6. In order to better analyze the differences between the targets, we repeated the experiment analyzing

the cells on day 3, 7, and 10. At this time, we also treated the cells for a second time on day 7 (Fig. 2.4). For most cases, we did not observe any growth inhibition on day 3 but instead noticed that some targets were promoting cell proliferation, in particular NTN1-1 and STAT3 doubled the DNA content extracted (Fig 2.4). The only inhibition that was observed on day 3 was of ~14% by targeting BCL2L12 with PEI 1.2 LA 6. However, after the second siRNA treatment on day 7 we are able to report up to 80% of growth inhibition by targeting RPS6K5A (RPS) with PEI 1.2 LA 6. By delivering two doses of siRNA on days 0 and 7, most of the targets were able to reduce cellular proliferation by at least 40% with PEI 1.2 LA 6 with the exceptions of CD29 and PIK3CB. With these conditions we also observed that the PEI 1.2 LA 6 carrier was more effective at inhibiting growth on day 10 than RNAiMAX.

We used the same transfection time frames and delivered different siRNAs to KG1A cells on days 0 and 7 (Fig 2.5). Six carriers were selected including RNAiMAX, PEI 1.2 LA 6, PEI 2 LA 9, PEI 1.2 St 4, PEI 1.2 Lau 4 and PEI 1.2 Lau 8. PEI 2 LA 9 gave the most increased proliferation with CDC 20, SOD-1 and survivin and thus was not used for further studies. Similarly, increased proliferation was observed by targeting RPS with RNAiMAX, PEI 1.2 LA 6, PEI 1.2 St 4, and PEI 1.2 Lau 8 (Fig 2.5).

In terms of growth inhibition, PEI 1.2 St 4 did not show any significant effect and was also not used for further studies. For KG1A cells, PEI 1.2 Lau 8 was the most successful carrier at significantly inhibiting cell growth with 4 out of 6 targets on day 10. On this day, the most inhibition was seen after targeting MAP2K3 with 5/6 carriers, SOD-1 with 4/6 carriers and BCL2L12 with 3 out of 6 carriers (Fig 2.5).

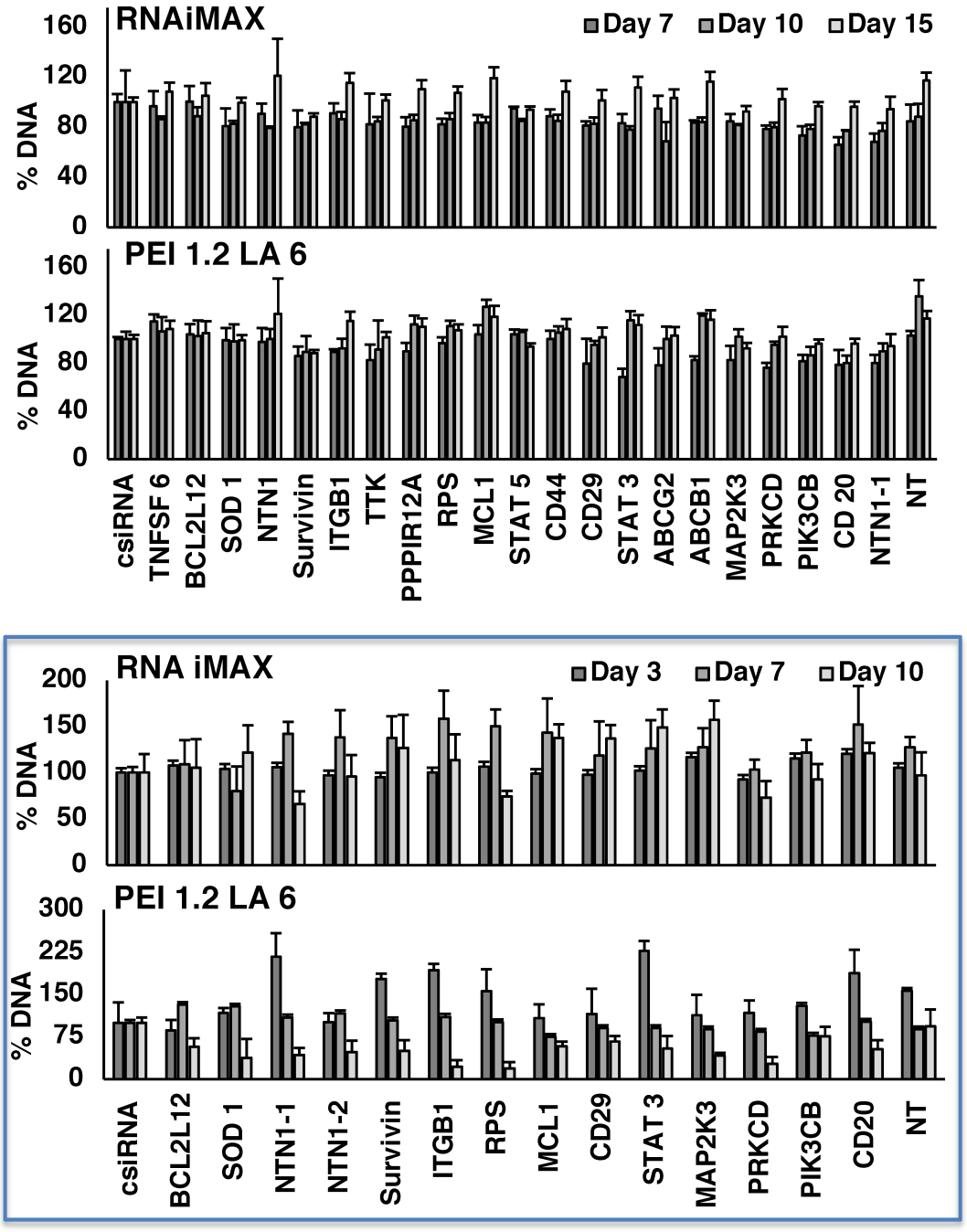

Figure 2.4. Long term and dosage effect on proliferation of siRNA treatment in a hematopoietic cell line model.

The effects of different siRNAs on DNA content were observed on days 7, 10 and 15 after a single transfection (on day 0) using a library of targets. We also analyzed the effects on day 3, 7, and 10 after transfection on day 0 and a second dose on day 7 (in box). siRNA concentration was 50 nM and PEI:siRNA used was 1:10. Percent DNA content is expressed compared to the control siRNA (csiRNA) sample.

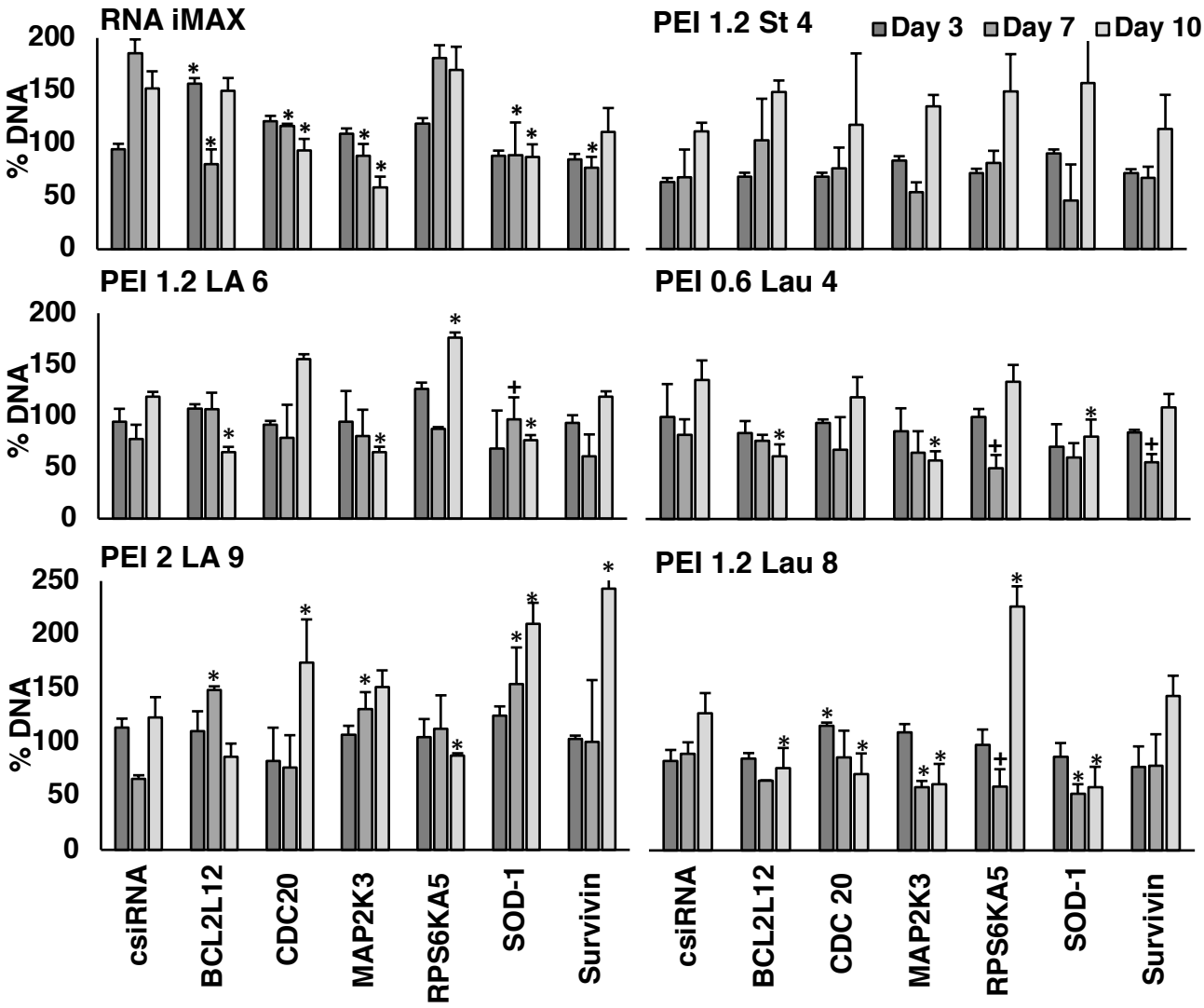

Figure 2.5. Effect of siRNA treatment on the proliferation of KG1A cells.

The effects of different siRNAs on DNA content were analyzed on days 3, 7 and 10 after siRNA treatments on days 0 and 7. By utilizing different transfection reagents, we aimed to select the most effective delivery vehicle to elicit an effect on the cells. Percent DNA is expressed compared to the no treatment control. siRNA:PEI ratio utilized was 10 and siRNA concentration was 50 nM.

We further analyzed the effect of siRNA delivery on KG1 cells using three carriers, RNAiMAX, PEI 1.2 LA 6 and PEI 1.2 Lau 8. For KG1 cells, the control siRNA impaired cellular proliferation on day 3 and more cell proliferation was observed with different targets and the three carriers instead of growth inhibition. On day 10, no growth inhibition was observed with any carrier, except when survivin was used with PEI 1.2 LA 6. Significant growth inhibition was also observed with PEI 1.2 Lau 8 on day 7 targeting MAP2K3 (Fig. 2.6).

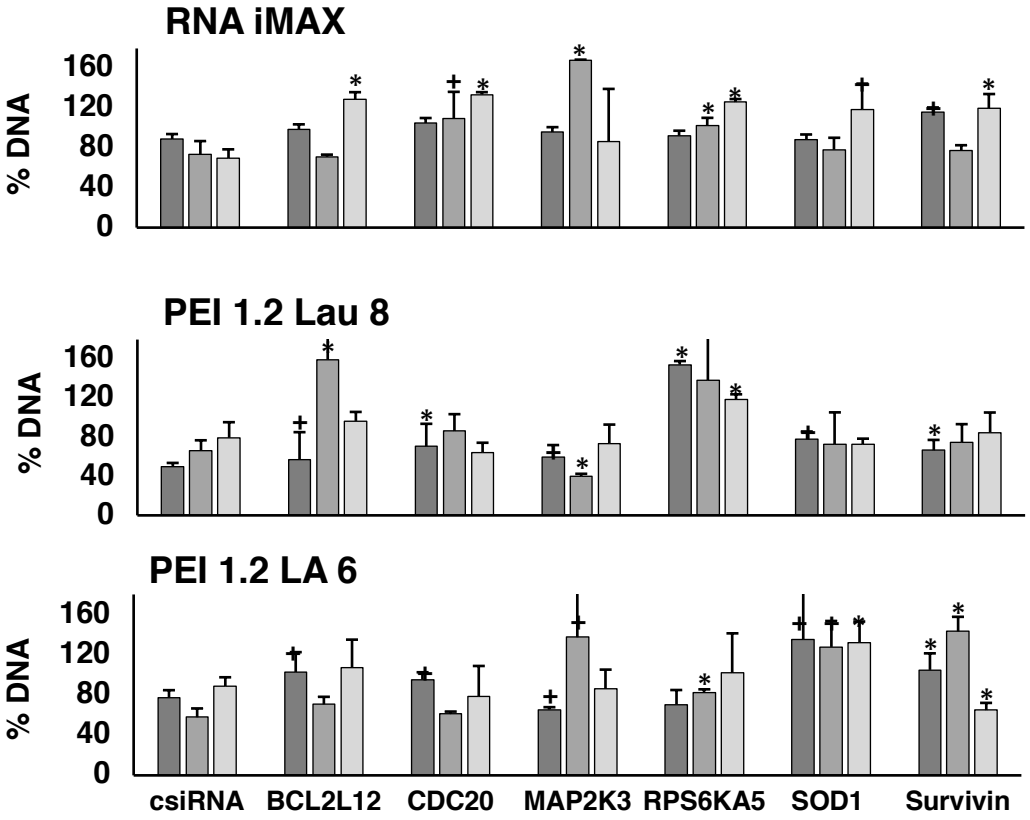

Figure 2.9. Effect of siRNA treatment on the proliferation of KG1 cells.

Effects of different siRNAs on DNA content were analyzed on days 3, 7 and 10 after siRNA treatment on days 0 and 7. Percent DNA is expressed compared to the no treatment control. siRNA:PEI ratio utilized was 10 and siRNA concentration was 50 nM.

As we observed some non-specific effects by the use of siRNA:PEI ratio 1:10 in both KG1A and KG1 cells, we decided to examine lower ratio with complexes (i.e., with a lower polymer amount that may cause non-specific toxicity) and employed ratio 1:6 focusing on two targets only, BCL2L12 and survivin (Fig. 2.7). In KG1 cells we had observed growth inhibition with the control siRNA at ratio 1:10, and by lowering the ratio to 1:6 we were able to mitigate these changes with PEI 1.2 LA 6, yet PEI 1.2 Lau8 still lowered the percentage of DNA recovered by about 30% on day 10. Nonetheless, for KG1 cells PEI 1.2 Lau 8 at the 1:6 ratio was the most effective carrier targeting BCL2L12 and survivin on day 7 by lowering proliferation by ~17% and ~10%, respectively. In KG1A cells, BCL2L12 siRNA resulted in decreased growth on day 10 with PEI 1.2 Lau 8 and PEI 0.6 Lau 4 by ~30%. Survivin decreased growth on day 10 with PEI 1.2 LA 6, yet this was only by about 10%. In contrast, we must note that survivin was more effectively targeted on day 3 with the three carriers used giving ~20% growth inhibition on average (Fig 2.7).

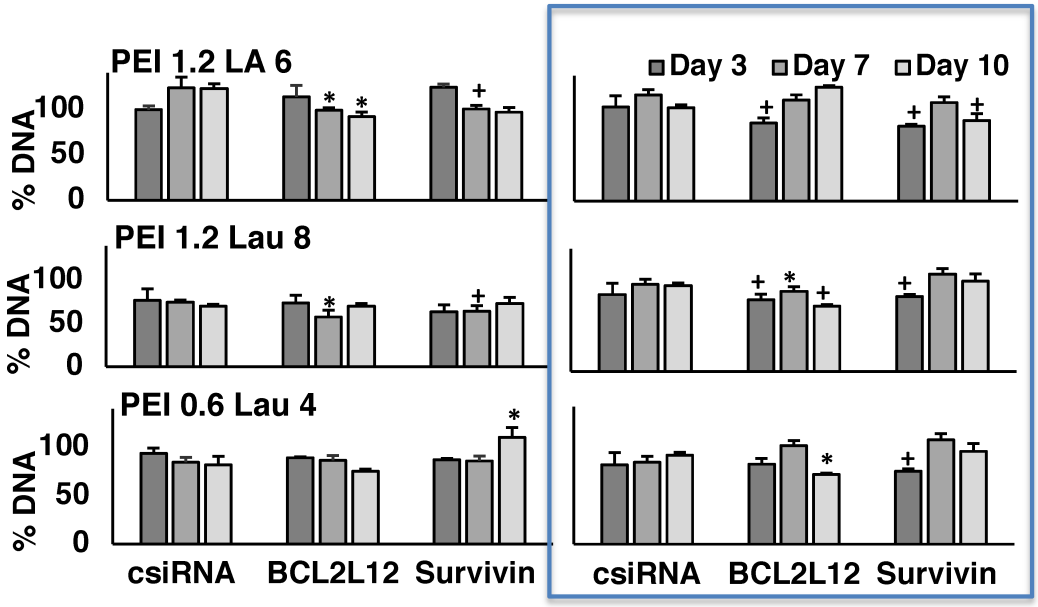

Figure 2.7. Effect of siRNA treatment on the proliferation of KG1A and KG1 cells.

The effects of different siRNAs on DNA content were analyzed on days 3, 7 and 10 after siRNA treatment on days 0 and 7 on KG1A (in box) and KG1 cells. Percent DNA is expressed compared to the no treatment control. siRNA:PEI ratio utilized was 1:6 and siRNA concentration was 50 nM.

2.3.3 mRNA silencing in KG1A and KG1 cells

We used RT-qPCR to assess the effect of siRNA delivery at the mRNA level. For KG1A cells we analyzed three targets: BCL2L12, survivin, and MAP2K3 at siRNA:PEI ratios of 1:10 and 1:6. At ratio 1:10, only PEI 1.2 Lau 8 effectively silenced BCL2L12 and survivin, yet the control siRNA elevated the transcript levels above the non-treatment sample (Fig. 2.8). At ratio 1:6, BCL2L12 was significantly silenced with all carriers, MAP2K3 was silenced with PEI 1.2 LA 6 and survivin with PEI 1.2 LA 6 and Lau 8 (Fig. 2.8). In contrast, MAP2K3 was upregulated with PEI 0.6 Lau 4 at ratio 1:6 and at ratio 1:10 with PEI 1.2 LA 6 and Lau 8.

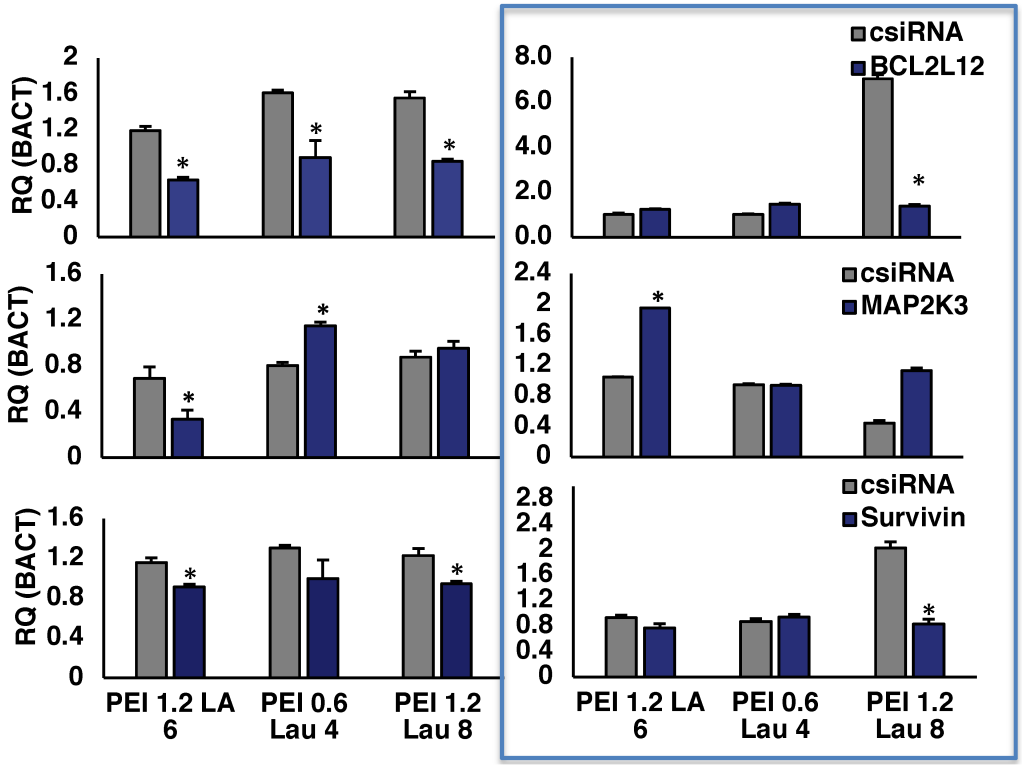

Figure 2.8. Silencing of BCL2L12, MAP2K3 and Survivin in KG1A cells at siRNA:PEI ratios of 6:1 and 10:1.

Silencing was assessed after 3 days of treatment by RT-qPCR using β-actin as the housekeeping gene reference. In addition, the effect of polymer concentration was assessed by analyzing siRNA:PEI ratios of 6:1 and 10:1 (in box) and the siRNA concentration was kept constant at 60 nM.

As most of the silencing effect was observed with ratio 6:1, we targeted BCL2L12 and survivin in KG1 cells (Fig. 2.9). For these cells, PEI 1.2 LA 6 was the most effective at silencing both BCL2L12 and survivin. PEI 0.6 Lau 4 also achieved some silencing with both targets, but the effect was not as pronounced, and PEI 1.2 Lau 8 did not have any effect on the mRNA transcripts (Fig. 2.9), even though at this ratio it had been the most effective at siRNA delivery for KG1 cells (Fig. 2.3).

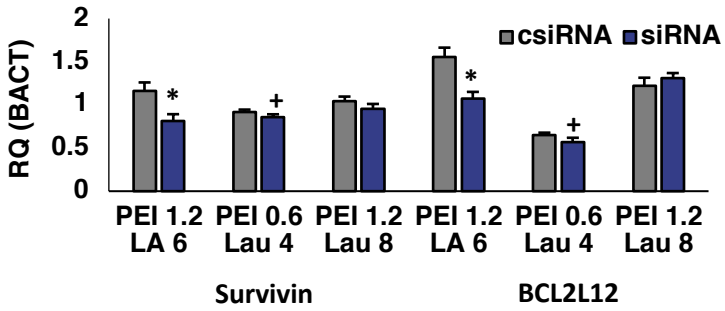

Figure 2.9. Silencing of BCL2L12 and Survivin in KG1 cells at siRNA:PEI ratio of 6:1. Silencing was assessed after 3 days of treatment by RT-qPCR using β-actin as the housekeeping reference gene. The siRNA concentration was 60 nM.

2.3.4 Apoptosis in KG1A cells

We then examined the levels of apoptosis and cell death in KG1A cells with ratio 1:6 as they demonstrated the most effects in proliferation and silencing with the selected carriers. Early apoptosis was achieved with PEI 1.2 LA 6 with the three chosen targets, BCL2L12, MAP2K3 and survivin. PEI 0.6 Lau 4 also allowed for the upregulation of early apoptosis when targeting survivin. Late apoptosis or cellular death was promoted by targeting MAP2K3 with PEI 1.2 Lau 8 (Fig. 2.10).

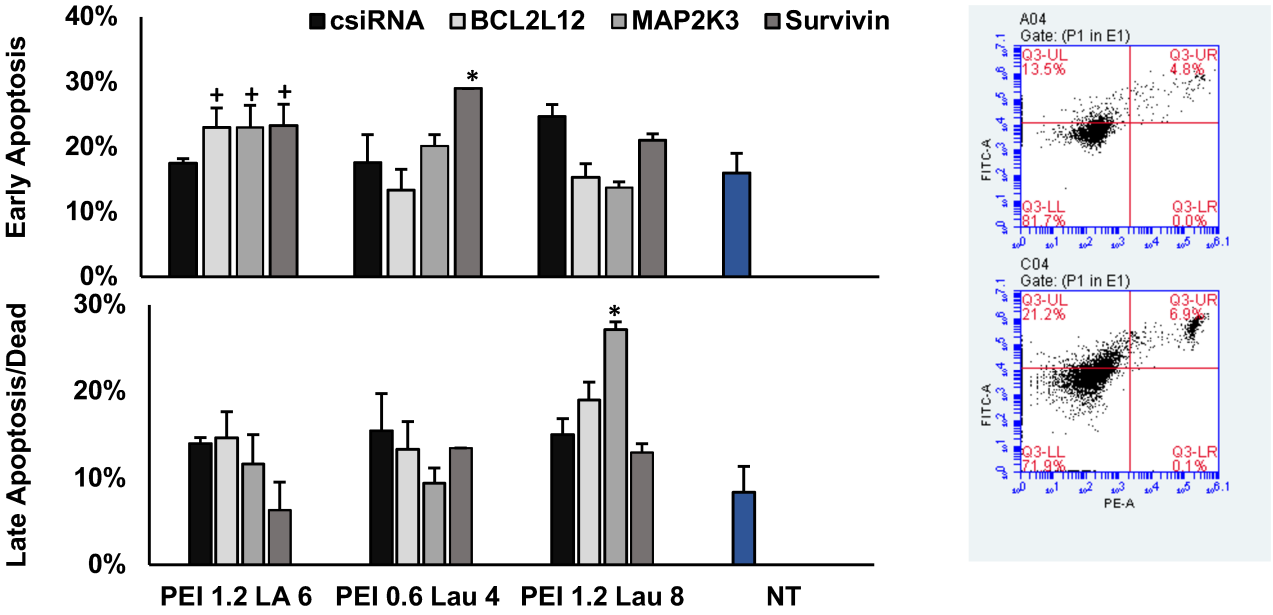

Figure 2.10. KG1A cell death after targeting BCL2L12, MAP2K3 and survivin with PEI 1.2 LA 6, PEI 0.6 Lau 4, and PEI 1.2 Lau 8.

The annexin V and PI stain were used to determine the percentage of early apoptotic cells (annexin V positive PI negative) or late apoptotic/dead cells (annexin V positive PI positive). The analysis was performed after 3 days of treatment. The boxed graph shows a representation of the no treatment sample (upper box) compared to a treatment sample (bottom box) and how there is a shift in the apoptotic cell population after the treatment.

2.3.5 mRNA silencing in AML patient cells

A total of four patient samples were obtained and analyzed for silencing using the three top carriers from the uptake study (Fig. 2.3). We reported the ratios of siRNA/csiRNA and csiRNA/NT to illustrate if there were significant differences in mRNA levels with the conditions we examined analyzing BCL2L12, CDC 20, survivin and RPS. PEI 1.2 LA 6 was able to significantly reduce the mRNA transcript level of BCL2L12 in one patient. PEI 0.6 St 4 also significantly reduced the mRNA content in one patient as well. We also observed that survivin

was downregulated consistently in more patients using PEI 1.2 Lau 8, yet this reduction was not significant (Fig .2.11).

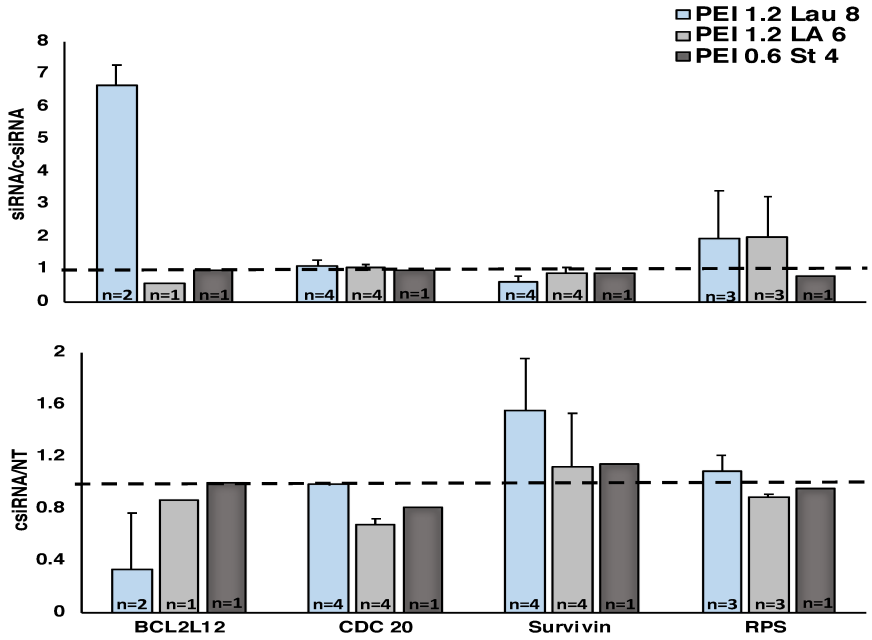

Figure 2.11. Silencing of BCL2L12, CDC20, Survivin and RPS6K5A using modified PEI carriers in AML patient samples.

A total of 4 patient cell samples were obtained and tested for silencing using PEI 1.2 Lau 8, PEI 1.2 LA 6, and PEI 1.2 St 4 polymers. The siRNA:polymer ratio used was 1:10 and the siRNA concentration was 60 nM. The results are reported as a ratio of silencing: siRNA/csiRNA combining the n=x number of patient samples tested for the specified target. Below we also plot the ratio of csiRNA/NT to examine the effect of csiRNA on the mRNA levels of the given targets.

2.4 Discussion

One of the main challenges with the current AML therapies is that about 10-40% of patients still do not achieve complete remission, meaning that their blast count does not go below 5% after 1-2 cycles of induction therapy and are therefore categorized as resistant or primary refractory [216-217]. Most of these patients are then advised to enroll in a clinical trial and reduce the disease burden before considering an HSCT if they are eligible for one [217]. Over the years, LSCs have been identified as the main culprit for the progression of leukemia as well as for patient relapse. Their self-renewal capacity, differentiation potential

and effector functions allow LSCs to maintain and regulate the disease leading to resistance to chemotherapy and other targeted therapies [152, 218]. As a result, focusing on LSCs is one of the most promising approaches to tackle chemo-resistance and decrease disease morbidity. For this reason, we have focused these studies on the identification of siRNA delivery systems to KG1 and KG1A stem cell models for AML that can also be translated for use in primary patient samples.

We demonstrated that PEI 1.2 Lau 8 was the most effective carrier for all cell lines studied as well as for primary samples (Fig. 2.1-2.3). This is promising as were able to identify that a chemical modification able to achieve delivery in up to 80% of KG1A cells also achieved delivery of up to 80% in one of the patient samples and an elevated MFI (Fig. 2.2-2.3). Lauric acid is a medium-length saturated fatty acid containing 12 carbons which is naturally sourced and metabolized [219]. In addition, this fatty acid has been found to have antiproliferative and pro-apoptotic effects in some cancer cells [220]. The use of lipids for drug delivery specifically in nano-carrier formulations is extremely popular as they increase membrane interactions and permeability promoting high levels of cellular uptake, with liposome delivery systems being the first to be translated into clinical applications [221]. In our case, we use lipids to increase the surface recognition and interactions between the PEI polymer and the cellular membrane [214-215, 222]. However, when using lipid formulations, we must also consider that lipids are highly involved in cell signaling pathways, gene expression regulation, apoptosis, metabolism, inflammation amongst other essential cellular functions [223-225]. Therefore, it is expected to observe some non-specific effects when studying lipid-based carriers as their interactions with the cellular membrane might trigger signaling cascades that might be independent from the target of interest. Such effects might be over-expressed in in vitro studies as the effective concentration of each carrier available to interact with each cell would be significantly greater than its bioavailability when used in vivo. In some of our studies, we noticed that our control treatments promoted cellular proliferation (Fig. 2.5) or led to an increase in transcript levels in BCL2L12 and survivin specially when the higher ratio of 1:10

of siRNA:PEI was used with control siRNA (Fig. 2.8). These effects might be caused by increased signaling from the lipids themselves, but also by endocytotic effects on proliferation which have been observed before via the Wnt/β-catenin pathway [226-227]. Also, we noted that the effects were more prominent with the carriers that had higher levels of lipid substitutions: PEI 2 LA 9 and PEI 1.2 Lau 8, and were decreased when the ratio was lowered to 1:6 which is why we hypothesize that the lipids themselves might be triggering cellular signals that we have yet to explore. Another reason for the non-specific effects observed could be from the siRNAs as these could arise when siRNA interacts with specific parts of the mRNA transcripts or with non-specific sequences, yet these can be reduced with ease by designing different siRNA sequences or by chemically modifying the siRNA [228-230]. Hence, even though some off-target effects in proliferation and mRNA transcript levels are observed there are various alternatives to mitigate these outcomes that could be explored in future work.

Focusing on the specific effects on proliferation after targeting genes involved in cell proliferation, apoptosis, and differentiation we demonstrated how when comparing growth inhibition on days 7, 10 and 15, the maximum effects are seen on day 7 as expected since the effects of siRNA are known to be transient, especially as cells proliferate (Fig. 2.4). However, proliferation can be successfully inhibited by transfecting the cells on day 0 and reinforcing the effects on day 7 as on this day we could still see some of the inhibition by a single transfection. By delivering siRNA twice, we were able to decrease growth inhibition by up to 80% and by at least 40% with all targets used (Fig. 2.4). We applied the same treatment schedule to KG1 and KG1A cells which from our experience are less responsive to treatment and more difficult to transfect. For KG1A cells, we were able to achieve up to 45% growth inhibition when targeting MAP2K3 and were able to decrease proliferation of all targets tested with different carriers by the 10 with the exception of survivin (Fig. 2.5). When testing the same transfection schedule on KG1 cells, we observed that they were less responsive, yet this was expected as they also had less cellular uptake of the particles that we tested than KG1A (Fig. 2.2, 2.6). Most of the effects were achieved on day 3 and only by targeting survivin

with PEI 1.2 LA 6 were we able to obtain about 40% decreased proliferation by day 10. In order to enhance these effects, we can design different carriers that are more specific and effective when transfecting KG1 cells. In this instance, we noticed how even though the carriers that we chose are able to effectively transfect suspension cells, they still hold high specificity and their effectiveness changes even when comparing two very similar cells that share the same origin. The specificity given by the simple design of the particles, without being targeted to any receptor or antigen, highlights the importance of the lipid membrane interactions themselves when considering a drug delivery vehicle.

To reduce some of the non-specific effects, we lowered the siRNA:PEI ratio to 1:6 and noticed that the KG1A cells still were more responsive to the transfections than the KG1 cells even though the effects were not as pronounced as when using the higher polymer ratio (Fig. 2.7). For both cells, PEI 1.2 Lau 8 was still the most effective carrier and both BCL2L12 and survivin were able to inhibit proliferation with effects lasting up to 10 days in KG1A cells (Fig 2.7).

To examine the outcomes of siRNA targeting at the molecular level, we analyzed the mRNA transcript levels using RT-qPCR. We tested ratios 1:10 and 1:6 in KG1A cells and noticed how ratio 1:6 was more effective at downregulating the mRNA levels on day 3 even though these effects were not translated to more effective proliferation inhibition (Fig. 2.8). We were able to achieve up to 40% reduction in mRNA content with the ratio of 1:6 when comparing the control siRNA to the treatment. With the ratio of 1:10, PEI 1.2 Lau 8 and the control siRNA showed non-specific transcript upregulation and, in this manner, using the effector siRNA targeting survivin, showed up to 500% reduction in mRNA content; however, this result is an artifact of the non-specific effect. The 1:6 ratio was also tested in KG1 cells and the most transcript suppression was achieved with using PEI 1.2 LA 6 and targeting survivin obtaining about 20% downregulation (Fig. 2.9). In our experience we have observed that when the lower siRNA:PEI ratio is used the dissociation of the siRNA from the carrier happens more readily and this could lead to more effective mRNA downregulation.

As we were examining targets that are highly involved in the regulation of apoptosis and proliferation, we looked into Annexin V staining and observed how PEI 1.2 LA 6 was the most effective carrier to increase apoptosis with all the targets tested. However, survivin with PEI 0.6 Lau 4 increased early apoptosis the most and MAP2K3 with PEI 1.2 Lau 8 was the most effective at promoting cellular death. With this assay we observe that each target behaves differently depending on the carrier that is used to deliver it again highlighting the importance of analyzing the effects and interactions that the carriers themselves might have which contribute to cellular outcomes. For a more thorough analysis on how silencing influences apoptosis, more time points can also be studied to get a better understanding of when the peak of the effect is and when it settles down. In this way we can also design a treatment regime that allows for reinforcement of the effect as we optimized for proliferation.

Finally, we analyzed the silencing effect on primary cells using the three top carriers and BCL2L12, CDC 20, survivin and RPS. By comparing the ratio of mRNA with the use of the control siRNA and the effector siRNAs we observed that with two patients we were able to obtain silencing with BCL2L12 and RPS. Also, we noticed how PEI 1.2 Lau 8 had the most effect on 4 patients when survivin was targeted. For this study the higher 1:10 ratio was used on the samples and now we understand that the lower ratio of 1:6 might be more effective to achieve silencing. Nonetheless, we must always keep the specific goals we aim to achieve when utilizing RNAi as in the example using KG1A the 1:6 ratio achieved more silencing, yet the 1:10 ratio was more effective at inhibiting cellular growth.

This chapter highlights the versatility and inherent specificity of the polymeric carriers after they are modified with aliphatic groups. By using modified PEI we have access to countless chemical modifications that in the future can be screened for individual patient samples to create personalized delivery systems. When an effective carrier is established, we can then design and optimize the siRNA personalizing it given the molecular information about the patients' transcriptome and genome making this system extremely potent to achieve

targeted therapy. For the use of RNAi in clinics we propose that most of its utility can be from providing an alternative to patients who do not respond to induction therapy or that are older and more vulnerable suffering from co-morbidities and previous malignancies. RNAi could be paired up with the current targeted therapies and chemotherapeutic reagents and allow for the use of lower dosage of the broad-mechanism drugs.

Chapter 3. Molecular targeting to detect of O^6-methylguanine (O^6-meG) using synthetic DNA surrogates

3.1. Background

3.1.2 O^6-Methylguanine (O^6-meG)

Exposure of DNA to chemicals and environmental carcinogens can result in the formation of DNA adducts, or covalently modified DNA bases [231]. However, these modified DNA bases do not remain in the genome for long as they are removed by specific DNA repair proteins. Thus, their presence can reflect exposure levels or aberrant metabolic pathways [232]. Of all known DNA adducts, O^6-methylguanine (O^6-meG) has the greatest mutagenic and carcinogenic potential [233]. Exposure to *N*-nitrosamines from materials such as rubber, tobacco, or dietary sources such as grilled foods and dairy [233-234], chemotherapeutic alkylating agents, cosmetics, hydraulic fluids [234-236], and endogenous methylation [236] can all lead to the formation of O^6-meG. The main mechanism of O^6-meG carcinogenic and cytotoxic effects are during replication; O^6-meG:thymine base pairs can form as readily as O^6-meG:cytosine leading to a G:C to A:T transition mutation during replication. However, such mutations are usually prevented as the O^6-methylguanine-DNA methyltransferase (MGMT) removes the methyl group from the O^6-meG transferring it to an internal cysteine residue of itself [233].

Besides causing mutations during replication, O^6-meG can also cause cytotoxicity by failure of the post-replication mismatch repair pathway to fix the aberrant base pair causing a double strand break in the DNA, a pathway that is readily exploited by many alkylating agents used for cancer treatment [235]. Consequently, O^6-meG detection in tissues has been highly investigated, but research has been hampered by the fact that DNA adducts are only typically found in very low concentrations: 2,000 O^6-meG /nmol dG or 50,000 O^6-meG per cell compared to approximately 3 billion canonical base pairs [236-237]. Additionally, these numbers are dynamic as the repair pathways are actively demethylating the adducts as previously described. Variations when comparing different tissues and individuals based on geographic regions have also been observed [238-241].

3.1.3 O^6-methylguanine detection

Since the discovery of the link between O^6-meG and its roles with cytotoxicity, mutagenesis and cancer, many detection methods have been developed to quantify and correlate the presence of the adduct to disease. One of the first assays for the detection of O^6-meG relied on the specificity of the O^6-alkylguanine-DNA-alkyltransferase repair enzyme. In this case, the amount of O^6-meG repair was compared against the amount in a known standard using immunoprecipitation and radiolabeling. With this method, O^6-meG was able to be detected at levels of 50 fmol/mg of DNA or a 0.5 fmol detection limit in vitro [242]. Other early detection methods included ^{32}P-postlabeling [243], immunoassays [244-245], and mass spectroscopy [246] along with combinations of analytical methods including high-performance liquid chromatography (HPLC) fractionation of the adduct before quantification to extend the sensitivity of the assays [247-249]. The main drawback from these assays is that none of them provide sequence specificity but instead they were meant to solely detect and quantify the amount of O^6-meG. With time, new assays were developed that provided sequence specificity of O^6-meG in the target of interest. This is extremely beneficial as advances in the genomic basis of distinct disease are made.

Amongst the first attempts to analyze the occurrence of O^6-meG and understand its distribution in a given sequence was to use radio-labelled guanine residues, but only short sequences could be analyzed [250-251]. Dolan et al., noticed an uneven distribution of the adduct in dodecamer sequences and found that when the modified guanine is preceded by a purine the incidence of the adduct is greater and the extent of repair is slower [250]. Shortly after, Richardson et al., elucidated that O^6-meG was preferentially formed in single-stranded oligonucleotides compared to double stranded and that the incidence of O^6-meG varies in a sequence-dependent manner [251]. Furthermore, it was highlighted that some regions of the genome may be more susceptible to mutagenesis by the formation of O^6-meG [251]. The first report of high throughput DNA sequencing including the detection of several adducts was in 2011 by Clark et al., where they applied single molecule real time (SMRT) DNA sequencing

previously used for the detection of DNA methylation on cytosine and adenine [252-253]. SMRT DNA sequencing relies on the differences in polymerase kinetics to incorporate modified DNA compared to an unmodified template [252]. Clark et al., used the same method to analyze methylated bases including O^6-meG, 1-methyladenine, and O^4-methylthymine. The kinetic signal generated by the incorporation of O^6-meG varied depending on its position. Yet, the distinct signature of the polymerase could still be used to detect the adduct in a sequence-specific manner [253]. Even though SMRT sequencing offers a potent method for the analysis of DNA damage, special instrumentation is required and quantification of the adduct abundance was not addressed. With the goal of obtaining sequence and quantitative information about DNA adducts, Sturla and co-workers have synthesized various synthetic DNA analogs that are able to pair preferentially to methylated bases including O^6-meG and O^6-benzylguanine (O^6-BnG) [254]. In this case, the analogs varied in their hydrogen bonding and pi-stacking interactions with the adducts and the canonical bases allowing them to form more stable interactions with the former [254]. In 2016, the Sturla group synthesized new surrogates that had even higher affinity to O^6-meG than to the unmodified base: 1′ -β -[1-naphtho[2,3-d]imidazol-2(3H)-one)]-2′ -deoxy-D -ribofuranose (ExBenzi) and 1′ -β -[1-naphtho[2,3-d]-imidazole]-2′ -deoxy-D -ribofuranose (ExBIM) with ExBIM being more selective [251]. In their report they were particularly interested in the detection and quantification of the adduct with sequence specificity in a particular mutagenic hotspot of the Kristen Ras proto-oncogene (KRAS) [255].

3.1.3 KRAS

The *KRAS* or Kristen Ras proto-oncogene belongs to a group of GTP-binding proteins, known as the Ras-like GTPases, that relay signals from extracellular growth factors and modulate gene expression and homeostasis. Specifically, *KRAS* expresses a guanosine triphosphate (GTP)/guanosine diphosphate (GDP) binding protein in the Ras/MAPK pathways [256]. Normally the protein remains inactive, but once it binds GTP it acts as a switch to activate genes and modulate intracellular activity [257]. The Ras/MAPK signaling pathways

affect cellular differentiation, growth, chemotaxis and apoptosis. Also, as a key regulator of cell survival, cancer cells that become resistant to chemotherapies often have *KRAS* mutations [258]. Commonly, activating mutations are linked to carcinogenesis, resistance to chemotherapy, and poor patient prognosis [259]. Dominant *KRAS* mutations are the most common ones in any type of cancer, thus, the *KRAS* gene has been highly studied [260]. The most common recurring mutation in the *KRAS* gene of cancer cells happens in codons 12 and 13 of exon 1 [261]. *KRAS* mutations are the most prominent in colorectal carcinomas, non-small cell lung cancer and pancreatic ductal carcinoma [262-263]; however, mutations are also found in biliary tract carcinomas, endometrial cancer, bladder cancer, breast cancer, liver cancer and myeloid leukemias amongst other types of cancer [264].

3.2 Introduction

This thesis presents a continuation of the work developed by the Sturla lab on the use of synthetic DNA surrogates to obtain sequence specificity and quantitative information of the presence of O^6-meG in the codon 13 hotspot of the *KRAS* proto-oncogene. Out of the surrogates developed, we focused on ExBIM, a synthetic nucleoside analogue with an elongated hydrophobic surface that was previously shown to preferentially bind to O^6-meG. Ioannis et al., elucidated that ExBIM interacts more strongly with O^6-meG based on its increased hydrophobicity due to the extra methyl group compared to a guanosine base [255]; O^6-meG and ExBIM are shown in Scheme 3.1.

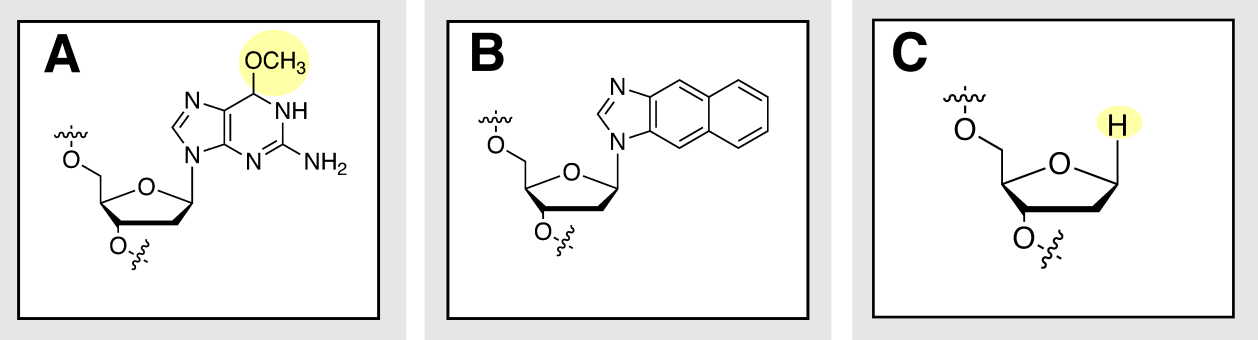

Figure 3.1. O^6-methylguanine structure highlighting the methylation on the oxygen group (A) and O^6-methylguanine synthetic complementary base, ExBIM (B) and abasic phosphoramidite nucleotide (C).

Previously, ExBIM containing oligonucleotides were attached to gold nanoparticles to achieve colorimetric detection in the presence of target DNA containing O^6-meG at specific locations [255]. We hypothesized that their limit of detection of 0.24% of O^6-meG in the presence of background non-methylated target could be expanded if we increased the selectivity of the probes and included a signal amplification step [255]. Therefore, the main objective of this project was to extend the selectivity of the ExBIM probes by pairing them to a ligation reaction that would happen only if O^6-meG was present (Scheme 3.2). For the ligation reaction, we designed a pair of recognition probes, each one binding one half of the *KRAS* DNA target (T_{KRAS}, T_{KRAS11} or T_{KRAS14}, where the number subscript represents the position of the methylated guanine) sequence in codon 13. The first probe contained ExBIM (DNA_{EI} or DNA_{EII}, depending on the position of the ExBIM) and the second one contained a fluorescein modified base to be able to detect the reaction using gel electrophoresis (DNA_{F0}, DNA_{F1}, or DNA_{F2} where F indicates the presence of a fluorescein and the number subscript indicates the presence of an abasic nucleotide). The abasic nucleotide is also displayed in Scheme 3.1 for reference. Our hypothesis was that only in the presence of O^6-meG the two probes could form a covalent bond by the ligation reaction of the T4 DNA ligase and the product could be later amplified to increase the observed signal from the formation of the product. Hence, for the

reaction to be selective we should observe no product formation in the absence of the methylated adduct.

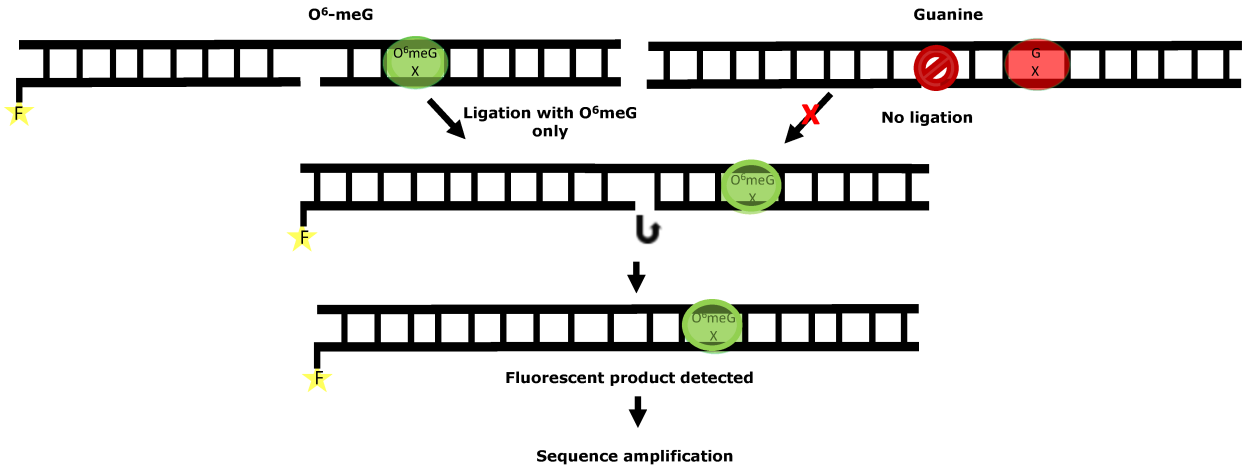

Figure 3.2. ExBIM recognition and hybridization with O6-meG drives the ligation reaction forming a product only in the presence of the methylated target.

The T4 DNA ligase is one of the most widely studied ligases for molecular biology applications and works by joining a 5'-phosphate with a 3'-hydroxyl group from oligonucleotides that are in close proximity by hybridization to a template forming a phosphodiester bond [265]. The T4 ligase is also known to be a high activity ligase with discriminatory activity for 3' mismatches and thus it has been used widely in diagnostic assays [265-266]. However, the mechanism of discrimination is thought to be by scanning the minor DNA grooves and the DNA structure not by interrogating each base pair and thus the T4 ligase has also been seen to tolerate base mis-pairings [266-268]. Therefore, to increase the selectivity of the probes besides relying on the selectivity of the ExBIM recognition, we also incorporated abasic sites that have been shown by our group to increase the discrimination of ligation reactions and mismatch recognition when detecting single nucleotide polymorphisms (SNPs) in the past [269]. In addition, we examined different parameters of the ligation reaction, probe modifications, and reaction conditions to increase the detection limit of ExBIM in the presence of non-methylated background DNA. By enhancing the selectivity of the ligation reaction with ExBIM and abasic sites we aimed to increase the

selectivity of the O^6-meG detection retaining sequence specificity so that in the future we can design a fast screening test for adduct formation that can be used as a biomarker test for hotspot mutation sites such as *KRAS* codon 13.

3.3 Materials and Methods

3.3.1 Materials

All materials for DNA synthesis, including phosphoramidites and reagents, were purchased from Glen Research (Sterling, VA). DNA synthesis was performed with the ABI 392 solid-phase synthesizer. T4 DNA ligase and 10x ligase buffer was purchased from New England Biolabs (NEB, Ipswich, MA, Cat M020T 2,000,000 units/mL). The DNA analysis was performed using polyacrylamide gel electrophoresis (PAGE) with 40% acrylamide/bis Solution from Bio-Rad (Cat. 1610156) and a Biorad Mini-PROTEAN Tetra Cell chamber. When the gels were finished running, they were imaged with an ImageQuant RT ECL imager from Healthcare Life Science using UV transillumination. For gel preparation, tris base (BP-152-1), boric acid (BP-168-1), urea (BP-169-212) and ethylenediamine tetraacetic acid (EDTA) (BP-120-500) were purchased from Thermo Fisher Scientific (Waltham, MA). Tetramethylethylenediamine (TEMED, BO-150-20) was also purchased from Fisher BioReagents. Ammonium persulfate solution (APS, A3678) was purchased from Sigma-Aldrich (St. Louis, MO) and prepared as a 10% w/v solution. For temperature regulation of the reactions we used a Torrey Pines Scientific Echotherm Chilling/Heating Plate model IC22.

3.3.2 DNA synthesis

DNA was prepared using the ABI 392 solid-phase synthesizer and Glen Research reagents. Standard phosphoramidites were used and fluorescein-dT phosphoramidite (Glen Research Cat. No. 10-1056-95), and abasic phosphoramidite (Glen Research Cat. No. 10-1914-90). Both abasic and fluorescein-dT phosphoramidites are shown in Scheme 3.3; when part of a strand the absic phosphoramidite is abbreviated as “ab” and the fluorescein-dT modification as “F”. All strands were purified using Glen-Pak DNA purification cartridges (Cat. # 60-5200-01) following the DMT-on protocol or reverse phase HPLC. After purification, the

samples were analyzed with matrix assisted laser desorption/ionization (MALDI). To prepare the DNA for MALDI we de-salted the samples using a C18 ZipTip (ThermoFisher Cat. No. 87782) following the manufacturer's protocol. For this, DNA samples (100-200 ng) were dissolved in 10 µL of 0.1 M triethylammonium acetate (TEAA, pH 7) before using the ZipTip. The last step of the de-salting process eluted the DNA in 5 µL of 1:1 acetonitrile:water solution by volume. For the sample analysis we then added 5 µL of matrix solution. Briefly, the matrix used contained 2,4,6-trihydroxylacetophenone (20 mg/mL) in a 1:1 ratio with acetonitrile:water combined in equal volume with an aqueous ammonium citrate solution (50 mg/mL). We used 1 µL of DNA:matrix mixture on the MALDI plate to be analyzed. For the analysis we used the Voyager Elite (Applied BioSystems, Foster City, CA) time of flight-mass spectrometer in linear positive mode. The ExBIM containing probes were prepared by alumni Ioannis Trantakis, PhD from the Sturla lab in the Department of Health Sciences and Technology, ETH Zu̇rich.

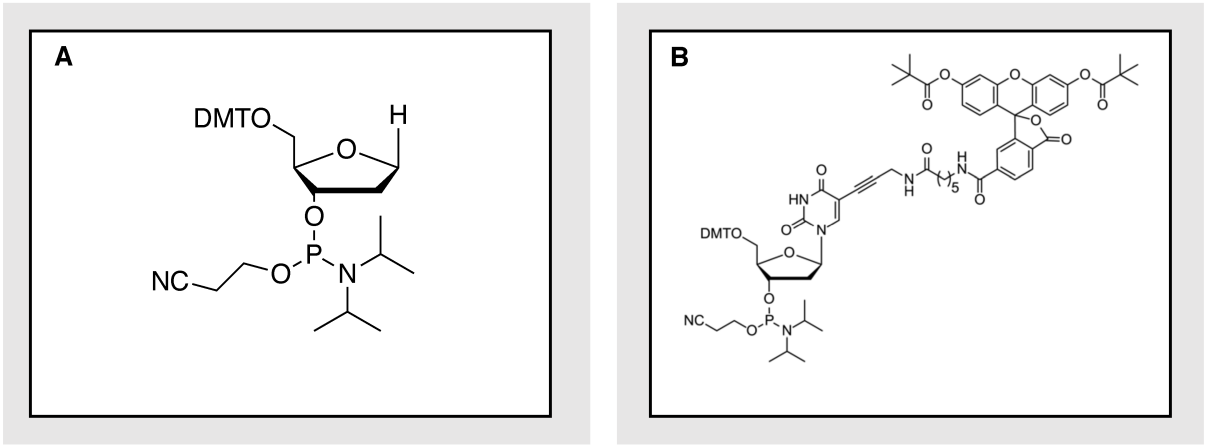

Figure 3.3. Abasic (A) and fluorescein-dT (B) phosphoramidites obtained from Glen Research and used for probe synthesis.

Table 3.1 DNA sequences and nomenclature

Name	Sequence
KRAS target (T_{Kras})	5′ GTT GGA GCTG GT GGC GTA 3′
Methylated KRAS target on 14th guanosine (T_{Kras14})	5′ GTT GGA GCTG GT GG $_{CH3}$C GTA 3′
Methylated KRAS target on 11th guanosine (T_{Kras11})	5′ GTT GGA GCT GG $_{CH3}$T GGC GTA 3′
ExBIM probe (DNA_{EI})	5′ TAC GE$_X$C CA 3′
ExBIM probe (DNA_{EII})	5′ TAC GCC AC E$_X$ 3′
Fluorescent probe 1 (DNA_{FII})	5′ $_P$CAG CTC*Ab* CAA *Ab*$_F$ 3′
Fluorescent probe 2 (DNA_{FI})	5′ $_P$CAG CTC CAA C$_F$ 3′
Fluorescent probe 3 (DNA_{F0})	5′ $_P$CAG CTC CAA C$_F$ 3′
Blocking probe	5′ TAC GCC ACA AA C3′
DNA-C	5′ AAAA CA CCG CAT 3′

3.3.3 DNA ligation experiments

DNA ligation experiments were performed by mixing 1 equivalent of target (either methylated or non-methylated KRAS), 1 equivalent of fluorescently-labeled probe, and 2 equivalents of the ExBIM containing probe, so that the complete consumption of the fluorescent probe indicated that 100% of the product had reacted. The final concentration of the probes was 1.4 μM and the reaction volume used was 7.5 μL. The master mix used per reaction was: Enzyme (1.0 μL), buffer (1.5 μL) and water (2.5 μL). The buffer was obtained with the T4 ligase from NEB and its composition was: Tris-HCl (50 mM), $MgCl_2$ (10 mM), ATP (1 mM), DTT (10 mM) at pH 7.5. Table 3.2 exemplifies the reaction volumes and mixtures. Reactions were performed at different temperatures: 10 °C, 13 °C, or 16 °C were tested, but most experiments were done at 16 °C unless otherwise specified. At the desired time points, samples (2.0 μL) from each reaction were collected and combined with "stop solution" (1.8 μL) to stop the ligations. The stop solution was prepared by combining 100 μL of bromophenol blue stock (11 mg of bromophenol blue in 1 mL of H_2O) with 800 μL of sucrose stock (4 g sucrose + 10 mL of 0.5 M EDTA). The reaction products were then analyzed using polyacrylamide gel electrophoresis (PAGE) and a UV transilluminator. For ligation experiments we used a denaturing polyacrylamide gel at a 15% concentration: urea (4.8 g, moles), 5x Tris Borate EDTA (TBE) buffer (1 mL), 40% acrylamide/bis 19:1 (5 mL) brought to a 10 mL

final volume with Millipore water. The solution was then polymerized by adding 10% (w/v) APS (80 µL) and TEMED (10.7 µL) and incubated in a 0.75 mm spacer plate. The 5x TBE buffer was made with TRIS (108 g), boric acid (55 g), 0.5M EDTA (40 mL) and brought to a 2L final volume with Millipore water. The buffer was diluted to 1x to run the gels using the electrophoretic chamber. The product percentage yield was calculated by comparing the fluorescent intensities of the reactant band with the ligation product band: $\frac{Iproduct\ band}{Iproduct\ band + Ireactant\ band}\ x\ 100\%$.

Table 3.2. T4 ligase reactions to detect methylated or non-methylated KRAS DNA. The reactions were performed by mixing the set volumes of reactants and collecting fractions at different time points and combining these with stop solution.

	Target (µL)	**DNA_{F0} (µL)**	**DNA_{EI} (µL)**	**H_2O (µL)**	**Master Mix (µL)**
T_{KRAs14}	0.625	0.625	1.25	2.5	2.5
T_{KRAS}	0.625	0.625	-	2.5	2.5
Control	-	0.625	1.25	3.13	2.5

Table 3.3. T4 ligase reactions to detect methylated or non-methylated KRAS DNA introducing a blocking step.

	Target (µL)	**DNA_{F0} (µL)**	**DNA_{EI} (µL)**	**Blocking probe (µL)**	**NEB buffer (µL)**
T_{KRAs14}	1.25	1.25	2.5	1.25	5
T_{KRAS}	1.25	1.25	2.5	1.25	5
Mixed	1.25 each	1.25	2.5	1.25	5

The reactions were performed by mixing the set volumes of reactants and collecting fractions at different time points and combining these with stop solution. In this reaction a blocking step was implementing by adding 1.25 µL of blocking probe 20 minutes prior to the addition of the rest of the probes tested.

3.3.4 DNA hybridization experiments

DNA hybridization experiments were performed by incubating the targets of interest with their complementary probes at 4 °C for 24 hours and at least 2.2 picomoles of reaction sample were run for PAGE analysis (3.7 μL of 1.4 μM reaction). In contrast to the ligation reactions, the hybridization reactions were run using a non-denaturing gel using 5.6 mL of acrylamide:bis 19:1, 4.0 mL of H_2O and 2.4 mL of 5x TBE buffer and polymerized with of 10% APS (200 μL) and TEMED 10 (μL). Hybridization reactions were run at 150 mV by keeping the electrophoresis chamber in ice.

Table 3.4. Hybridization reaction set up to detect methylated or non-methylated KRAS DNA.

The reactions were performed by incubating the set volumes of reactants at 4 °C overnight. For the PAGE analysis 5 μL of sample were combined with 2 μL of sucrose solution and 1 μL of bromophenol blue solution (3.7 μL from the prepared samples were ran in the non-denaturing gel). We must note that the samples containing two targets had lower $MgCl_2$ concentrations as less NEB buffer (10 mM $MgCl_2$) was used for their hybridizations.

	Target (μL)	**DNA_{F0} (μL)**	**DNA_{EI} (μL)**	**DNA-C (μL)**	**NEB buffer (μL)**
T_{KRAs11}	3.45	5.25	1.45	-	4.85
T_{KRAS}	3.45	5.25	1.45	-	4.85
Mixed	3.45 each	5.25	1.45	-	1.4

3.4 Results and Discussion

3.4.1 Selectivity of ExBIM in ligation reactions

3.4.1.1 Destabilization and ExBIM selectivity

To increase the sensitivity of ExBIM for the detection of O^6-meG we started by modifying the DNA probe with the fluorescein label by introducing abasic sites as in the past abasic sites have shown to increase the selectivity of SNP detection [269]. First, we observed that if no abasic sites were used we obtained approximately 63% product formation when the non-methylated guanosine was present and 82% product formation with O^6-meG after 5 minutes at 16 ^{o}C (Fig. 3.1). Thus, ExBIM has some preference for O^6-meG, yet the ExBIM probe by itself was not enough to be selective during the ligation reaction with T4 ligase. As we mentioned before, T4 ligase is known to tolerate mismatches. In this case, we believed that the change in the DNA hybrid structure was not sufficiently different when there was methylation or not for the ligase to differentiate between the non-ideal base pairing [266]. As the ExBIM probe is able to hybridize with non-methylated guanosine non-selectively, we hypothesized that the abasic sites on the complementary probe might disrupt the stability of the hybrids, especially if the interactions were not as favorable as for ExBIM:G. By increasing the number of abasic sites to one and two we obtained yields of 23% or 0%, respectively, with the non-methylated target and 20% and 15% with O^6-meG after 5 minutes (Fig. 3.1). Therefore, the addition of abasic sites on the fluorescein probe increased the selectivity of the ExBIM probe as well. However, after 60 minutes, even when the two abasic sites were used we still observed 10% product formation without the presence of methylation (Fig 3.1). Consequently, the dynamic nature of the DNA hybrid formation, regardless of destabilization with the introduction of abasic sites, allowed for the product formation between the ExBIM:G if given enough time utilizing the T4 ligase.

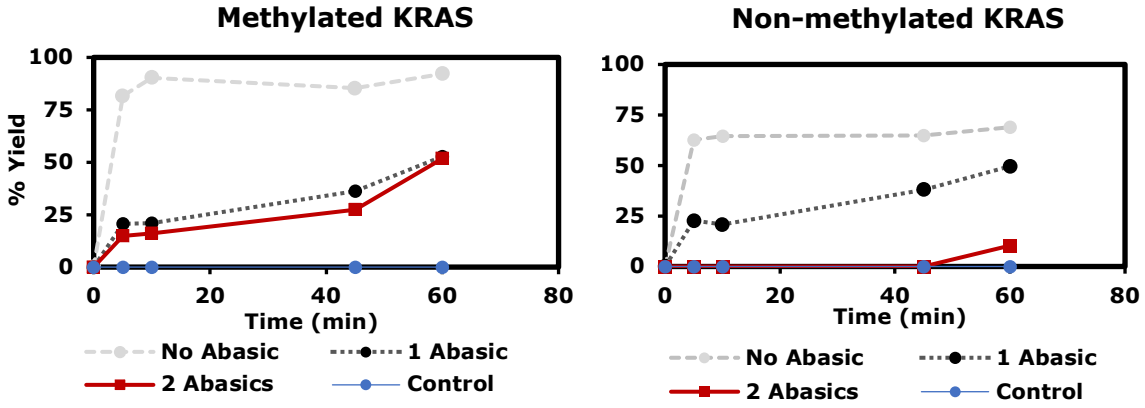

Reactions: 5′ GTTGGAGCTG——GTGGCGTA 3′
3′$_{F}$CAAC*Ab*TCGA*Ab*$_{p}$CACExGCAT 5′

Figure 3.4. Selectivity of methylated KRAS recognition using abasic destabilization.

Ligation reactions were performed with the methylated or non-methylated KRAS targets on position G_{14}. The fluorescently labeled probes contained one, two or no abasic sites. The ligation reaction was performed at 16 °C and analyzed with PAGE. The control reaction was performed without target DNA using the two abasic probe. Percent yield was obtained by comparing the product and reactant intensities. The reaction sequences are color-coded, where green shading highlights the guanine where the methylation may be present. Light blue shading indicates the fluorescent probe and grey shading shows the probe which contains the ExBIM. Finally, *"Ab"* indicates an abasic nucleoside, E_x indicates ExBIM, and F indicates fluorescein.

For the ligations reactions we also analyzed the activity of a less concentrated ligase, 1 unit compared with 5-units which we used for all of the presented experiments. Yet at the 1-unit concentration we were only able to observe a maximum of 6% product yield when using the two abasics and the methylated KRAS target, and 12% product yield with the one abasic probe. However, the abasic probe also allowed for product formation with non-methylated target (Fig. 3.2). Therefore, to be able to increase the product yield we utilized the 5-units of enzyme for all ligation experiments.

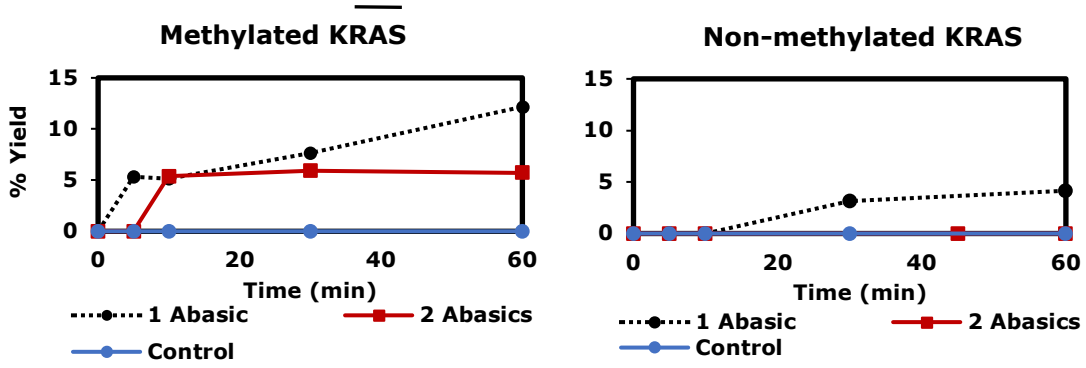

Reactions: 5′ GTTGGAGCTG──GTGGCGTA 3′
3′FCAACAbTCGAAbpCACExGCAT 5′

Figure 3.5. Selectivity of methylated KRAS recognition using 1-unit T4 ligase. Ligation reactions were performed with the methylated or non-methylated KRAS targets on position G_{14}. The fluorescently labeled probes contained one or two abasic sites. The ligation reaction was performed at 16 °C and analyzed with PAGE. The control reaction was performed without target DNA using the two abasic probe. Percent yield was obtained by comparing the product and reactant intensities. The reaction sequences are color-coded, where green shading highlights the guanine where the methylation may be present. Light blue shading indicates the fluorescent probe and grey shading shows the probe which contains the ExBIM. Finally, *"Ab"* indicates an abasic nucleoside, E_x indicates ExBIM, and F indicates fluorescein.

3.4.1.2 Temperature effects on ligation kinetics with ExBIM

Next, we analyzed temperature variations and how these affect the rates of the ligation reactions (Fig. 3.3). Temperature is one of the most important parameters for nucleic acid-based diagnostic assays as DNA hybridization is dictated by its dissociation, or melting temperature (T_m), and therefore altering the temperatures in a reaction can have a huge impact on the selectivity and sensitivity of an assay without changing any other parameter [270-271]. As expected, we observed that product formation and temperature were inversely related; as we lowered the temperature from 16 °C to 10 °C we were able to obtain 100% product formation after 60 minutes when the methylated KRAS target was present. However, at 10 °C and after 60 minutes 74% product was formed without methylation (Fig. 3.3). By selecting 16 °C and two abasic sites on the fluorescent probe we were able to increase the

selectivity of the ExBIM probe. We also analyzed the reaction at 23 °C yet at this temperature there was no discrimination between methylated and non-methylated target.

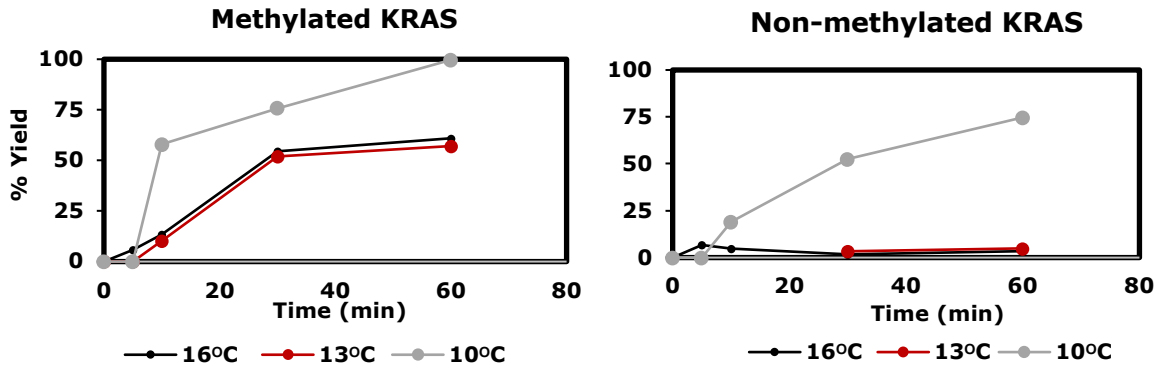

Reactions: 5′ GTTGGAGCTG——GTGGCGTA 3′
3′$_{F}$CAAC*Ab*TCGA*Ab*$_{p}$CACExGCAT 5′

Figure 3.6. Selectivity of methylated KRAS recognition using temperature variations. Ligation reactions were performed with the methylated or non-methylated KRAS targets on position G_{14}. The fluorescently labeled probe contained two abasic sites. The ligation reactions were performed at 16 °C, 13 °C, and 10 °C and monitored after 5, 10, 45 and 60 minutes and analyzed with PAGE. Percent yield was obtained by comparing the product and reactant intensities.

3.4.1.3 ExBIM recognition site

Next, we looked into moving the methylation site with respect to the ligation site, to the guanosine at the 11th position (Fig. 3.4). It is known that T4 ligase is more selective at the ligation site and thus we hypothesized that this position would allow for the maximum discrimination between methylated target and non-methylated [264]. However, when the ExBIM:O^{6}-meG or ExBIM:G were at the enzyme ligation site, we observed no product formation, even after 60 minutes (Fig. 3.4). This lack of reactivity was likely due to the ligase not being able to detect the DNA nick when the ExBIM was at the site of ligation, one possibility for this is that the ExBIM changed the conformation of the duplex structure when positioned at the ends of a strand yet this would need to be confirmed with further analysis.

Reactions:

A) **5′ GTTGGAGCTG——GTGGCGTA 3′**
3′$_F$CAAC*Ab*TCGA*Ab*$_p$E$_x$ACCGCAT 5′

B) **5′ GTTGGAGCTG——GTGGCGTA 3′**
3′$_F$CAAC*Ab*TCGA*Ab*$_p$ CACE$_x$GCAT 5′

Figure 3.7. Selectivity of methylated KRAS recognition by changing the position of the O^6-meG.

Ligation reactions were performed with the methylated or non-methylated KRAS targets on position G_{11} (A) or G_{14} (B). The fluorescently labeled probe contained one abasic site. The ligation reactions were performed at 16 ^oC and analyzed with PAGE. Lane 1 includes no template, lane 2 T_{KRAS} and lane 3 T_{KRAS11}.

3.4.1.4 ExBIM selectivity with mixed samples

After selecting the parameters of the ligations reactions that were the most selective to discriminate between methylated and non-methylated target, we then analyzed the detection when the targets were mixed together (Fig. 3.5). When 1% of the original methylated target was present no product formation was observed, even after 240 minutes. Here, we realized that the detection limit of our gel imaging technique had a threshold for allowing the visualization of the product that might be higher than the amount that we should observe. However, by doing target mixtures or analyzing 99% of the non-methylated target alone we observed that the parameters we had selected were not stringent enough to allow for the discrimination between the methylated and non-methylated targets (Fig. 3.5). For

example, after four hours, 23% of product had formed with 99% of non-methylated target alone, (Fig. 3.5); unexpectedly adding 1% methylated target reduced this product to 13%. However, even though there might be some inhibition by the combination of methylated and non-methylated target, evidently the ExBIM probe is not sufficiently discriminatory with mixed samples using ligation reactions.

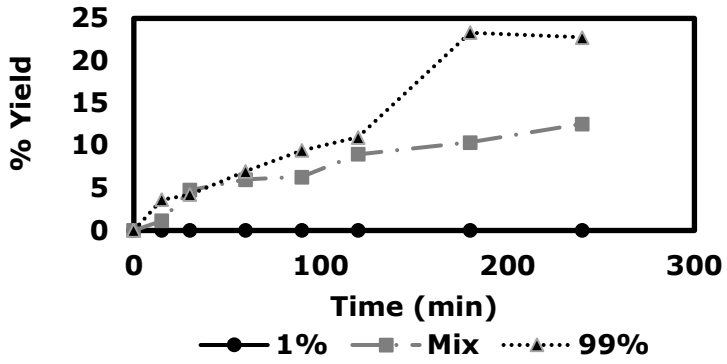

Reactions: 5′ GTT GGA GCT G GT GGC GTA 3′
3′$_{F}$CAA C^{Ab}T CGA ^{Ab}p CA CE$_{x}$G CAT 5′

Figure 3.8. Selectivity of ExBIM probe to O^6-meG in the presence of background non-methylated target.

Mixtures of methylated and non-methylated targets were made 1% methylated and 99% non-methylated DNA to examine the selectivity of ExBIM. In the legend,1% refers to 1% methylated target only, "Mix" refers to 1% methylated target and 99% non-methylated target, and 99% refers to non-methylated target only. The fluorescently labeled probe in the reactions contained two abasic probes and the reactions were performed at 16 °C. Samples were analyzed by PAGE.

In order to increase the discrimination of the O^6-meG detection in a mixed sample we hypothesized that we could introduce a "blocking step" in the reaction to reduce the effective concentration of non-methylated guanine encountered by the ExBIM probe. To achieve this, we added an extra blocking step with a probe containing a cytosine instead of ExBIM to observe if the cytosine could have higher affinity towards the non-methylated target and allow for the methylated target to be free for detection by the ExBIM. Sturla and co-workers had reported that the approximate T_m of the DNA hybrid with C:G is 66 °C while that with C:O^6-

meG is 55.2 °C. For hybrids with ExBIM:G the T_m was 51.7 °C and 54 °C for ExBIM O^6-meG hybrid strands [251]. Therefore, the C:G bond is significantly more stable than the ExBIM:G by a difference of around 15 °C, yet there is only a 2.3 °C difference in T_m that gives ExBIM selectivity towards O^6-meG. Therefore, we expected that if given the choice to hybridize non-methylated guanine or O^6-meG, a cytosine containing probe would preferentially bind and "capture" the non-methylated guanines. Next, in order to actually block the ligation reaction, we added three extra adenine bases at the ligation site so that no nick could be recognized by the T4 ligase once the cytosine-probe bound. We analyzed the selectivity of the ExBIM probe by combining 5% methylated target with 95% non-methylated target (Fig. 3.6). First, we analyzed the reaction without the blocking probe, and observed that by 30 minutes both the 5% methylated target only and 95% non-methylated target only had similar product yields of approximately 16% (Fig. 3.6). When the blocking probe was introduced by incubating the probe alone with the targets for 20 minutes at 4 °C prior to the addition of the fluorescein and ExBIM probes, we observed that the reaction had a slower kinetic rate, and by 30 minutes the maximum product yield was about 5% (Fig 3.5). In this reaction, the 5% methylated target and 95% non-methylated target still resulted in similar product yields by 30 minutes meaning that the blocking probe could bind to either target as well as the ExBIM probe and thus no discrimination was observed. We can improve this experiment by incubating the blocking probe with cytosine at a temperature that is above the T_m of C:O^6-meG yet still below the T_m of C:G. Yet to do this study we expect that more time would be required for the blocking step and we would need to analyze the optimal time for maximum blocking before the cytosine target hybridizes with the O^6-meG. In the future, to increase the selectivity of the ligation reaction we could also examine different ligase enzymes that are more stringent than the T4 ligase and observe if this could increase the selectivity of the O^6-meG recognition along with changing some of the physiochemical parameters as we have done in this project.

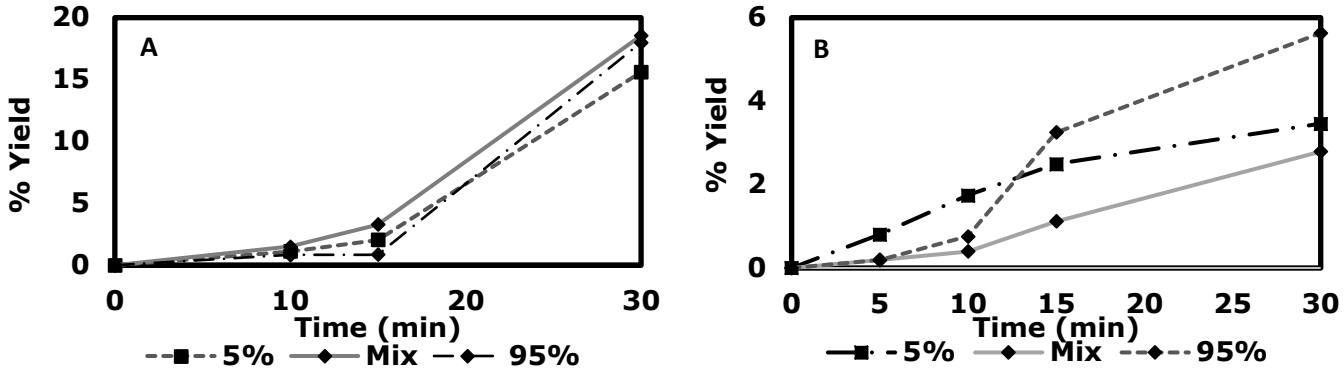

Reactions: 5′ GTT GGA GCT G GT GGC GTA 3′

3′$_{F}$CAA C*Ab*T CGA *Ab*$_{p}$ CA CE$_{x}$G CAT 5′

Or

5′ GTT GGA GCT G GT GGC GTA 3′

3′FCAA C*Ab*T CGA *Ab*$_{p}$ $_{AAA}$CA CCG CAT 5′

Figure 3.9. Selectivity of ExBIM probe to O^{6}-meG in the presence of background non-methylated target.

Mixtures of methylated and non-methylated targets were made by combining 5% methylated and 95% non-methylated DNA. A) We mixed the T_{KRAS14} target with complementary ExBIM probe and fluorescein labeled probe with two abasic sites. B) We included a blocking step by incubating the targets with a probe equal to ExBIM with extra bases at the ligation site at 4 ^{o}C before adding the ExBIM probe 20 minutes later. In the legend, 5% refers to 5% methylated target only, "Mix" refers to 5% methylated target and 95% non-methylated target, and 95% refers to non-methylated target only. The ligations were performed at 16 ^{o}C and samples were analyzed by PAGE.

3.4.2 Analysis of probe hybridization utilizing ExBIM

To further understand the selectivity and discrimination capacity of the ExBIM probe we decided to analyze the hybridization of the probes alone without the addition of the T4 ligase as we noticed that the ligations were not stringent enough to recognize methylated target from non-methylated. To analyze probe hybridizations, we included non-methylated targets and methylated targets at the 11th position of the guanine to further understand if the inability for the T4 ligase to ligate the product at this site had to do with probe hybridization itself. To perform hybridizations, we compared an ExBIM probe with a similar probe that

contained cytosine instead (DNA-C). To distinguish between the products formed, we added extra adenine bases to the 5' end of the cytosine probe expecting that the extra bases would increase the molecular weight of the probe and the resulting product would then be slower running through the polyacrylamide gel compared to the product from the ExBIM. We analyzed methylated and non-methylated targets by themselves with both DNA-C and ExBIM probes and also target mixtures. Moreover, for the hybridization reactions, the fluorescein probe contained no abasic sites to analyze the selectivity of ExBIM by itself without any other modifications. Figure 3.7 displays a representation of the expected outcome of the experiment, highlighting how if the DNA-C and DNA_{F0} are bound to the target the expected duplex band is of higher molecular weight (Lane 2) than if ExBIM and DNA_{F0} are bound (Lane 1) and thus the band should be higher in the gel. In lane 3 the target was incubated with both DNA-C and ExBIM probes and thus we expect that both duplexes formed are apparent in the gel. Finally, as a control we only incubated the target with DNA_{F0} and analyzed its position in the gel relative to the other samples as well (Lane 4).

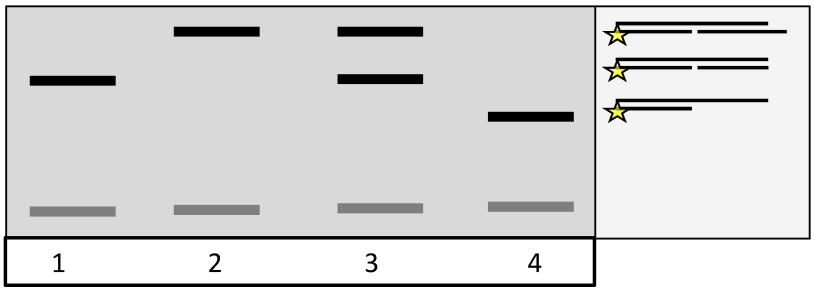

Figure 3.10. Expected hybridization results when either ExBIM (Lane 1), DNA-C (Lane 2) or both probes (Lane 3) hybridize to a target strand.
Lanes 1-3 include fluorescently labeled probe DNA_{F0} in addition to ExBIM or DNA-C probes whereas lane 4 is used as a control where only the fluorescently labeled probe is used with the target. The three hybridization possibilities are shown in the right panel.

We performed the hybridization reactions at 4 °C for 24 hours and target and probes were combined in equal concentrations; when two probes were combined with one target each probe was given at a 1:1 ratio to the target. All groups included DNA_{F0} for visualization

on the polyacrylamide gel (Lanes 1-9, Fig. 3.8). Lanes 1-3 compared T_{kras11} methylated target with ExBIM probe (DNA_{EII}) or non-methylated T_{kras} target with ExBIM probe (DNA_{EII}) or both targets with DNA_{EII}. As shown, when the ExBIM probes are hybridized to either methylated or non-methylated targets their resulting duplexes are unable to be differentiated on a gel as their molecular weights are too close to each other (Fig. 3.8). Thus, in order to observe the difference between ExBIM binding a methylated or unmethylated target another type of analysis must be performed. In the future the ExBIM probe could contain a fluorophore moiety and one of the targets a quencher, and thus be able to differentiate which target is bound based on fluorescent intensity changes.

We then analyzed the hybridization products with DNA-C with non-methylated (Lane 4) or methylated target (Lane 5). As expected, when DNA-C formed a duplex with the non-methylated target, we were able to observe a band that ran higher when compared to when the ExBIM probe was bound (Lane 4) but, surprisingly, the duplex formed between the methylated target and the DNA-C probe appeared at a slightly lower position (Lane 5) when compared to the ExBIM probe duplex (Lane 1). From our analysis it was unclear if the DNA-C probe was not able to bind to the target at all, since the band seemed to be at a similar position as the target and fluorescein probe only duplex (Lane 9) or if another DNA structure was being formed that prevented the observation of the DNA-C probe hybridized with methylated target. In lanes 6-7, we analyzed the hybridization product formed when either non-methylated (lane 6) or methylated (lane 7) targets were given the choice to either bind DNA_{EII} or DNA-C. In this case, the non-methylated target formed a hybrid product with DNA-C only. This is observed by comparing the positions of lane 6 and lane 4 where only DNA-C was given as an option for binding to the target. Similarly, the methylated target seems to bind only to the DNA_{EII} probe by comparing the position of the duplex with the duplex formed when only DNA_{EII} was given as an option for binding (Lane 1). To summarize, by doing the hybridization reactions we learned that the ExBIM probe will detect and hybridize to a non-

methylated target in a similar manner as a methylated target, producing product bands of the same length (Fig. 3.8). Thus, the non-specific hybridization when performing the ligation reactions can explain why the discrimination of the ExBIM was not sufficient to obtain selectivity even after adjusting the physiochemical characteristics of the reaction. Sturla and co-workers had also observed that a hybrid containing C:O^6-meG had a slightly higher T_m (55.2 °C) than with the ExBIM:O6-meG pair (54 °C) and thus if given enough time O^6-meG can hybridize as readily with ExBIM or cytosine. However, their reported melting temperatures correspond to the bases located in the middle of the target strand and not at the ends as in figure 3.8 and thus we expect melting temperature changes in our analysis. We want to highlight that when the probes are analyzed with only one target, we can observe how the ExBIM probe hybridizes with methylated target and the "c" probe hybridizes with the non-methylated target preferentially indicating that ExBIM offers some affinity towards O^6-meG. Yet, in mixed reactions this affinity needs to be enhanced for an effective detection assay (Fig. 3.7). In the future, we can exploit the affinity differences between guanine binding cytosine preferentially compared to ExBIM (Lane 6) when at the end of a strand and devise an assay that is able to block guanine targets but not targets with O^6-meG.

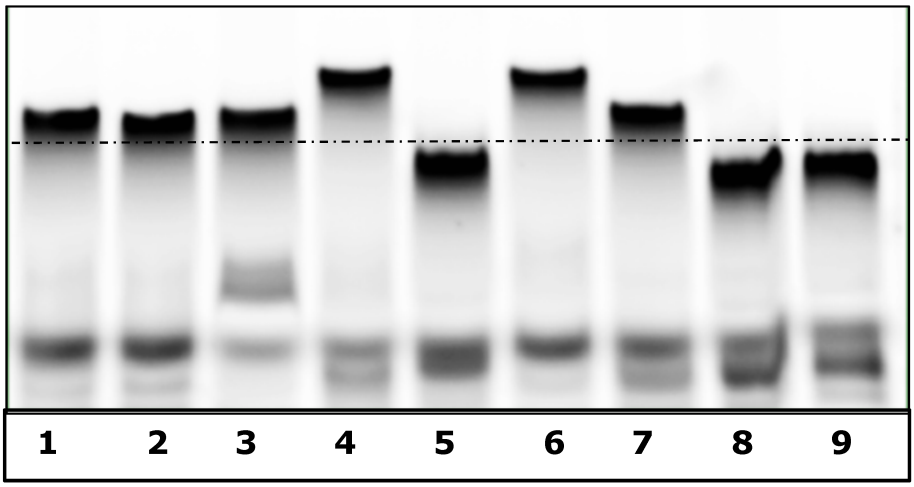

Lane 1: T_{KRAS11} + DNA_{EII}
Lane 2: T_{KRAS} + DNA_{EII}
Lane 3: T_{KRAS11} + T_{KRAS} & DNA_{EII}
Lane 4: T_{KRAS} + DNA_{C}
Lane 5: T_{KRAS11}+ DNA_{C}
Lane 6: T_{KRAS} + DNA_{EII} + DNA_{C}
Lane 7: T_{KRAS11} + DNA_{EII} + DNA_{C}
Lane 8: T_{KRAS} + DNA_{F0}
Lane 9: T_{KRAS11} + DNA_{F0}

TKRAS: 5′ GTT GGA GCT G GT GGC GTA 3′
DNA_{EII}: 3′$_F$CAA CCT CGA C$_p$ XA CCG CAT 5′
DNA_{C}: 3′$_F$CAA CCT CGA C$_p$ CA CCG CAT AAAA 5′

Figure 3.11. Hybridization of ExBIM probe to O^6-meG in the presence of background non-methylated target.

Hybridization reactions including non-methylated or methylated targets at the guanine in the 11thposition with ExBIM probe or a cytosine probe with extra bases. Reactions were performed by adding 0.65 nmoles of KRAS target and 0.65 nmoles of its complementary probes in 15 µL total volume using NEB buffer and incubated at 4 ^{o}C before analyzing after 24 or 48 hours on a non-denature polyacrylamide gel. The gel was run at 150 mV on ice.

3.5 Conclusion

In this chapter we analyzed the selectivity of an ExBIM modified probe with the main objective of utilizing it for detection of the O^6-meG in the hotspot mutation site of *KRAS* codon 13. We analyzed different parameters that might affect its discrimination including optimizing temperature, recognition site and introduction of abasic lesions that were aimed to increase the discrimination capacity of the ExBIM containing probe. However, using the T4 DNA ligase to perform the ligation reactions did not offer selectivity after one hour even when changing the said parameters. Thus, when analyzing reaction mixtures, the ExBIM probes were not able to discriminate between methylated or non-methylated targets even when we aimed to block the non-methylated target. Adding a blocking step could be beneficial in the future. However, from our observations the cytosine base can also bind and hybridize to O^6-meG when the adduct is found in the middle of a sequence and thus it also blocks the recognition

of the target of interest, however, we might be able to obtain better selectivity when the adduct is found at the end of the sequence. The ideal option would be to either further modify the O^6-meG to enhance its discrimination between O^6-meG or guanine or to include a step that completely removes the non-methylated targets. In the future we could also increase the discrimination of the detection reactions by selecting a more stringent enzyme or by exploring other detection methods that do not rely on an enzyme.

Chapter 4. Conclusion and Future Work

This thesis exemplifies the versatility of nucleic acids for the development of targeted therapies and biomarker detection methods. By their nature, nucleic acids allow for the development of specific targeting based on base pairing interactions and are highly modifiable which allows for enhanced detection and reduced side effects [62-65]. Moreover, in Chapter Two we highlighted how some of the limitations of working with siRNA including its lack of stability in vivo and its low efficiency to pass through cellular membranes can be overcome with the use of synthetic delivery systems.

The main goal in Chapter Two was to exploit the potential of RNA interference using lipid-substituted polyethylenimine carriers as an alternative to current AML therapeutics that focus on protein targeting or have broader mechanisms of action. We selected lipid modifications that increased the potential of the carriers and mRNA targets that responded to silencing and resulted in the reduction of cellular proliferation. However, we observed that not all targets allowed for the same level of mRNA reduction or even though silencing was observed, the effect did not correlate with a reduction in proliferation or increase in apoptosis as expected. Thus, in the future to have a better insight on the effect of mRNA downregulation, we can expand the time points that we do the analysis on proliferation and apoptosis and directly analyze protein downregulation as well. In the past, correlating mRNA levels with protein levels have also not always been successful as the proteins that are already in the cell might have longer half-lives than expected to be downregulated with one mRNA treatment. Or, de novo protein synthesis might not be as active in the given cell. Also, genome correlations have been studied to understand in what cases mRNA might not match protein abundance levels. Greenbaum et al., elucidated how there are target categories that might be more or less susceptible to correlations based on the localization of the protein [272]. For example, proteins that act on the nucleolus were found to be better correlated with mRNA levels when compared to proteins that have their major effects in the mitochondria or cellular rescue. Another factor that could be hampering the outcome of mRNA downregulation is that

some genes have shown less variation in mRNA levels during cellular division and instead their protein levels are controlled at the translational or post-translational level [272]. To overcome these limitations, siRNA targeting could be analyzed across a group of genes in the same cellular pathway as each one might have variations in the processes mentioned above yet still allow for similar therapeutic outcomes lowering cellular proliferation, inducing apoptosis or differentiation. Also, combinational targeting of siRNAs could be employed in the future to study synergistic effects in one specific cellular pathway or in pathways that result in two different outcomes. For example, targeting the Ras/MAPK pathway involved in cellular differentiation, growth, chemotaxis and apoptosis and the BCL-2 intrinsic apoptotic pathway. Other considerations for future work are the introduction of modifications to the siRNA itself to increase its stability and have more potent effects on mRNA content with lower doses [230]. Besides focusing on the siRNA itself, to increase the potential of RNAi for the treatment of AML we can further examine the delivery systems and the specific interactions each lipid modification we introduced has on enhancing cell membrane interactions or triggering non-specific cellular pathways. For in vivo delivery, the carriers could also be further modified to target a specific antigen on the surface of the desired cells.

In Chapter Three the main objective was to introduce the ExBIM base surrogate to a ligation-mediated detection method for the in-sequence recognition of O^6-meG so that the ligated product could be further amplified. From our observations, when O^6-meG is in the middle of the target sequence the T4 ligase which catalyzes product formation tolerates less than optimal base pairing and thus the selectivity of the assay was not optimal. By changing the O^6-meG to the recognition site we aimed to increase the discrimination of the ligase; however, the rate of the reaction was significantly diminished. As an alternative to ligation-based detection, we can introduce the ExBIM modification to other types of oligonucleotide probes that are still able to hybridize to a target for detection such as molecular beacons (MB). MBs are synthetic oligonucleotides that include a stem structure of hybridized bases and a loop portion with unhybridized bases that are able to detect a target of interest [273-

274]. MBs are also commonly modified with a reporter feature by having a fluorophore and a quencher at the ends of the stem so that when the loop section hybridizes to its complementary target the MB changes its conformation and the fluorophore and quencher separate allowing for the emission of fluorescence [273-274]. In the past the most optimal lengths for the loop portion are 15-25 and 5-7 for the stem [275] and in the past they have been paired with signal amplification steps including PCR for detecting single nucleotide polymorphisms [276]. Thus, as an alternative for O^6-meG ligation-based detection, a MB could be designed with an ExBIM base in the loop sequence and abasic sites that enhance the specificity of the hybridization. By optimizing the position of the abasic sites in relationship to the ExBIM we could survey the maximum discrimination without the loss of signal from the fluorophore. Another advantage of using MB for the assay would be the analysis of the detection by fluorescence in contrast to gel electrophoresis which is less sensitive and more time consuming [277].

Finally, the projects presented in Chapters Two and Three of these thesis illustrate the various approaches that can be examined when developing a nucleic acid-based therapy or detection method. Pairing nucleic acids with synthetic materials makes them potent in-cell targeting moieties and introducing chemical modifications into a sequence can further increase their selectivity. Targeting genetic sequences of interest or introducing genetic modifications is considered as an alternative and/or complement to the treatment and diagnosis of different disease and in the future, we will only experience more developments in the area.

Bibliography

1. Rothemund, P. W. K. (2006). Folding DNA to create nanoscale shapes and patterns. Nature, 440, 297. Retrieved from https://doi.org/10.1038/nature04586

2. Hong, F., Zhang, F., Liu, Y., & Yan, H. (2017). DNA origami: Scaffolds for creating higher order structures. *Chemical Reviews*, 117(20), 12584-12640. doi:10.1021/acs.chemrev.6b00825

3. Juliano, R.L. (2016). The delivery of therapeutic oligonucleotides. *Nucleic Acids Research*, 44(14), 6518-6548. doi:10.1093/nar/gkw236.

4. Khvorova, A., Scaringe, S., Boese, Q., Leake, D., Reynolds, A., & Marshall, W. S. (2004). Rational siRNA design for RNA interference. *Nature Biotechnology*, 22(3), 326-330. doi:10.1038/nbt936

5. Liu, X., Zhang, F., Jing, X., Pan, M., Liu, P., Li, W., . . . Fan, C. (2018). Complex silica composite nanomaterials templated with DNA origami. *Nature*, 559(7715), 593-598. doi:10.1038/s41586-018-0332-7

6. McGinn, S., Bauer, D., Brefort, T., Dong, L., El-Sagheer, A., Elsharawy, A., . . . Gut, I. G. (2016). New technologies for DNA analysis – a review of the READNA project. *New Biotechnology*, 33(3), 311-330. doi://doi.org/10.1016/j.nbt.2015.10.003Nature04586

7. Peng, P., Shi, L., Wang, H., & Li, T. (2016). A DNA nanoswitch-controlled reversible nanosensor. *Nucleic Acids Research*, 45(2), 541-546. doi:10.1093/nar/gkw1146

8. Stoler, A. B. (1991). Genes and cancer. Br Med Bull, 64-75. Retrieved from https://www.ncbi.nlm.nih.gov/pubmed/1863849

9. National Cancer Institute. (2017). The genetics of cancer. Retrieved from https://www.cancer.gov/about-cancer/causes-prevention/genetics

10. Weinstein, I.B., Arcoleo, J., Backer, J., Jeffrey, A., Hsiao, W.L., Gattoni-Celli, S., Kirschmeier, P., Okin, E. (1983). Molecular mechanisms of tumor promotion and multistage carcinogenesis. *Princess Takamatsu Symp*osyum,14, 59-74.

11. Weinstein, B. (1988). The Origins of Human Cancer: Molecular Mechanisms of Carcinogenesis and Their Implications for Cancer Prevention and Treatment—Twenty-seventh G. H. A. Clowes. Memorial Award Lecture. *Cancer Res.* (48) (15) 4135-4143.

12. Pearson, P.L., Van der Luijt, R.B., The genetic analysis of cancer. *J Intern Med*, 243(6), 413-7.

13. Devereux, T.R., Risinger, J.I., Barrett, J.C. (1999). Mutations and altered expression of the human cancer genes: what they tell us about causes. *IARC Sci Publ*, 146, 19-42.

14. Berger, A. C., Korkut, A., Kanchi, R. S., Hegde, A. M., Lenoir, W., Liu, W., . . . Akbani, R. (2018). A comprehensive pan-cancer molecular study of gynecologic and breast cancers. *Cancer Cell, 33*(4), 705.e9. doi://doi.org/10.1016/j.ccell.2018.03.014

15. Ilyas, A. M., Ahmad, S., Faheem, M., Naseer, M. I., Kumosani, T. A., Al-Qahtani, M. H., Gari, M., … Ahmed, F. (2015). Next generation sequencing of acute myeloid leukemia: influencing prognosis. *BMC genomics*, *16 Suppl 1*(Suppl 1), S5.

16. Katona, B. W., & Rustgi, A. K. (2017). Gastric Cancer Genomics: Advances and Future Directions. *Cellular and molecular gastroenterology and hepatology*, *3*(2), 211-217. doi:10.1016/j.jcmgh.2017.01.003

17. Siegel, M. B., He, X., Hoadley, K. A., Hoyle, A., Pearce, J. B., Garrett, A. L., Kumar, S., Moylan, V. J., Brady, C. M., Van Swearingen, A. E., Marron, D., Gupta, G. P., Thorne, L. B., Kieran, N., Livasy, C., Mardis, E. R., Parker, J. S., Chen, M., Anders, C. K., Carey, L. A., … Perou, C. M. (2018). Integrated RNA and DNA sequencing reveals early drivers of metastatic breast cancer. *The Journal of clinical investigation*, *128*(4), 1371-1383.

18. Fujimoto, A., Totoki, Y., Abe, T., Boroevich, K. A., Hosoda, F., Nguyen, H. H., . . . Nakagawa, H. (2012). Whole-genome sequencing of liver cancers identifies etiological influences on mutation patterns and recurrent mutations in chromatin regulators. *Nature Genetics, 44*, 760. Retrieved from https://doi.org/10.1038/ng.2291

19. Hoang, P. H., Dobbins, S. E., Cornish, A. J., Chubb, D., Law, P. J., Kaiser, M., & Houlston, R. S. (2018). Whole-genome sequencing of multiple myeloma reveals oncogenic pathways are targeted somatically through multiple mechanisms. *Leukemia, 32*(11), 2459-2470. doi:10.1038/s41375-018-0103-3

20. Lu, X., Kensche, P. R., Huynen, M. A., & Notebaart, R. A. (2013). Genome evolution predicts genetic interactions in protein complexes and reveals cancer drug targets. *Nature Communications, 4*, 2124. Retrieved from https://doi.org/10.1038/ncomms3124

21. Ricketts, C. J., De Cubas, A. A., Fan, H., Smith, C. C., Lang, M., Reznik, E., . . . Linehan, W. M. (2018). The cancer genome atlas comprehensive molecular characterization of renal cell carcinoma. *Cell Reports, 23*(1), 326.e5. doi://doi.org/10.1016/j.celrep.2018.03.075

22. Wedge, D. C., Gundem, G., Mitchell, T., Woodcock, D. J., Martincorena, I., Ghori, M., . . . The, T. C. (2018). Sequencing of prostate cancers identifies new cancer genes, routes of progression and drug targets. *Nature Genetics, 50*(5), 682-692. doi:10.1038/s41588-018-0086-z

23. NIH. (2018). TCGA releases the pan-cancer atlas. Retrieved from https://cancergenome.nih.gov/newsevents/newsannouncements/pancancer_atlas

24. Roth, J. A., & Cristiano, R. J. (1997). Gene therapy for cancer: What have we done and where are we going? *JNCI: Journal of the National Cancer Institute, 89*(1), 21-39. Retrieved from http://dx.doi.org/10.1093/jnci/89.1.21

25. Roth, J.A., Swisher, S.G., Meyn, R.E. (1999). p53 tumor suppressor gene therapy for cancer. *Oncology;* 13; 148-54.

26. Valente, J. Queiroz, J. Sousa, F. (2018). p53 as the Focus of Gene Therapy: Past, Present and Future. *Current Drug Targets.*;19(15):1801-1817. doi 10.2174/ 1389450119666180115165447.

27. Zhang, W., Li, L., Li, D., Liu, J., Li, X., Li, W., Xu, x., Zhang, M.J., Chandler, L.A., Lin, H., Hu, A., Xu, W., and Lam, D.M. (2018). The First Approved Gene Therapy

Product for Cancer Ad-*p53* (Gendicine): 12 Years in the Clinic. *Human Gene Therapy*, 29(2), 160-179.

28. National Cancer Institute. (2017). CAR T cells: Engineering patients' immune cells to treat their cancers. Retrieved from https://www.cancer.gov/about-cancer/treatment/research/car-t-cells

29. June, C.H., Blazar, B.R., Riley, J.L. (2009). Engineering lymphocyte subsets: Tools, trials and tribulations. *Nature Review Immunology*, 9, 704–716.

30. 29.Frey, N. V. and Porter, D. L. (2016), CAR T-cells merge into the fast lane of cancer care. *American Journal Hematology,* 91, 146-150. doi:10.1002/ajh.24238

31. Park, J. H., Geyer, M. B., & Brentjens, R. J. (2016). CD19-targeted CAR T-cell therapeutics for hematologic malignancies: interpreting clinical outcomes to date. Blood, 127(26), 3312-3320. https://doi.org/10.1182/blood-2016-02-629063

32. U.S. Food and Drug Administration. (2017). FDA approves novel gene therapy to treat patients with a rare form of inherited vision loss. Retrieved from https://www.fda.gov/newsevents/newsroom/pressannouncements/ucm589467.htm

33. Gu, S., Thompson, D. A., Srikumari, C. R. S., Lorenz, B., Finckh, U., Nicoletti, A., . . . Gal, A. (1997). Mutations in RPE65 cause autosomal recessive childhood–onset severe retinal dystrophy. *Nature Genetics, 17*, 194. Retrieved from https://doi.org/10.1038/ng1097-194

34. Novartis Media Relations. (2018). Novartis announces positive CHMP opinion for one-time gene therapy luxturna® to treat children and adults with rare inherited retinal disease. Retrieved from https://www.novartis.com/news/media-releases/novartis-announces-positive-chmp-opinion-one-time-gene-therapy-luxturna-treat-children-and-adults-rare-inherited-retinal-disease

35. Goodsell, D.S. (1999). The Molecular Perspective: The *ras* Oncogene. *The Oncologist*. Voll. 4no. 3 263-264.

36. Simanshu, K. D., Nissley, D. V., McCormick, F. (2017). RAS Proteins and Their Regulators in Human Disease. *Cell,* 170 (1): 17-33. doi;https://doi.org/10.1016/j.cell.2017.06.009

37. Réjiba, S. , Wack, S. , Aprahamian, M. and Hajri, A. (2007). K-ras oncogene silencing strategy reduces tumor growth and enhances gemcitabine chemotherapy efficacy for pancreatic cancer treatment*. Cancer Science*, 98: 1128-1136. doi:10.1111/j.1349-7006.2007.00506.x

38. Zhou, L., Jiang, Y., Tan, A., Greenlee, A.R., Shen, Y., Liu, L., Yang, Q., (2008). Silencing of N-Ras Gene Expression Using shRNA Decreases Transformation Efficiency and Tumor Growth in Transformed Cells Induced by Anti-BPDE, *Toxicological Sciences*, 105 (2,1) : 286–294, https://doi.org/10.1093/toxsci/kfn122

39. Mukhopadhyay, T., Tainsky, M., Cavender, A.C., Roth, JA. Specific inhibition of K-ras expression and tumorigenicity of lung cancer cells by antisense RNA (1991). *Cancer Res* , vol. 51 (pg. 1744-8)

40. Hanahan, D. & Weinberg, R. A. (2000). The hallmarks of cancer. *Cell* 100, 57–70.

41. Elmore S. (2007). Apoptosis: a review of programmed cell death. *Toxicologic pathology*, *35*(4), 495-516.

42. Inoue-Yamauchi, A., Jeng, P. S., Kim, K., Chen, H., Han, S., Ganesan, Y. T., . . . Cheng, E. H. (2017). Targeting the differential addiction to anti-apoptotic BCL-2 family for cancer therapy. *Nature Communications, 8*, 16078. Retrieved from https://doi.org/10.1038/ncomms16078

43. Letai, A. G. (2008) Diagnosing and exploiting cancer's addiction to blocks in apoptosis. *Nat. Rev. Cancer* 8, 121.

44. Cheng, Emily H. -Y. A., Wei, M. C., Weiler, S., Flavell, R. A., Mak, T. W., Lindsten, T., & Korsmeyer, S. J. (2001). BCL-2, BCL-XL sequester BH3 domain-only

molecules preventing BAX- and BAK-mediated mitochondrial apoptosis. *Molecular Cell, 8*(3), 705-711. doi://doi.org/10.1016/S1097-2765(01)00320-3

45. Kim, H., Rafiuddin-Shah, M., Tu, H., Jeffers, J. R., Zambetti, G. P., Hsieh, J. J. -., & Cheng, E. H. -. (2006). Hierarchical regulation of mitochondrion-dependent apoptosis by BCL-2 subfamilies. *Nature Cell Biology, 8*, 1348. Retrieved from https://doi.org/10.1038/ncb1499

46. Willis, S. N., Fletcher, J. I., Kaufmann, T., van Delft, M. F., Chen, L., Czabotar, P. E., . . . Huang, D. C. S. (2007). Apoptosis initiated when BH3 ligands engage multiple bcl-2 homologs, not bax or bak. *Science, 315*(5813), 856. doi:10.1126/science.1133289

47. Anderson, M. A., Deng, J., Seymour, J. F., Tam, C., Kim, S. Y., Fein, J., Yu, L., Brown, J. R., Westerman, D., Si, E. G., Majewski, I. J., Segal, D., Heitner Enschede, S. L., Huang, D. C., Davids, M. S., Letai, A., … Roberts, A. W. (2016). The BCL2 selective inhibitor venetoclax induces rapid onset apoptosis of CLL cells in patients via a TP53-independent mechanism. *Blood*, *127*(25), 3215-24.

48. Choudhary, G. S., Al-harbi, S., Mazumder, S., Hill, B. T., Smith, M. R., Bodo, J., . . . Almasan, A. (2015). MCL-1 and BCL-xL-dependent resistance to the BCL-2 inhibitor ABT-199 can be overcome by preventing PI3K/AKT/mTOR activation in lymphoid malignancies. *Cell Death &Amp; Disease, 6*, e1593. Retrieved from https://doi.org/10.1038/cddis.2014.525

49. Takahashi, H., Chen, M. C., Pham, H., Matsuo, Y., Ishiguro, H., Reber, H. A., Takeyama, H., Hines, O. J., … Eibl, G. (2013). Simultaneous knock-down of Bcl-xL and Mcl-1 induces apoptosis through Bax activation in pancreatic cancer cells. *Biochimica et biophysica acta*, *1833*(12), 2980-2987.

50. Lee, Y. J., Hwang, I. S., Lee, Y. J., Lee, C. H., Kim, S. H., Nam, H. S., Choi, Y. J., … Lee, S. H. (2014). Knockdown of Bcl-xL enhances growth-inhibiting and apoptosis-inducing effects of resveratrol and clofarabine in malignant mesothelioma H-2452 cells. *Journal of Korean medical science*, *29*(11), 1464-72.

51. Denoyelle, C., Abeilard, E., Brotin, E., Varin, E., Giffard, F., Meryet-Figuière, M., . . . Goux, D. (2010). Downregulation of bcl-x L and mcl-1 is sufficient to induce cell death in mesothelioma cells highly refractory to conventional chemotherapy. *Carcinogenesis, 31*(6), 984-993. doi:10.1093/carcin/bgq026

52. Ma, L., Han, M., Keyoumu, Z., Wang, H., & Keyoumu, S. (2017). Immunotherapy of Dual-Function Vector with Both Immunostimulatory and B-Cell Lymphoma 2 (Bcl-2)-Silencing Effects on Gastric Carcinoma. *Medical science monitor: international medical journal of experimental and clinical research*, *23*, 1980-1991. doi:10.12659/MSM.900418

53. Schölch, S., Rauber, C., Tietz, A., Rahbari, N. N., Bork, U., Schmidt, T., Kahlert, C., Haberkorn, U., Tomai, M. A., Lipson, K. E., Carretero, R., Weitz, J., Koch, M., … Huber, P. E. (2014). Radiotherapy combined with TLR7/8 activation induces strong immune responses against gastrointestinal tumors. *Oncotarget*, *6*(7), 4663-76.

54. Fabian, M. R., Sonenber, N. (2012). The mechanics of miRNA-mediated gene silencing: a look under the hood of miRISC. Nature Structural & Molecular Biology, 19; 586–593.

55. Pai, S. I., Lin, Y., Macaes, B., Meneshian, A., Hung, C., & Wu, T. (2005). Prospects of RNA interference therapy for cancer. *Gene Therapy, 13*, 464. Retrieved from https://doi.org/10.1038/sj.gt.3302694

56. Feng, M., Cabrera, G., Deshane, J., Scanlon, K. J., and Curiel, D.T. (1995). Neoplastic Reversion Accomplished by High Efficiency Adenoviral-mediated Delivery of an Anti-ras Ribozyme. *Cancer Res.* 55(10), 2024-2028.

57. Baranyi, L., Slepushkin, V., & Dropulic, B. (2014). Chapter 1 - ex vivo gene therapy: Utilization of genetic vectors for the generation of genetically modified cell products for therapy. In E. C. Lattime, & S. L. Gerson (Eds.), *Gene therapy of cancer (third edition)* (3-18). San Diego: Academic Press. doi://doi.org/10.1016/B978-0-12-394295-1.00001-9.

58. Dambournet, D., Hong, S. H., Grassart, A., & Drubin, D. G. (2014). Chapter seven - tagging endogenous loci for live-cell fluorescence imaging and molecule counting using ZFNs, TALENs, and Cas9. In J. A. Doudna, & E. J. Sontheimer (Eds.), *Methods in enzymology* (pp. 139-160) Academic Press. doi://doi.org/10.1016/B978-0-12-801185-0.00007-6 Retrieved from http://www.sciencedirect.com/science/article/pii/B9780128011850000076

59. Zhan, T., Rindtorff, N., Betge, J., Ebert, M. P., & Boutros, M. (2018). CRISPR/Cas9 for cancer research and therapy. *Seminars in Cancer Biology,* doi://doi.org/10.1016/j.semcancer.2018.04.001.

60. Stephenson, ML., Zamecnik, PC. (1978). Inhibition of Rous sarcoma viral RNA translation by a specific oligodeoxyribonucleotide. *Proc Natl Acad Sci U S A. 1978 Jan; 75(1):285-8.*

61. Opalinska, J. B. & Gewirtz, A. M. (2002). Nucleic-acid therapeutics: basic principles and recent applications. *Nat. Rev. Drug Discov.* 1, 503–514.

62. Watts, J. K., & Corey, D. R. (2011). Silencing disease genes in the laboratory and the clinic. *The Journal of pathology*, *226*(2), 365-79.

63. Sharma, V. K., Sharma, R. K., & Singh, S. K. (2014). Antisense oligonucleotides: Modifications and clinical trials. *MedChemComm, 5*(10), 1454-1471. doi:10.1039/C4MD00184B

64. J. Micklefield. (2001). Backbone modification of nucleic acids: synthesis, structure and therapeutic applications, *Curr. Med. Chem;* 8, 1157–1179

65. J. Zang, J. T. Shaw and M. D. Matteucci. (1999). Synthesis and hybridisation property of an oligonucleotide containing a 3’-thioformacetal linked pentathymidylate, *Bioorg. Med. Chem. Lett;* 9, 319–327

66. S. M. Rahman, T. Baba, T. Kodama, M. A. Islam and S. Obika. (2012). Hybridising ability and nuclease resistance profile of backbone modified cationic phosphorothioate oligonucleotides, *Bioorg. Med. Chem;* 20, 4098–4102

67. Libini, P., Zurcher, W., Egli, M. (1994). Stabilizing effects of the RNA 2′-substituent: crystal structure of an oligodeoxynucleotide duplex containing 2′-*O*-methylated adenosines. *Chem Biol*. 1(1):39-45.

68. Vickers, T. A., Wyatt, J. R., Burckin, T., Bennett, C. F., & Freier, S. M. (2001). Fully modified 2' MOE oligonucleotides redirect polyadenylation. *Nucleic acids research*, *29*(6), 1293-9.

69. Havens, M. A., & Hastings, M. L. (2016). Splice-switching antisense oligonucleotides as therapeutic drugs. *Nucleic acids research*, *44*(14), 6549-63.

70. van Deutekom J.C., Bremmer-Bout M., Janson A.A., Ginjaar I.B., Baas F., den Dunnen J.T., van Ommen G.J. (2001). Antisense-induced exon skipping restores dystrophin expression in DMD patient derived muscle cells. *Hum. Mol. Genet*;10:1547–1554.

71. Yokota, T., Duddy, W. & Partridge, T. (2007). Optimizing exon skipping therapies for DMD. *Acta Myol.* 26, 179–184.

72. Pratt, A. J., & MacRae, I. J. (2009). The RNA-induced silencing complex: a versatile gene-silencing machine. *The Journal of biological chemistry*, *284*(27), 17897-901.

73. Lam, J. K., Chow, M. Y., Zhang, Y., & Leung, S. W. (2015). siRNA Versus miRNA as Therapeutics for Gene Silencing. *Molecular therapy. Nucleic acids*, *4*(9), e252. doi:10.1038/mtna.2015.23

74. Rao, DD, Vorhies, JS, Senzer, N and Nemunaitis, J. (2009). siRNA vs. shRNA: similarities and differences. *Adv Drug Deliv Rev*. 61: 746–759.

75. Huntzinger, E., & Izaurralde, E. (2011). Gene silencing by microRNAs: contributions of translational repression and mRNA decay. *Nat Rev Genet.* 12: 99–110.

76. Kim, VN., Han, J & Siomi., MC. (2009). Biogenesis of small RNAs in animals. *Nat Rev Mol Cell Biol*. 10: 126–139.

77. Hayes, J., Peruzzi, PP., and Lawler, S. (2014). MicroRNAs in cancer: biomarkers, functions and therapy. *Trends Mol Med.* 20: 460–469.

78. Esquela-Kerscher, A., & Slack, F. J. (2006). Oncomirs — microRNAs with a role in cancer. *Nature Reviews Cancer, 6*, 259. Retrieved from https://doi.org/10.1038/nrc1840

79. Daka, A., & Peer, D. (2012). RNAi-based nanomedicines for targeted personalized therapy. *Advanced Drug Delivery Reviews; Personalized Nanomedicine, 64*(13), 1508-1521. doi://doi.org/10.1016/j.addr.2012.08.014

80. Gallo, V., Egger, M., McCormack, V., Farmer, P. B., Ioannidis, J. P. A., Kirsch-Volders, M., . . . Vineis, P. (2011). STrengthening the reporting of OBservational studies in Epidemiology—Molecular epidemiology (STROBE-ME): An extension of the STROBE statement.*European Journal of Epidemiology, 26*(10), 797-810. doi:10.1007/s10654-011-9622-1

81. Manolio, T. A. (2010). Genomewide association studies and assessment of the risk of disease. *N Engl J Med, 363*(2), 166-176. doi:10.1056/NEJMra0905980

82. Lim, S. Y., Lee, J. H., Diefenbach, R. J., Kefford, R. F., & Rizos, H. (2018). Liquid biomarkers in melanoma: Detection and discovery. *Molecular Cancer, 17*(1), 8. doi:10.1186/s12943-018-0757-5

83. Ziegler, A., Koch, A., Krockenberger, K., & Grosshennig, A. (2012). Personalized medicine using DNA biomarkers: a review. *Human genetics*, *131*(10), 1627-38.

84. Han, X., Wang, J., & Sun, Y. (2017). Circulating Tumor DNA as Biomarkers for Cancer Detection. Genomics, proteomics and bioinformatics. 15; 59-72.

85. Grimwade, D., Walker, H., Oliver, F., Wheatley, K., Harrison, C., Harrison, G., Rees, J., Hann, I., Stevens, R., Burnett, A., & Goldstone, A. (1998). The Importance of Diagnostic Cytogenetics on Outcome in AML: Analysis of 1,612 Patients Entered Into the MRC AML 10 Trial. Blood, 92(7), 2322-2333. Retrieved from http://www.bloodjournal.org/content/92/7/2322.

86. Byrd, J. C., Mrózek, K., Dodge, R. K., Carroll, A. J., Edwards, C. G., Arthur, D. C., Pettenati, M. J., Patil, S. R., Rao, K. W., Watson, M. S., Koduru, P. R., Moore, J. O., Stone, R. M., Mayer, R. J., Feldman, E. J., Davey, F. R., Schiffer, C. A., Larson, R. A., & Bloomfield,

C. D. (2002). Pretreatment cytogenetic abnormalities are predictive of induction success, cumulative incidence of relapse, and overall survival in adult patients with de novo acute myeloid leukemia: results from Cancer and Leukemia Group B (CALGB 8461). *Blood*, 100(13), 4325-4336. https://doi.org/10.1182/blood-2002-03-0772.

87. Grimwade, D. (2001). The predictive value of hierarchical cytogenetic classification in older adults with acute myeloid leukemia (AML): analysis of 1065 patients entered into the United Kingdom Medical Research Council AML11 trial. *Blood*, 98 (5) pp. 1312-1320

88. Campo, E., Swerdlow, S.H., . Harris, N.L., Pileri, S., Stein, H., Jaffe, E.S. (2011). The 2008 WHO classification of lymphoid neoplasms and beyond: evolving concepts and practical applications. *Blood*, 117: 19; pp. 5019-5032

89. Hatzimichael, E., Georgiou, G., Benetatos, L., & Briasoulis, E. (2013). Gene mutations and molecularly targeted therapies in acute myeloid leukemia. *Am J Blood Res*, 3, 29-51

90. Prada-Arismendy, J., Arroyave, J. C., & Röthlisberger, S. (2017). Molecular biomarkers in acute myeloid leukemia. *Blood Reviews, 31*(1), 63-76. doi://doi.org/10.1016/j.blre.2016.08.005

91. Meshinchi, S., & Appelbaum, F. R. (2009). Structural and functional alterations of FLT3 in acute myeloid leukemia. *Clin Cancer Res, 15*(13), 4263. doi:10.1158/1078-0432.CCR-08-1123

92. M. Nakao, S. Yokota, T. Iwai, H. Kaneko, S.Horiike, K. Kashima, *et al. (*1996). Internal tandem duplication of the flt3 gene found in acute myeloid leukemia. *Leukemia*, 10 (12). pp. 1911-1918

93. Bienz, M., Ludwig, M., Mueller, B. U., Oppliger Leibundgut, E., Ratschiller, D., Solenthaler, M., . . . Pabst, T. (2005). Risk assessment in patients with acute myeloid leukemia and a normal karyotype. *Clin Cancer Res, 11*(4), 1416. doi:10.1158/1078-0432.CCR-04-1552

94. Fröhling, S., Schlenk, R. F., Breitruck, J., Benner, A., Kreitmeier, S., Tobis, K., Döhner, H., & Döhner, K. (2002). Prognostic significance of activating FLT3 mutations in younger adults (16 to 60 years) with acute myeloid leukemia and normal cytogenetics: a study of the AML Study Group Ulm. *Blood*, 100(13), 4372-4380. Accessed January 24, 2019. https://doi.org/10.1182/blood-2002-05-1440.

95. Ozeki, K., Kiyoi, H., Hirose, Y., Iwai, M., Ninomiya, M., Kodera, Y., Miyawaki, S., Kuriyama, K., Shimazaki, C., Akiyama, H., Nishimura, M., Motoji, T., Shinagawa, K., Takeshita, A., Ueda, R., Ohno, R., Emi, N., & Naoe, T. (2004). Biologic and clinical significance of the FLT3 transcript level in acute myeloid leukemia. *Blood*, 103(5), 1901-1908. Accessed January 24, 2019. https://doi.org/10.1182/blood-2003-06-1845.

96. Levis, M., Allebach, J., Tse, K., Zheng, R., Baldwin, B. R., Smith, B. D., Jones-Bolin, S., Ruggeri, B., Dionne, C., & Small, D. (2002). A FLT3-targeted tyrosine kinase inhibitor is cytotoxic to leukemia cells in vitro and in vivo. *Blood*, 99(11), 3885-3891. https://doi.org/10.1182/blood.V99.11.3885.

97. El Fakih, R., Rasheed, W., Hawsawi, Y., Alsermani, M., & Hassanein, M. (2018). Targeting FLT3 Mutations in Acute Myeloid Leukemia. *Cells*, *7*(1), 4. doi:10.3390/cells7010004

98. Antar A, Kharfan-Dabaja MA, Mahfouz R, Bazarbachi A. (2015). Sorafenib Maintenance Appears Safe and Improves Clinical Outcomes in FLT3-ITD Acute Myeloid Leukemia After Allogenic Hematopoietic Cell Transplantation. *Clinical Lymphoma Myeloma Leuk. May; 15(5):298-302. Epub.*

99. Stone, R. M., Mandrekar, S., Sanford, B. L., Geyer, S., Bloomfield, C. D., Dohner, K., Thiede, C., Marcucci, G., Lo-Coco, F., Klisovic, R. B., Wei, A., Sierra, J., Sanz, M. A., Brandwein, J. M., de Witte, T., Niederwieser, D., Appelbaum, F. R., Medeiros, B. C., Tallman, M. S., Krauter, J., Schlenk, R. F., Ganser, A., Serve, H., Ehninger, G., Amadori, S., Larson, R. A., & Dohner, H. (2015). The Multi-Kinase Inhibitor Midostaurin (M) Prolongs Survival Compared with Placebo (P) in Combination with Daunorubicin (D)/Cytarabine (C)

Induction (ind), High-Dose C Consolidation (consol), and As Maintenance (maint) Therapy in Newly Diagnosed Acute Myeloid Leukemia (AML) Patients (pts) Age 18-60 with FLT3 Mutations (muts): An International Prospective Randomized (rand) P-Controlled Double-Blind Trial (CALGB 10603/RATIFY [Alliance]). Blood, 126(23), 6. Retrieved from http://www.bloodjournal.org/content/126/23/6.

100. Rasmussen, S. L., Krarup, H. B., Sunesen, K., Johansen, M. B., Stender, M. T., Pedersen, I. S., . . . Thorlacius-Ussing, O. (2017). Hypermethylated DNA, a circulating biomarker for colorectal cancer detection. *Plos One, 12*(7), e0180809. Retrieved from https://doi.org/10.1371/journal.pone.0180809

101. Barault, L., Amatu, A., Siravegna, G., Ponzetti, A., Moran, S., Cassingena, A., . . . Di Nicolantonio, F. (2018). Discovery of methylated circulating DNA biomarkers for comprehensive non-invasive monitoring of treatment response in metastatic colorectal cancer. *Gut, 67*(11), 1995. doi:10.1136/gutjnl-2016-313372

102. Jin, B., Li, Y., & Robertson, K. D. (2011). DNA methylation: superior or subordinate in the epigenetic hierarchy?. *Genes & cancer*, *2*(6), 607-17.

103. Lister, R., Pelizzola, M., Dowen, R. H., Hawkins, R. D., Hon, G., Tonti-Filippini, J., Nery, J. R., Lee, L., Ye, Z., Ngo, Q. M., Edsall, L., Antosiewicz-Bourget, J., Stewart, R., Ruotti, V., Millar, A. H., Thomson, J. A., Ren, B., … Ecker, J. R. (2009). Human DNA methylomes at base resolution show widespread epigenomic differences. *Nature*, *462*(7271), 315-

104. Zhu J. K. (2009). Active DNA demethylation mediated by DNA glycosylases. *Annual review of genetics*, *43*, 143-66.

105. *Feinberg AP, Ohlsson R, Henikoff S.* (2006). The epigenetic progenitor origin of human cancer. *Nat Rev Genet; 7(1):21-33*

106. Deaton, A. M., & Bird, A. (2011). CpG islands and the regulation of transcription. *Genes & development*, *25*(10), 1010-22.

107. Hemminki K, Dipple A, Shuker DEG, Kadlubar FF, Segerback D,Bartsch H. (1994). DNA Adducts: Identification and Biological Significance. IARC Scientific Publication No 125, IARC, Lyon, France.

108. Groopman. JD., Kensler, TW. (1993). Molecular markers for human chemical carcinogen exposures. *Chem. Res. Toxicol.* 6: 764-770.

109. Warren, J. J., Forsberg, L. J., & Beese, L. S. (2006). The structural basis for the mutagenicity of O(6)-methyl-guanine lesions. *Proceedings of the National Academy of Sciences of the United States of America*, *103*(52), 19701-6.

110. Perera, F.P., Weinstein, I.B. (1982). Molecular epidemiology and carcinogen-DNA adduct detection: new approaches to studies of human cancer causation. *J. Chronic Dis.*, 35(7). 581-600

111. N. Rothman., W. Stewart, P. Schulte. (1995). Incorporating biomarkers into cancer epidemiology: a matrix of biomarker and study design categories. *Cancer Epidemiol. Biomarkers Prev.* 4. 301-311.

112. K. Hemminki, M. Koskinen, H. Rajaniemi, C. Zhao. (2000). DNA adducts, mutations, and cancer 2000. Regul. Toxicol. Pharmacol; 32. 264-275

113. Poirier M. C. (1997). DNA adducts as exposure biomarkers and indicators of cancer risk. *Environmental health perspectives*, *105 Suppl 4*(Suppl 4), 907-12.

114. Kurdyukov, S., & Bullock, M. (2016). DNA Methylation Analysis: Choosing the Right Method. *Biology*, *5*(1), 3. doi:10.3390/biology5010003

115. Lee Y.K., Jin S., Duan S., Lim Y.C., Ng D.P., Lin X.M., Yeo G., Ding C. (2014). Improved reduced representation bisulfite sequencing for epigenomic profiling of clinical samples. Biol. Proced. Online. 16:1. doi: 10.1186/1480-9222-16-1.

116. Song, L., James, SR., Kazim, L., Karpf, AR. (2005). Specific method for the determination of genomic DNA methylation by liquid chromatography-electrospray ionization tandem mass spectrometry. *Anal Chem; 77(2):504-10.*

117. Le, T., Kim, K. P., Fan, G., & Faull, K. F. (2011). A sensitive mass spectrometry method for simultaneous quantification of DNA methylation and hydroxymethylation levels in biological samples. *Analytical biochemistry*, *412*(2), 203-9.

118. Liu, Z., Wu, J., Xie, Z., Liu, S., Fan-Havard, P., Huang, T. H., Plass, C., Marcucci, G., … Chan, K. K. (2009). Quantification of regional DNA methylation by liquid chromatography/tandem mass spectrometry. *Analytical biochemistry*, *391*(2), 106-13.

119. Shim, J., Humphreys, G. I., Venkatesan, B. M., Munz, J. M., Zou, X., Sathe, C., . . . Bashir, R. (2013). Detection and quantification of methylation in DNA using solid-state nanopores. *Scientific Reports, 3*, 1389. Retrieved from https://doi.org/10.1038/srep01389

120. Wang, Y., Zhang, Y., Guo, Y., & Kang, X. F. (2017). Fast and precise detection of DNA methylation with tetramethylammonium-filled nanopore. *Scientific reports*, *7*(1), 183. doi:10.1038/s41598-017-00317-2

121. Ding, Y., Fleming, A. M., White, H. S., & Burrows, C. J. (2015). Differentiation of G:C vs A:T and G:C vs G:mC Base Pairs in the Latch Zone of α-Hemolysin. *ACS nano*, *9*(11), 11325-32.

122. Powell, J. R., Bennett, M. R., Evans, K. E., Yu, S., Webster, R. M., Waters, R., Skinner, N., … Reed, S. H. (2015). 3D-DIP-Chip: a microarray-based method to measure genomic DNA damage. *Scientific reports*, *5*, 7975. doi:10.1038/srep07975

123. J.E. Klaunig, L.M. Kamendulis. (2010). Toxicology Testing and Evaluation. Comprehensive Toxicology.

124. Kaina, B., Margison, G. P., & Christmann, M. (2010). Targeting O6-methylguanine-DNA methyltransferase with specific inhibitors as a strategy in cancer therapy. *Cellular and Molecular Life Sciences, 67*(21), 3663-3681. doi:10.1007/s00018-010-0491-7

125. Mojas, N., Lopes, M., & Jiricny, J. (2007). Mismatch repair-dependent processing of methylation damage gives rise to persistent single-stranded gaps in newly replicated DNA. *Genes & development*, *21*(24), 3342-55.

126. Kraus, A., McKeague, M., Seiwert, N. et al. (2018). Immunological and mass spectrometry-based approaches to determine thresholds of the mutagenic DNA adduct O^6-methylguanine in vivo. Arch Toxicol. https://doiorg.login.ezproxy.library.ualberta.ca/10.1007/s00204-018-2355-0

127. Wyss, L. A., Nilforoushan, A., Williams, D. M., Marx, A., & Sturla, S. J. (2016). The use of an artificial nucleotide for polymerase-based recognition of carcinogenic O6-alkylguanine DNA adducts. *Nucleic acids research*, *44*(14), 6564-73.

128. Wyss L.A., Nilforoushan A., Eichenseher F., Suter U., Blatter N., Marx A., Sturla S.J. (2015). Specific incorporation of an artificial nucleotide opposite a mutagenic DNA adduct by a DNA polymerase. J. Am. Chem. Soc, 137, 30–33.

129. Trantakis, I. A., Nilforoushan, A., Dahlmann, H. A., Stäuble, C. K., & Sturla, S. J. (2016). In-Gene Quantification of O(6)-Methylguanine with Elongated Nucleoside Analogues on Gold Nanoprobes. *Journal of the American Chemical Society*, *138*(27), 8497-504.

130. Thaxton, C. S., Georganopoulou, D. G., Mirkin, C. A. (2006). Gold nanoparticle probes for the detection of nucleic acid targets. *Clin. Chim. Acta, 363*, 120-126.

131. Adams, N. M.; Jackson, S. R.; Haselton, F. R.; Wright, D. W. (2012). Design, synthesis, and characterization of nucleic-acid-functionalized gold surfaces for biomarker detection. *Langmuir, 28*, 1068-1082.

132. Elghanian, R., Storhoff, J. J., Mucic, R. C., Letsinger, R. L., & Mirkin, C. A. (1997). Selective colorimetric detection of polynucleotides based on the distance-dependent optical properties of gold nanoparticles. *Science, 277*(5329), 1078. doi:10.1126/science.277.5329.1078

133. Jin, R., Wu, G., Li, Z., Mirkin, C., & Schatz, G. (2003). What controls the melting properties of DNA-linked gold nanoparticle assemblies. *J. Am. Chem. Soc.,* 125, 1643-1654.

134. Kelloff, G., and Sigman, C. C. (2012). Cancer biomarkers: selecting the right drug for the right patient. *Nat. Rev. Drug Discovery* 11, 201-2014.

135. Papaemmanuil, E., Gerstung, M., Bullinger, L., Gaidzik, V., Paschka, P., ...Campbell, P. (2016). Genomic classification and prognosis in acute myeloid leukemia. *N. Engl. J. Med*, 374, 2209-2221.

136. Döhner, H., Estey, E., Grimwade, D., Amadori, S., Appelbaum, F. R., Büchner, T., Dombret, H., Ebert, B. L., Fenaux, P., Larson, R. A., Levine, R. L., Lo-Coco, F., Naoe, T., Niederwieser, D., Ossenkoppele, G. J., Sanz, M., Sierra, J., Tallman, M. S., Tien, H. F., Wei, A. H., Löwenberg, B., … Bloomfield, C. D. (2017). Diagnosis and management of AML in adults: 2017 ELN recommendations from an international expert panel. *Blood*, *129*(4), 424-447.

137. Tyner, J. W., Tognon, C. E., Bottomly, D., Wilmot, B., Kurtz, S. E., Savage, S. L., … Druker, B. J. (2018). Functional genomic landscape of acute myeloid leukaemia. *Nature*, *562*(7728), 526–531. https://doi.org/10.1038/s41586-018-0623-z

138. Stornetta, A., Zimmermann, M., Cimino, G. D., Henderson, P. T., & Sturla, S. J. (2017). DNA adducts from anticancer drugs as candidate predictive markers for precision medicine. *Chemical Research in Toxicology, 30*(1), 388-409. doi:10.1021/acs.chemrestox.6b00380

139. Wang, R., Han, Y., Sun, B., Zhao, Z., Opoku-Damoah, Y., Cheng, H., . . . Ding, Y. (2018). Deep tumor penetrating bioparticulates inspired burst intracellular drug release for precision chemo-phototherapy. *Small, 14*(12), 1703110. doi:10.1002/smll.201703110

140. Bhujwalla, Z. M., Kakkad, S., Chen, Z., Jin, J., Hapuarachchige, S., Artemov, D., & Penet, M. (2018). Theranostics and metabolotheranostics for precision medicine in oncology. *Journal of Magnetic Resonance, 291*, 141-151. doi://doi.org/10.1016/j.jmr.2018.03.004

141. Wu, Y., Wu, H., Kuan, C., Lin, C., Wang, L., Chang, C., & Wang, T. (2016). Multi-functionalized carbon dots as theranostic nanoagent for gene delivery in lung cancer therapy. *Scientific Reports, 6*, 21170. Retrieved from https://doi.org/10.1038/srep21170

142. Estey, E., & Döhner, H. (2006). Acute myeloid leukaemia. *The Lancet, 368*(9550), 1894-1907. 10.1016/S0140-6736(06)69780-8 Retrieved from https://www.sciencedirect.com/science/article/pii/S0140673606697808

143. Abelson, S., Collord, G., Ng, S. W. K., Weissbrod, O., Mendelson Cohen, N., Niemeyer, E., Shlush, L. I. (2018). Prediction of acute myeloid leukaemia risk in healthy individuals. *Nature, 559*(7714), 400-404. 10.1038/s41586-018-0317-6 Retrieved from https://doi.org/10.1038/s41586-018-0317-6

144. Gallipoli, P., Giotopoulos, G., & Huntly, B. J. P. (2015). Epigenetic regulators as promising therapeutic targets in acute myeloid leukemia. *Therapeutic Advances in Hematology, 6*(3), 103-119. 10.1177/2040620715577614 Retrieved from http://www.ncbi.nlm.nih.gov/pmc/articles/PMC4480521/

145. Grimwade, D., Ivey, A., & Huntly, B. J. P. (2016). Molecular landscape of acute myeloid leukemia in younger adults and its clinical relevance. *Blood, 127*(1), 29-41. 10.1182/blood-2015-07-604496 Retrieved from https://www.ncbi.nlm.nih.gov/pubmed/26660431

146. Lamble, A., Kosaka, Y., Lo, P., Huang, F., Sasser, K., Tognon, C. E., . . . Lind, E. F. (2015). Defining the immune microenvironment in patients with acute myeloid leukemia. *Blood, 126*(23), 1374. Retrieved from http://www.bloodjournal.org/content/126/23/1374.abstract

147. Olsson, I., Bergh, G., Ehinger, M., & Gullberg, U. (1996). Cell differentiation in acute myeloid leukemia. *European Journal of Haematology, 57*(1), 1-16. 10.1111/j.1600-0609.1996.tb00483.x Retrieved from https://www.ncbi.nlm.nih.gov/pubmed/8698118

148. Dombret, H., & Gardin, C. (2015). An update of current treatments for adult acute myeloid leukemia. *Blood, 127*(1), 53-61. 10.1182/blood-2015-08-604520 Retrieved from http://www.ncbi.nlm.nih.gov/pmc/articles/PMC4705610/

149. Pan, R., Hogdal, L. J., Benito, J. M., Bucci, D., Han, L., Borthakur, G., . . . Letai, A. G. (2013). Selective BCL-2 inhibition by ABT-199 causes on target cell death in acute

myeloid leukemia. *Cancer Discovery, 4*(3), 362-375. 10.1158/2159-8290.CD-13-0609 Retrieved from http://www.ncbi.nlm.nih.gov/pmc/articles/PMC3975047/

150. van Rhenen, A., Feller, N., Kelder, A., Westra, A. H., Rombouts, E., Zweegman, S., . . . Schuurhuis, G. J. (2005). High stem cell frequency in acute myeloid leukemia at diagnosis predicts high minimal residual disease and poor survival. *Clin Cancer Res, 11*(18), 6520. Retrieved from http://clincancerres.aacrjournals.org/content/11/18/6520.abstract

151. Reinisch, Andreas|Chan, Steven M.|Thomas, Daniel Majeti, Ravindra. (2015). Biology and clinical relevance of acute myeloid leukemia stem cells. *Seminars in Hematology, 52*(3), 150-164. 10.1053/j.seminhematol.2015.03.008 Retrieved from https://www.clinicalkey.es/playcontent/1-s2.0-S0037196315000323

152. She, M., Niu, X., Chen, X., Li, J., Zhou, M., He, Y., . . . Guo, K. (2012). Resistance of leukemic stem-like cells in AML cell line KG1a to natural killer cell-mediated cytotoxicity. *Cancer Letters, 318*(2), 173-179. //doi.org/10.1016/j.canlet.2011.12.017 Retrieved from http://www.sciencedirect.com/science/article/pii/S0304383511007646

153. Quillet-Mary, A., Mansat, V., Duchayne, E., Come, M. G., Allouche, M., Bailly, J. D., . . . Laurent, G. (1996). Daunorubicin-induced internucleosomal DNA fragmentation in acute myeloid cell lines. *Leukemia, 10*(3), 417-425.

154. Bailly, J. D., Skladanowski, A., Bettaieb, A., Mansat, V., Larsen, A. K., & Laurent, G. (1997). Natural resistance of acute myeloid leukemia cell lines to mitoxantrone is associated with lack of apoptosis. *Leukemia, 11*(9), 1523-1532. 10.1038/sj.leu.2400762 Retrieved from https://www.ncbi.nlm.nih.gov/pubmed/9305608

155. Bettaieb, A., Record, M., Côme, M. G., Bras, A. C., Chap, H., Laurent, G., & Jaffrézou, J. P. (1996). Opposite effects of tumor necrosis factor alpha on the sphingomyelin-ceramide pathway in two myeloid leukemia cell lines: Role of transverse sphingomyelin distribution in the plasma membrane. *Blood, 88*(4), 1465. Retrieved from https://www.ncbi.nlm.nih.gov/pubmed/8695867

156. Fire, A., Xu, S., Montgomery, M. K., Kostas, S. A., Driver, S. E., & Mello, C. C. (1998). Potent and specific genetic interference by double-stranded RNA in caenorhabditis elegans. *Nature, 391*, 806. Retrieved from https://doi.org/10.1038/35888

157. Hannon, G. J. (2002). RNA interference. *Nature, 418*, 244. Retrieved from http://dx.doi.org/10.1038/418244a

158. Elbashir, S. M., Harborth, J., Lendeckel, W., Yalcin, A., Weber, K., & Tuschl, T. (2001). Duplexes of 21-nucleotide RNAs mediate RNA interference in cultured mammalian cells. *Nature, 411*, 494. Retrieved from https://doi.org/10.1038/35078107

159. Kim, D.H., & Rossi, J.J. (2007). Strategies for silencing human disease using RNA interference. *Nat. Rev. Genetics*. 8(3):173-84. http://dx.doi.org/10.1038/nrg2006

160. K. Imai, A. Takaoka. (2006). Comparing antibody and small-molecule therapies for cancer. *Nat. Rev. Cancer.* 6: 714–727.

161. Kaczmarek, J. C., Kowalski, P. S., & Anderson, D. G. (2017). Advances in the delivery of RNA therapeutics: From concept to clinical reality. *Genome Medicine, 9*(1), 60. doi:10.1186/s13073-017-0450-0

162. Raemdonck, K., Vandenbroucke, R. E., Demeester, J., Sanders, N. N., & De Smedt, S. C. (2008). Maintaining the silence: Reflections on long-term RNAi. *Drug Discovery Today, 13*(21), 917-931. doi://doi.org/10.1016/j.drudis.2008.06.008

163. Dykxhoorn, D. M., Palliser, D., & Lieberman, J. (2006). The silent treatment: siRNAs as small molecule drugs. *Gene Therapy, 13*, 541. Retrieved from https://doi.org/10.1038/sj.gt.3302703

164. Kanasty, R., Dorkin, J. R., Vegas, A., & Anderson, D. (2013). Delivery materials for siRNA therapeutics. *Nature Materials, 12*, 967. Retrieved from https://doi.org/10.1038/nmat3765

165. Wang, J., Lu, Z., Wientjes, M. G., & Au, J. L.-S. (2010). Delivery of siRNA Therapeutics: Barriers and Carriers. *The AAPS Journal*, *12*(4), 492–503. http://doi.org/10.1208/s12248-010-9210-4

166. Pack, D. W., Hoffman, A. S., Pun, S., & Stayton, P. S. (2005). Design and development of polymers for gene delivery. *Nature Reviews Drug Discovery, 4*, 581. Retrieved from https://doi.org/10.1038/nrd1775

167. B. Landry, H.M. Aliabadi, A. Samuel, H. Gül-Uludag, J. Xiiaoyan, O. Kutsch, et al., (2012). Effective non-viral delivery of siRNA to acute myeloid leukemia cells with lipid substituted polyethylenimines, PLoS One 7, e44197http://dx.doi.org/10.1371/journal.pone.0044197.

168. Behr, J. (1997). The proton sponge: A trick to enter cells the viruses did not exploit [Abstract]. *CHIMIA International Journal for Chemistry, 51*(1-2) 34-36. Retrieved from https://www.ingentaconnect.com/content/scs/chimia/1997/00000051/f0020001/art00026

169. Rehman, Z. u., Hoekstra, D., & Zuhorn, I. S. (2013). Mechanism of polyplex- and lipoplex-mediated delivery of nucleic acids: Real-time visualization of transient membrane destabilization without endosomal lysis. *ACS Nano, 7*(5), 3767-3777. doi:10.1021/nn3049494

170. [Guideline] NCCN Clinical Practice Guidelines in Oncology: Acute Myeloid Leukemia Version 1.2015. National Comprehensive Cancer Network. Available at http://www.nccn.org/professionals/physician_gls/pdf/aml.pdf. Accessed: September 10, 2018.

171. Döhner, H., Weisdorf, D. J., & Bloomfield, C. D. (2015). Acute myeloid leukemia. *N Engl J Med, 373*(12), 1136-1152. doi:10.1056/NEJMra1406184

172. Bishop, J., Matthews, J., Young, G., Szer, J., Gillett, A., Joshua, D., Bradstock, K., Enno, A., Wolf, M., & Fox, R. (1996). A randomized study of high-dose cytarabine in induction in acute myeloid leukemia. *Blood*, 87(5), 1710-1717. Retrieved from http://www.bloodjournal.org/content/87/5/1710.

173. Dombret, H., & Gardin, C. (2016). An update of current treatments for adult acute myeloid leukemia. *Blood,* 127(1), 53-61. Accessed September 19, 2018. https://doi.org/10.1182/blood-2015-08-604520.

174. McGowan, J. V., Chung, R., Maulik, A., Piotrowska, I., Walker, J. M., & Yellon, D. M. (2017). Anthracycline Chemotherapy and Cardiotoxicity. *Cardiovascular Drugs and Therapy*, *31*(1), 63–75. http://doi.org/10.1007/s10557-016-6711-0

175. Lamba, J. K. (2009). Genetic factors influencing cytarabine therapy. *Pharmacogenomics*, *10*(10), 1657–1674. http://doi.org/10.2217/pgs.09.118

176. Weick, J., Kopecky, K., Appelbaum, F., Head, D., Kingsbury, L., Balcerzak, S., Bickers, J., Hynes, H., Welborn, J., Simon, S., & Grever, M. (1996). A randomized investigation of high-dose versus standard-dose cytosine arabinoside with daunorubicin in patients with previously untreated acute myeloid leukemia: a Southwest Oncology Group study. *Blood,* 88(8), 2841-285. doi: http://www.bloodjournal.org/content/88/8/2841.

177. Levis, M. (2017). Midostaurin approved for FLT3-mutated AML. *Blood,* 129(26),3403-3406. https://doi.org/10.1182/blood-2017-05-782292.

178. Appelbaum, F. R., & Bernstein, I. D. (2017). Gemtuzumab ozogamicin for acute myeloid leukemia. *Blood,* 130(22), 2373-2376. https://doi.org/10.1182/blood-2017-09-797712.

179. Motyckova, G., Stone, RM. (2015). Development of midostaurin as a tyrosine kinase inhibitor in:.*Targeted Therapy of Acute Myeloid Leukemia*. New York, NY: Springer-Verlag; 2014:201-214. https://doi.org/10.1007/978-1-4939-1393-0

180. Stone, R. M., Manley, P. W., Larson, R. A., & Capdeville, R. (2018). Midostaurin: its odyssey from discovery to approval for treating acute myeloid leukemia and advanced systemic mastocytosis. *Blood Advances*, *2*(4), 444–453. http://doi.org/10.1182/bloodadvances.2017011080

181. Rowe, J. M., & Löwenberg, B. (2013). Gemtuzumab ozogamicin in acute myeloid leukemia: a remarkable saga about an active drug. *Blood,* 121(24),4838-4841. Retrieved from: https://doi.org/10.1182/blood-2013-03-490482.

182. U.S Food & Drug Administration. FDA approves ivosidenib for relapsed or refractory acute myeloid leukemia. (2018). Retrieved from: https://www.fda.gov/Drugs/InformationOnDrugs/ApprovedDrugs/ucm614128.htm

183. Pollyea, D. (2018). Enasidenib for the treatment of acute myeloid leukemia AU - dugan, james. *Expert Review of Clinical Pharmacology, 11*(8), 755-760. doi:10.1080/17512433.2018.1477585

184. Schnittger, S., Haferlach, C., Ulke, M., Alpermann, T., Kern, W., & Haferlach, T. (2010). IDH1 mutations are detected in 6.6% of 1414 AML patients and are associated with intermediate risk karyotype and unfavorable prognosis in adults younger than 60 years and unmutated NPM1 status. Blood, 116(25), 5486-5496. https://doi.org/10.1182/blood-2010-02-267955.

185. Chen, E. C., Fathi, A. T., & Brunner, A. M. (2018). Reformulating acute myeloid leukemia: liposomal cytarabine and daunorubicin (CPX-351) as an emerging therapy for secondary AML. *OncoTargets and therapy*, *11*, 3425-3434. doi:10.2147/OTT.S141212

186. Lancet, J. E., Uy, G. L., Cortes, J. E., Newell, L. F., Lin, T. L., Ritchie, E. K., . . . Medeiros, B. C. (2018). CPX-351 (cytarabine and daunorubicin) liposome for injection versus conventional cytarabine plus daunorubicin in older patients with newly diagnosed secondary acute myeloid leukemia. *Jco, 36*(26), 2684-2692. doi:10.1200/JCO.2017.77.6112

187. Ossenkoppele, G., & Löwenberg, B. (2015). How I treat the older patient with acute myeloid leukemia. *Blood,* 125(5), 767-774. Accessed September 23, 2018. https://doi.org/10.1182/blood-2014-08-551499.

188. Löwenberg, B., Ossenkoppele, G. J., van Putten, W., Schouten, H. C., Graux, C., Ferrant, A., . . . Verhoef, G. (2009). High-dose daunorubicin in older patients with acute myeloid leukemia. *N Engl J Med, 361*(13), 1235-1248. doi:10.1056/NEJMoa0901409

189. O'Dwyer, K., Freyer, D. R., & Horan, J. T. (2018). Treatment strategies for adolescent and young adult patients with acute myeloid leukemia. *Blood,*132(4), 362-368. Accessed September 20, 2018.https://doi.org/10.1182/blood-2017-12-778472

190. Tomizawa, D., Watanabe, T., Hanada, R., Horibe, K., Horikoshi, Y., Iwamoto, S., . . . Adachi, S. (2015). Outcome of adolescent patients with acute myeloid leukemia treated with pediatric protocols. *International Journal of Hematology, 102*(3), 318-326. doi:10.1007/s12185-015-1825-x

191. Canner, J., Alonzo, T. A., Franklin, J., Freyer, D. R., Gamis, A., Gerbing, R. B., Lange, B. J., Meshinchi, S., Woods, W. G., Perentesis, J., … Horan, J. (2013). Differences in outcomes of newly diagnosed acute myeloid leukemia for adolescent/young adult and younger patients: a report from the Children's Oncology Group. *Cancer*, *119*(23), 4162-9.

192. Wouters, B. J., Löwenberg, B., & Delwel, R. (2009). A decade of genome-wide gene expression profiling in acute myeloid leukemia: flashback and prospects. *Blood,* 113(2), 291-298.

193. Cioca, D. P., Aoki, Y., & Kiyosawa, K. (2003). RNA interference is a functional pathway with therapeutic potential in human myeloid leukemia cell lines. *Cancer Gene Therapy, 10*, 125. Retrieved from https://doi.org/10.1038/sj.cgt.7700544

194. Calabretta, B., Sims, R. B., Valtieri, M., Caracciolo, D., Szczylik, C., Venturelli, D., Ratajczak, D., Beran, M., Gewirtz, A. M. (1991). Normal and leukemic hematopoietic cells manifest differential sensitivity to inhibitory effects of c-myb antisense oligodeoxynucleotides: an in vitro study relevant to bone marrow purging. *Proceedings of the National Academy of Sciences of the United States of America*, *88*(6), 2351–2355.

195. Citro, G., Perrotti, D., Cucco, C., D'Agnano, I., Sacchi, A., Zupi, G., Calabretta, B. (1992). Inhibition of leukemia cell proliferation by receptor-mediated uptake of c-myb antisense oligodeoxynucleotides. Proc Natl Acad Sci U S A. Aug 1992, 89 (15) 7031-7035; DOI:10.1073/pnas.89.15.7031

196. Walters, D. K., Stoffregen, E. P., Heinrich, M. C., Deininger, M. W., & Druker, B. J. (2005). RNAi-induced down-regulation of FLT3 expression in AML cell lines increases sensitivity to MLN518. Blood, 105(7), 2952-2954. https://doi.org/10.1182/blood-2004-07-2758.

197. Merkerova, M., Klamova, H., Brdicka R., Bruchova, H. (2007). Targeting of gene expression by siRNA in CML primary cells. Mol Biol Rep, 34, 27. https://doi.org/10.1007/s11033-006-9006-x

198. Lostale-Seijo, I., & Montenegro, J. Synthetic materials at the forefront of gene delivery. (2018*). Nature Reviews Chemistry*. 2; 258–277.

199. Wang, R., Chow T. Y., Chen, S., Ma, D., Luo, T., Tan, Y., Dong, S. (2018). Magnetic Force-driven in Situ Selective Intracellular Delivery. *Scientific Reports*. 8:14205. DOI:10.1038/s41598-018-32605-w

200. Ansari, A. S., Santerre, P. J., & Uludağ, H. (2017). Biomaterials for polynucleotide delivery to anchorage-independent cells. *Journal of Materials Chemistry B, 5*(35), 7238-7261. doi:10.1039/C7TB01833A

201. Basiouni, S., Fuhrmann, H., & Schumann, J. (2012). High-efficiency transfection of suspension cell lines. *BioTechniques, 53*(2), 1-4. doi:10.2144/000113914

202. Alshamsan, A. Haddadi, V. Incani, J. Samuel, A. Lavasanifar, H. Uludag. (2009). Formulation and delivery of siRNA by oleic acid and stearic acid modified polyethylenimine, Mol. Pharm; 6: 121–133.

203. Love, K. T., Mahon, K. P., Levins, C. G., Whitehead, K. A., Querbes, W., Dorkin, J. R., . . . Anderson, D. G. (2010). Lipid-like materials for low-dose, in vivo gene silencing. *Proc Natl Acad Sci USA, 107*(5), 1864. doi:10.1073/pnas.0910603106

204. Thapa, B., Pilanwong, S., KC, B. R., Rutherford, B., Uludag, H. (2016). Small hydrophobe substitution on polyethylenimine for plasmid DNA delivery: Optimal substitution is critical for effective delivery. *Acta Biomaterialia;* 33: 213–224. Doi: http://dx.doi.org/10.1016/j.actbio.2016.01.025

205. Nishioka, C., Ikezoe, T., Takeuchi, A., Nobumoto, A., Tsuda, M., Yokoyama, A. (2015). The novel function of CD82 and its impact on BCL2L12 via AKT/STAT5 signal pathway in acute myelogenous leukemia cells. *Leukemia;* 29: 2296–2306.

206. Thomadaki, H., Floros, KV., Pavlovic, S., Tosic, N., Gourgiotis, D., Colovic M *et al*. (2012). Overexpression of the novel member of the BCL2 gene family, BCL2L12, is associated with the disease outcome in patients with acute myeloid leukemia. *Clin Biochem*; 45: 1362–1367.

207. Papageorgiou, S. G., Kontos, C. K., Pappa, V., Thomadaki, H., Kontsioti, F., Dervenoulas, J., Papageorgiou, E., Economopoulos, T., … Scorilas, A. (2011). The novel member of the BCL2 gene family, BCL2L12, is substantially elevated in chronic lymphocytic leukemia patients, supporting its value as a significant biomarker. *The oncologist*, *16*(9), 1280-91.

208. Altieri, D. C. (2015). SURVIVIN - THE *INCONVENIENT* IAP. *Seminars in Cell & Developmental Biology*, *39*, 91–96. http://doi.org/10.1016/j.semcdb.2014.12.007

209. Carter, B. Z., Qiu, Y., Huang, X., Diao, L., Zhang, N., Coombes, K. R., … Kornblau, S. M. (2012). Survivin is highly expressed in CD34+38− leukemic stem/progenitor cells and predicts poor clinical outcomes in AML. *Blood; 120*(1), 173–180. http://doi.org/10.1182/blood-2012-02-409888

210. Carter, Z. B., Milella, M., Altieri, C. D., Andreeff, M. (2001). Cytokine-regulated expression of *survivin* in myeloid leukemia. Blood; 97:2784-2790; doi: https://doi.org/10.1182/blood.V97.9.2784

211. Small, S., Keerthivasan, G., Huang, Z., Gurbuxani, S., & Crispino, J. D. (2010). Overexpression of Survivin Initiates Hematologic Malignancies In Vivo. *Leukemia*, *24*(11), 1920–1926. http://doi.org/10.1038/leu.2010.198

212. Remant K.C., Landry B., Aliabadi H.M., Lavasanifar A, Uludag H. (2011). Lipid substitution on low molecular weight (0.6–2.0 kDa) polyethylenimine leads to a higher zeta

potential of plasmid DNA and enhances transgene expression. *Acta Biomaterialia*. 7, 2209-2217.

213. Parmar, M.B., Arteaga, B., Fu, T., Bahadur, KC., Aliabadi, H.M., Hugh J.C., Löbenberg, R., Uludağ, H. (2016). Multiple siRNA delivery against cell cycle and anti-apoptosis proteins using lipid-substituted polyethylenimine in triple-negative breast cancer and non-malignant cells. *J. Biomed. Mat. Res. A*, 104, 3031-304

214. Gül-Uludağ, HH., Valencia-Serna ,J., Kucharski, C., Marquez-Curtis, LA., Xiaoyan, J., Larratt, LM., Janowska-Wieczorek, A., Uludağ, H. (2014). Polymeric Nanoparticle-Mediated Silencing of CD44 in CD34+ Acute Leukemia Blasts. *Leuk Res*, 11, 1299-308. doi: 10.1016/j.leukres.

215. Landry, B., Gül-Uludağ, H., Plianwong, S., Kucharski, C., Zak, Z., Parmar, M. B., . . . Uludağ, H. (2016). Targeting CXCR4/SDF-1 axis by lipopolymer complexes of siRNA in acute myeloid leukemia. *Journal of Controlled Release, 224*, 8-21. doi://doi.org/10.1016/j.jconrel.2015.12.052

216. Cheson, B. D., Bennett, J. M., Kopecky, K. J., Büchner, T., Willman, C. L., Estey, E. H., . . . Bloomfield, C. D. (2003). Revised recommendations of the international working group for diagnosis, standardization of response criteria, treatment outcomes, and reporting standards for therapeutic trials in acute myeloid leukemia. *Jco, 21*(24), 4642-4649. doi:10.1200/JCO.2003.04.036

217. Thol, F., Schlenk, R. F., Heuser, M., & Ganser, A. (2015). How I treat refractory and early relapsed acute myeloid leukemia. *Blood,* 126(3), 319-327. https://doi.org/10.1182/blood-2014-10-551911.

218. Puneet, A. & Ravi, B. (2015). Influence of Bone Marrow Microenvironment on Leukemic Stem Cells: Breaking Up an Intimate Relationship. *Advances in Cancer Research*, 127, 227-52.

219. McCarty, M. F., & DiNicolantonio, J. J. (2016). Lauric acid-rich medium-chain triglycerides can substitute for other oils in cooking applications and may have limited pathogenicity. *Open heart*, *3*(2), e000467. doi:10.1136/openhrt-2016-000467

220. Rosamaria Lappano, Anna Sebastiani, Francesca Cirillo, Damiano Cosimo Rigiracciolo, Giulia Raffaella Galli, Rosita Curcio, . . . Marcello Maggiolini. (2017). The lauric acid-activated signaling prompts apoptosis in cancer cells. *Cell Death Discovery, 3*, 17063. doi:10.1038/cddiscovery.2017.63

221. Bulbake, U., Doppalapudi, S., Kommineni, N., & Khan, W. (2017). Liposomal Formulations in Clinical Use: An Updated Review. *Pharmaceutics*, *9*(2), 12. doi:10.3390/pharmaceutics9020012

222. Meneksedag-Erol, D., Sun, C., Tang, T., Uludag, H. (2014). Molecular Dynamics Simulations of Polyplexes and Lipoplexes Employed in Gene Delivery. *Intracellular Delivery II*. Fundamental Biomedical Technologies. DE: Springer Verlag.

223. Bocca, C., Bozzo, F., Gabriel, L., & Miglietta, A. (2007). Conjugated linoleic acid inhibits caco-2 cell growth via ERK-MAPK signaling pathway. *The Journal of Nutritional Biochemistry, 18*(5), 332-340. doi://doi.org/10.1016/j.jnutbio.2006.07.001

224. Engelbrecht, A., Toit-Kohn, J., Ellis, B., Thomas, M., Nell, T., & Smith, R. (2008). Differential induction of apoptosis and inhibition of the PI3-kinase pathway by saturated, monounsaturated and polyunsaturated fatty acids in a colon cancer cell model. *Apoptosis, 13*(11), 1368. doi:10.1007/s10495-008-0260-3

225. Jump, D. B., & Clarke, S. D. (1999). Regulation of gene expression by dietary fat. *Annual Review of Nutrition, 19*(1), 63-90. doi:10.1146/annurev.nutr.19.1.63

226. Lian, G., Dettenhofer, M., Lu, J., Downing, M., Chenn, A., Wong, T., & Sheen, V. (2016). Filamin A- and formin 2-dependent endocytosis regulates proliferation via the canonical Wnt pathway. *Development (Cambridge, England)*, *143*(23), 4509-4520.

227. Shojima, K., Sato, A., Hanaki, H., Tsujimoto, I., Nakamura, M., Hattori, K., . . Kikuchi, A. (2015). Wnt5a promotes cancer cell invasion and proliferation by receptor-

mediated endocytosis-dependent and -independent mechanisms, respectively. *Scientific Reports, 5*(1), 8042. doi:10.1038/srep08042

228. Caffrey, D. R., Zhao, J., Song, Z., Schaffer, M. E., Haney, S. A., Subramanian, R. R., Seymour, A. B., … Hughes, J. D. (2011). siRNA off-target effects can be reduced at concentrations that match their individual potency. *PloS one*, *6*(7), e21503.

229. Khvorova, A., Scaringe, S., Boese, Q., Leake, D., Reynolds, A., & Marshall, W. S. (2004). Rational siRNA design for RNA interference. *Nature Biotechnology, 22*(3), 326-330. doi:10.1038/nbt936

230. Dar, S. A., Thakur, A., Qureshi, A., & Kumar, M. (2016). siRNAmod: A database of experimentally validated chemically modified siRNAs. *Scientific Reports, 6*(1), 20031. doi:10.1038/srep20031

231. Hemminki, K., Dipple, A., Shuker, D.E.G., Kadlubar, F.F., Segerback. D., Bartsch, H. (1994). DNA Adducts: Identification and Biological Significance*. IARC Scientific Publication No 125*, IARC, Lyon, France.

232. Groopman, J.D., Kensler, T.W. (1993). Molecular markers for human chemical carcinogen exposures. *Chem Res Toxicol,* 6, 764-770.

233. Warren, J. J., Forsberg, L. J., & Beese., L. S. (2006). The structural basis for the mutagenicity of O(6)-methyl-guanine lesions. *Proceedings of the National Academy of Sciences of the United States of America*, *103*(52), 19701-6.

234. Reh, B. D., DeBord, D. G., Butler, M. A., Reid, T. M., Mueller, C., & Fajen, J. M. (2000). O6-methylguanine DNA adducts associated with occupational nitrosamine exposure. *Carcinogenesis, 21*(1), 29-33. doi:10.1093/carcin/21.1.29

235. Verbeek, B., Gilham, D. E., Southgate, T. D., & Margison, G. P. (2008). O6-methylguanine-DNA methyltransferase inactivation and chemotherapy. *British Medical Bulletin, 85*(1), 17-33. doi:10.1093/bmb/ldm036

236. Preussmann, R., & Eisenbrand, G. (1984). N-Nitroso carcinogens in the environment. In: Searle, C.E. (Ed) Chemical Carcinogens, Vol. 2, ACS Monograph 182, pp. 829-868.American Chemical Society, Washington, DC.

237. Harrison, K. L., Jukes, R., Cooper, D. P., & Shuker, D. E. G. (1999). Detection of concomitant formation of O6-carboxymethyl- and O6-methyl-2‘-deoxyguanosine in DNA exposed to nitrosated glycine derivatives using a combined immunoaffinity/HPLC method. *Chemical Research in Toxicology, 12*(1), 106-111. doi:10.1021/tx980057n

238. Frederick A. Beland, Miriam C. Poirier. Edited by R. G. Tardiff, P. H. M. Lohman and G. N. Wogan. (1994). Methods to Assess DNA Damage and Repair: lnterspecies Comparisons.SCOPE Published by John Wiley & Sons Ltd.

239. Pegg, A. E. (2000). Repair of O6-alkylguanine by alkyltransferases. *Mutation Research/Reviews in Mutation Research; Special Issue in Honor of Ruggiero Montesano, 462*(2), 83-100. doi://doi.org/10.1016/S1383-5742(00)00017-X

240. Andrew C. Povey (2000). DNA Adducts: Endogenous and Induced. Toxicologic Pathology, Volume 28, No 3, pp 405-414.

241. Inside Life Science. 2012. Chelsea Toledo and Kristie Saltsman. https://publications.nigms.nih.gov/insidelifescience/genetics-numbers.html

242. Souliotis, V. L., & Kyrtopoulos, S. A. (1989). A novel, sensitive assay for O^6-methyl- and O^6-ethylguanine in DNA, based on repair by the enzyme O^6-alkylguanine-DNA-alkyltransferase in competition with an oligonucleotide containing O^6-methylguanine. *Cancer Res, 49*(24), 6997. Retrieved from http://cancerres.aacrjournals.org/content/49/24_Part_1/6997.abstract

243. Wilson, V. L., Basu, A. K., Essigmann, J. M., Smith, R. A., & Harris, C. C. (1988). O^6-alkyldeoxyguanosine detection by ^{32}P-postlabeling and nucleotide chromatographic analysis. *Cancer Res, 48*(8), 2156. Retrieved from http://cancerres.aacrjournals.org/content/48/8/2156.abstract

244. Foiles, P. F., Trushin, N., & Castonguay, A. (1985). Measurement of O*-methyldeoxyguanosine in DNA methylated by the tobacco specific carcinogen 4-(methylnitrosamino)-l-(3-pyridyl)-l-butanone using a biotin-avidin enzyme linked-immunoassay. *Carcinogenesis*, 6(7), 989-993.

245. Wild, C.P., Smart, G., Saffhill, R., & Boyle, J.M. (1983), Radioimmunoassay of C-methyldeoxyguanosine in DNA of cells alkylated in vitro and in vivo, *Carcinogenesis*, 4, 1605-1609

246. Tretyakova, N., Goggin, M., & Janis, G. (2012). Quantitation of DNA adducts by stable isotope dilution mass spectrometry. *Chemical Research in Toxicology*, 25(10), 2007–2035.

247. Kang, H., Konishi, C., Eberle, G., Rajewsky, M., Kuroki, T., and Huh, N. (1992). Highly Sensitive, Specific Detection of O6-Methylguanine, O4-Methylthymine, and O4-Ethylthymine by the Combination of High-Performance Liquid Chromatography Prefractionation, 32P Postlabeling, and Immunoprecipitation. *Cancer Research*, 52, 5307-5312.

248. Kang, H., Konishi, C., Kuroki, T., and Huh, N. (1993). A highly sensitive and specific method for quantitation of O-alkylated DNA adducts and its application to the analysis of human tissue DNA. Environmental Health Perspectives, 99, 269–271.

249. Kaur, H., & Halliwell, B. (1996). Measurement of oxidized and methylated DNA bases by HPLC with electrochemical detection. Biochemical Journal, 318(Pt 1), 21–23.

250. Dolan, M.E., Oplinger, M., Pegg, A.E. (1988). Sequence specificity of guanine alkylation and repair. *Carcinogenesis,* 9(11), 2139–2143.

251. Richardson, F.C., Boucheron, J.A., Skopek, T.R., & Swenberg, J.A. (1989). Formation of O6-methyldeoxyguanosine at specific sites in a synthetic oligonucleotide designed to resemble a known mutagenic hotspot. *J. Biol. Chem*, 2(15), 838-841.

252. Flusberg, B. A., Webster, D. R., Lee, J. H., Travers, K. J., Olivares, E. C., Clark, T. A., . . . Turner, S. W. (2010). Direct detection of DNA methylation during single-molecule,

real-time sequencing. *Nature Methods, 7*, 461. Retrieved from https://doi.org/10.1038/nmeth.1459

253. Clark, T. A., Spittle, K. E., Turner, S. W., & Korlach, J. (2011). Direct detection and sequencing of damaged DNA bases. *Genome integrity*, *2*, 10. doi:10.1186/2041-9414-2-10

254. Gahlon, L.H., & Sturla, S.J. (2013). Hydrogen Bonding or Stacking Interactions in Differentiating Duplex Stability in Oligonucleotides Containing Synthetic Nucleoside Probes for Alkylated DNA. *Chemistry European Journal,* 19(33), 11062-11067.

255. Trantakis, I. A., Nilforoushan, A., Dahlmann, H. A., Stäuble, C. K., & Sturla, S. J. (2016). In-gene quantification of O6-methylguanine with elongated nucleoside analogues on gold nanoprobes. *Journal of the American Chemical Society, 138*(27), 8497-8504. doi:10.1021/jacs.6b03599

256. Wennerberg, K., Rossman, K. L., & Der, C. J. (2005). The ras superfamily at a glance. *Journal of Cell Science, 118*(5), 843. doi:10.1242/jcs.01660

257. Downward, J. (2003). Targeting RAS signalling pathways in cancer therapy. *Nature Reviews Cancer, 3*, 11. Retrieved from https://doi.org/10.1038/nrc969

258. Fernández-Medarde, A., & Santos, E. (2011). Ras in cancer and developmental diseases. *Genes & cancer*, *2*(3), 344-58.

259. Zuber, J., Tchernitsa, O. I., Hinzmann, B., Schmitz, A., Grips, M., Hellriegel, M., . . . Schäfer, R. (2000). A genome-wide survey of RAS transformation targets. *Nature Genetics, 24*, 144. Retrieved from https://doi.org/10.1038/72799

260. Barbacid, M. (1990). ras oncogenes: their role in neoplasia. *European Journal of Clinical Investigation*, 20(3), 225–235. doi: 10.1111/j.1365-2362.1990.tb01848.x

261. Tran, E., Robbins, P. F., Lu, Y., Prickett, T. D., Gartner, J. J., Jia, L., . . . Rosenberg, S. A. (2016). T-cell transfer therapy targeting mutant KRAS in cancer. N Engl J Med, 375(23), 2255-2262. doi:10.1056/NEJMoa1609279

262. Bos, J. L., Fearon, E. R., Hamilton, S. R., Vries, M. V., van Boom, J. H., van, d. E., & Vogelstein, B. (1987). Prevalence of ras gene mutations in human colorectal cancers. *Nature, 327*(6120), 293-297. doi:10.1038/327293a0

263. Downward, J. (2003). Role of receptor tyrosine kinases in G-protein-coupled receptor regulation of Ras: transactivation or parallel pathways?. *Biochemical Journal,* 376, e9–e10.

264. Pylayeva-Gupta, Y., Grabocka, E., & Bar-Sagi, D. (2011). RAS oncogenes: weaving a tumorigenic web. *Nature reviews. Cancer*, *11*(11), 761-74. doi:10.1038/nrc3106

265. Shi, K., Bohl, T. E., Park, J., Zasada, A., Malik, S., Banerjee, S., Tran, V., Li, N., Yin, Z., Kurniawan, F., Orellana, K., … Aihara, H. (2018). T4 DNA ligase structure reveals a prototypical ATP-dependent ligase with a unique mode of sliding clamp interaction. *Nucleic acids research*, *46*(19), 10474-10488.

266. Lohman, G. J., Bauer, R. J., Nichols, N. M., Mazzola, L., Bybee, J., Rivizzigno, D., Cantin, E., … Evans, T. C. (2015). A high-throughput assay for the comprehensive profiling of DNA ligase fidelity. *Nucleic acids research*, *44*(2), e14.

267. Barany F. (1991). Genetic disease detection and DNA amplification using cloned thermostable ligase. *Proceedings of the National Academy of Sciences of the United States of America*, *88*(1), 189-93.

268. Liu, P., Burdzy, A., & Sowers, L. C. (2004). DNA ligases ensure fidelity by interrogating minor groove contacts. *Nucleic acids research*, *32*(15), 4503-11. doi:10.1093/nar/gkh781

269. Kausar, A., Osman, E., Gadzikwa, T., Gibbs-Davis, J. (2016). The presence of a 5’-abasic lesion enhances discrimination of single nucleotide polymorphisms while inducing an isothermal ligase chain reaction. Analyst, 141, 4272-4277. doi: 10.1039/C6AN00614K

270. Maskos, U,. & Southern, E.M. (1992). Parallel analysis of oligodeoxyribonucleotide (oligonucleotide) interactions analysis of factors influencing oligonucleotide duplex formation. *Nucleic Acids Res*., 20, 1675–1678.

271. Fiche, J. B., Buhot, A., Calemczuk, R., & Livache, T. (2006). Temperature effects on DNA chip experiments from surface plasmon resonance imaging: isotherms and melting curves. *Biophysical journal*, *92*(3), 935-46.

272. Greenbaum, D., Colangelo, C., Williams, K., & Gerstein, M. (2003). Comparing protein abundance and mRNA expression levels on a genomic scale. *Genome Biology*, *4*(9), 117.

273. Tyagi, S,. & Kramer, F.R. (1996) Molecular beacons: probes that fluoresce upon hybridization. *Nature Biotechnology*, 14, 303–308.

274. Fang, X., Li, J.J., Perlette, J., Tan, W,. & Wang, K. (2000). Molecular beacons: novel fluorescent probes. *Analytical Chem*istry, 72(23), 747A–753A.

275. Owczarzy, R. , Vallone, P. M., Gallo, F. J., Paner, T. M., Lane, M. J. and Benight, A. S. (1997), Predicting sequence-dependent melting stability of short duplex DNA oligomers. Biopolymers, 44: 217-239. doi:10.1002/(SICI)1097-0282(1997)44:3<217::AID-BIP3>3.0.CO;2-Y

276. Li, X., Huang, Y., Guan, Y., Zhao, M., Li, Y. (2006). Universal molecular beacon-based tracer system for real-time polymerase chain reaction. *Analytical Chemistry*, 78(22),7886–7890. doi: 10.1021/ac061518+

277. Tang, Z., Wang, K., Tan, W., Li, J., Liu, L., Guo, Q., Meng, X., Ma, C., … Huang, S. (2003). Real-time monitoring of nucleic acid ligation in homogenous solutions using molecular beacons. *Nucleic acids research*, *31*(23), e148.